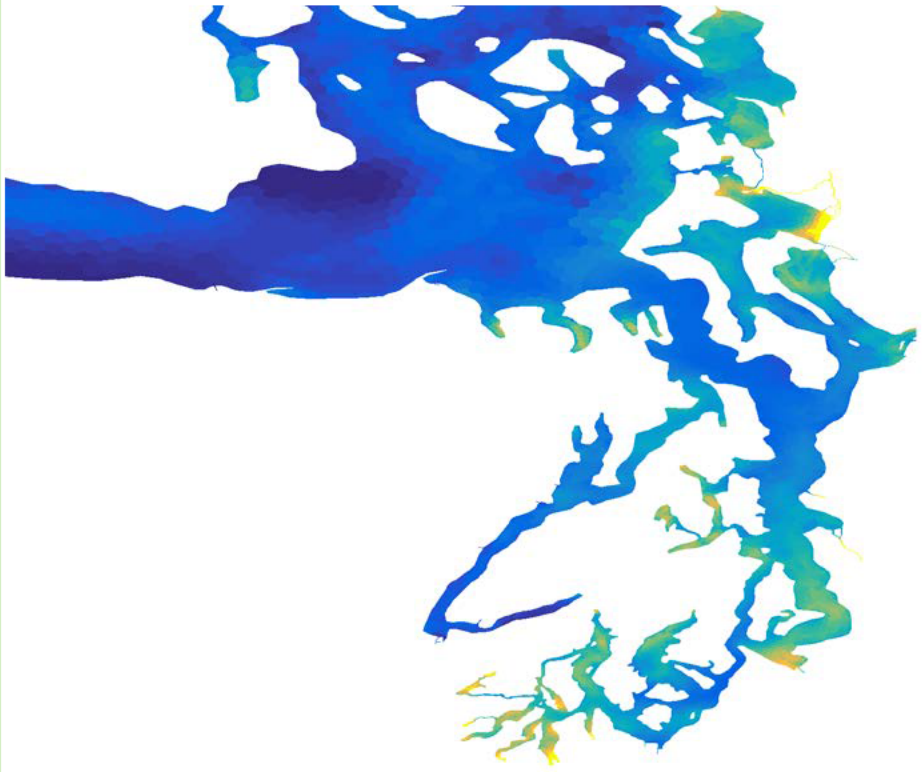

Salish Sea Model

Sediment Diagenesis Module

DEPARTMENT OF ECOLOGY
State of Washington

June 2017

Publication No. 17-03-010

Publication and contact information

This report is available on the Department of Ecology's website at
https://fortress.wa.gov/ecy/publications/SummaryPages/1703010.html

The Activity Tracker Code for this study is 14-017 (Sediment Diagenesis Module)

For more information contact:

Publications Coordinator
Environmental Assessment Program
P.O. Box 47600, Olympia, WA 98504-7600
Phone: (360) 407-6764

Washington State Department of Ecology - www.ecy.wa.gov

o	Headquarters, Olympia	(360) 407-6000
o	Northwest Regional Office, Bellevue	(425) 649-7000
o	Southwest Regional Office, Olympia	(360) 407-6300
o	Central Regional Office, Union Gap	(509) 575-2490
o	Eastern Regional Office, Spokane	(509) 329-3400

Cover image: Average sediment oxygen demand (SOD) during 2006, ranging from about 0.4 $gO_2/m^2/d$ (*dark blue*) to about 1.3 $gO_2/m^2/d$ (*bright yellow*).

Salish Sea Model

Sediment Diagenesis Module

by

Greg Pelletier[1], Laura Bianucci[2], Wen Long[2], Tarang Khangaonkar[2],
Teizeen Mohamedali[1], Anise Ahmed[1], and Cristiana Figueroa-Kaminsky[1]

[1]Environmental Assessment Program
Washington State Department of Ecology
Olympia, Washington 98504-7710

[2]Coastal Science Division
Pacific Northwest National Laboratory
Seattle, Washington 98109

This page is purposely left blank

Table of Contents

Page

List of Figures and Tables....6

Abstract....7

Acknowledgements....8

Introduction....9
- Study Area and Surroundings....9
- Project Description....13

Methods....16
- Model Selection....16
- Model Theory....17
- Model Development and Testing....23

Results....25
- Model Procedure and Calibration....25
- Predicted Sediment Fluxes during 2006....37

Discussion....41

Conclusions and Recommendations....43

References....44

Appendices....50
- Appendix A. Detailed Description of the Sediment Diagenesis Module (SDM)....51
- Appendix B. Comparison of Ecology's SedFlux.xlsm with Professor James Martin's SED_JLM.FOR....81
- Appendix C. Results of Model Quality Assurance Testing with SedFlux.xlsm....90
- Appendix D. Binders of Comparison of Predicted and Observed Water Quality Variables in Time Series and Profile Plots....93
- Appendix E. Listing of Key Model Parameters – Salish Sea Model (SSM) Water Quality Model (FVCOM-ICM) with pH and Sediment Diagenesis....94
- Appendix F. Glossary, Acronyms, and Abbreviations....111

List of Figures and Tables

Page

Figures

Figure 1. Salish Sea with land areas discharging to marine waters within the model domain. 10
Figure 2. Salish Sea Model (SSM) computational grid. 11
Figure 3. Sediment diagenesis schematic. 14
Figure 4. Basic structure of the Sediment Diagenesis Module (SDM)....19
Figure 5. Comparison of model-predicted concentrations of water quality variables with observed data. 28
Figure 6. Comparison of time-series of model-predicted concentrations of dissolved oxygen with observed data for the surface layer and bottom layer of selected stations. 29
Figure 7. Comparison of time-series of model-predicted concentrations of chlorophyll-a with observed data for the surface layer and bottom layer of selected stations. 30
Figure 8. Comparison of time-series of model-predicted concentrations of nitrate for the surface layer and bottom layer of selected stations.. 31
Figure 9. Comparison of time-series of model-predicted concentrations of ammonia for the surface layer and bottom layer of selected stations.. 32
Figure 10. Average sediment oxygen demand (SOD) during 2006....38
Figure 11. Average sediment flux of ammonia during 2006. 39
Figure 12. Average sediment flux of nitrate+nitrite during 2006. 40

Tables

Table 1. General information for benthic chamber sites in Puget Sound. 33
Table 2. Comparison of model-predicted and observed sediment oxygen demand (SOD)[1] 34
Table 3. Comparison of model-predicted and observed flux of ammonia 35
Table 4. Comparison of model-predicted and observed flux of nitrate+nitrite 36

Abstract

Low concentrations of dissolved oxygen (DO) have been measured throughout the Salish Sea. Recent modeling investigations indicate that low concentrations occur throughout much of the Salish Sea due to the intrusion of water with naturally occurring low DO from the Pacific Ocean. However, some regions of Puget Sound are also significantly influenced by human nutrient contributions. Sediment-water interactions strongly influence oxygen levels. A previous version of the Salish Sea Model, which simulated Salish Sea hydrodynamics and water quality, did not include the capability of dynamically simulating sediment-water interactions. Instead, it used a simpler approach of specifying sediment fluxes which limited our ability to distinguish the effect of individual nutrient sources on sediment fluxes, and thus, on DO levels in the Salish Sea.

This study added the capability to dynamically simulate the sediment-water exchanges into the water quality dynamics of the model, through a process called *sediment diagenesis*. Material fluxes to the sediment from the water column fuel biogeochemical processes that release some of the nutrients back to the water column and consume oxygen in the process. We set up and tested the model code to ensure that sediment-water exchanges were incorporated appropriately.

We applied the revised water quality model to the Salish Sea and compared simulation results against monitoring data to assess the model skill, a process that required recalibration. The updated Salish Sea Model, including simulation of sediment diagenesis and fluxes of oxygen and nitrogen between the water and sediment, was re-calibrated to the observed data. The model skill with the new Sediment Diagenesis Module was comparable to the previous version of the model, with improvement in skill for simulating DO levels in the lower ranges. Model skill in predicting observed data is reasonable and acceptable.

The revised and recalibrated Salish Sea Model, which now includes sediment diagenesis, will be used in future studies to reevaluate the relative influence on DO of climate effects, local human nutrient sources, and the Pacific Ocean.

Acknowledgements

This project is funded wholly or in part by grants to the Washington State Department of Ecology from the United States Environmental Protection Agency (EPA), National Estuarine Program, under EPA grant agreements PC-00J20101 and PC00J89901, Catalog of Domestic Assistance Number 66.123, Puget Sound Action Agenda: Technical Investigations and Implementation Assistance Program. The contents of this document do not necessarily reflect the views and policies of EPA, nor does mention of trade names or commercial products constitute endorsement or recommendation for use.

The authors of this report thank the following people for their contributions to this study:

- Mindy Roberts (Washington Environmental Council) and Brandon Sackmann (Integral Consulting, Inc.) led the project while they were employed at the Department of Ecology. Mindy contributed to the *Introduction* and *Discussion* sections of this report. Brandon created Matlab scripts that were used to process model input and output data.
- The PNNL Institutional Computing (PIC) program at Pacific Northwest National Laboratory (PNNL) provided access to a High Performance Computing facility.
- The following scientists reviewed this report:
  - Ben Cope (EPA)
  - Will Hobbs, Tom Gries, and Dustin Bilhimer (Department of Ecology)

Introduction

Study Area and Surroundings

The Salish Sea refers to Puget Sound, the Strait of Georgia, and the Strait of Juan de Fuca (Figure 1). Pacific Ocean water enters the Salish Sea primarily through the Strait of Juan de Fuca, with a lesser exchange around the north end of Vancouver Island in Canada through Johnstone Strait. The marine water model domain (Figure 2) includes portions of the U.S. and Canada.

Freshwater enters the Salish Sea from rivers, streams, and other inflows, where they mix with the marine waters (Mohamedali et al., 2011). The Fraser River represents the largest single source of freshwater overall and much of the 4,200 m^3/s of Canadian freshwater inflow in 2006. The largest source of freshwater to Puget Sound is the Skagit River. U.S. watershed inflows totaled 1,500 m^3/s to Puget Sound and an additional 300 m^3/s to the Straits in 2006 with some inter-annual variability. These freshwater inflows deliver nitrogen, predominantly in nitrate form, to the estuarine environment.

In 2006, U.S. watersheds delivered 27,500 kg/d of dissolved inorganic nitrogen (DIN) to Puget Sound and an additional 7,300 kg/d to the Straits from the combined effect of natural and human sources. Canadian watersheds delivered 44,400 kg/d of DIN, dominated by the Fraser River with 33,500 kg/d. These include the combined effect of natural and human sources within the watersheds. Mackas and Harrison (1997) estimated the annual average net flux of oceanic nitrate as 400,000 to 600,000 kg/d at the Strait of Juan de Fuca, and 117,000 kg/d at Admiralty Inlet.

Wastewater treatment plants (WWTPs) also discharge nutrient-laden freshwater, including the nutrients carbon and nitrogen. Inventoried point sources discharging directly into marine waters deliver much less flow than the watersheds. U.S. marine point sources produce 20 m^3/s, and Canadian marine point sources produce about 16 m^3/s (Mohamedali et al., 2011). However, nitrogen is more concentrated in WWTP effluent and can be 10 to 30 mg/L of total nitrogen, nearly all of which is DIN. This results in nutrient loads from treated wastewater of 34,700 kg/d from U.S. WWTPs and 29,100 kg/d of DIN from Canadian WWTPs in 2006. Nearly all of the wastewater is from municipal wastewater; a small fraction is from industrial wastewater.

The ratio of WWTP and river DIN loads varies in different regions of Puget Sound and at different times of the year. Overall, river DIN loads are slightly greater than WWTP DIN loads on an average annual basis, while WWTP loads are slightly greater in the summer when stream flows are much lower. Point sources of DIN within the U.S. are almost three times greater than human nonpoint sources (Mohamedali et al., 2011).

The largest wastewater inputs serve the largest metropolitan areas. Five WWTPs serve the greater Vancouver, BC population of 2.2 million people and produced 25,800 kg/d of DIN in 2006. Two outfalls serve the Seattle metropolitan area with about 1.8 million people, delivering 19,500 kg/d of DIN in 2006.

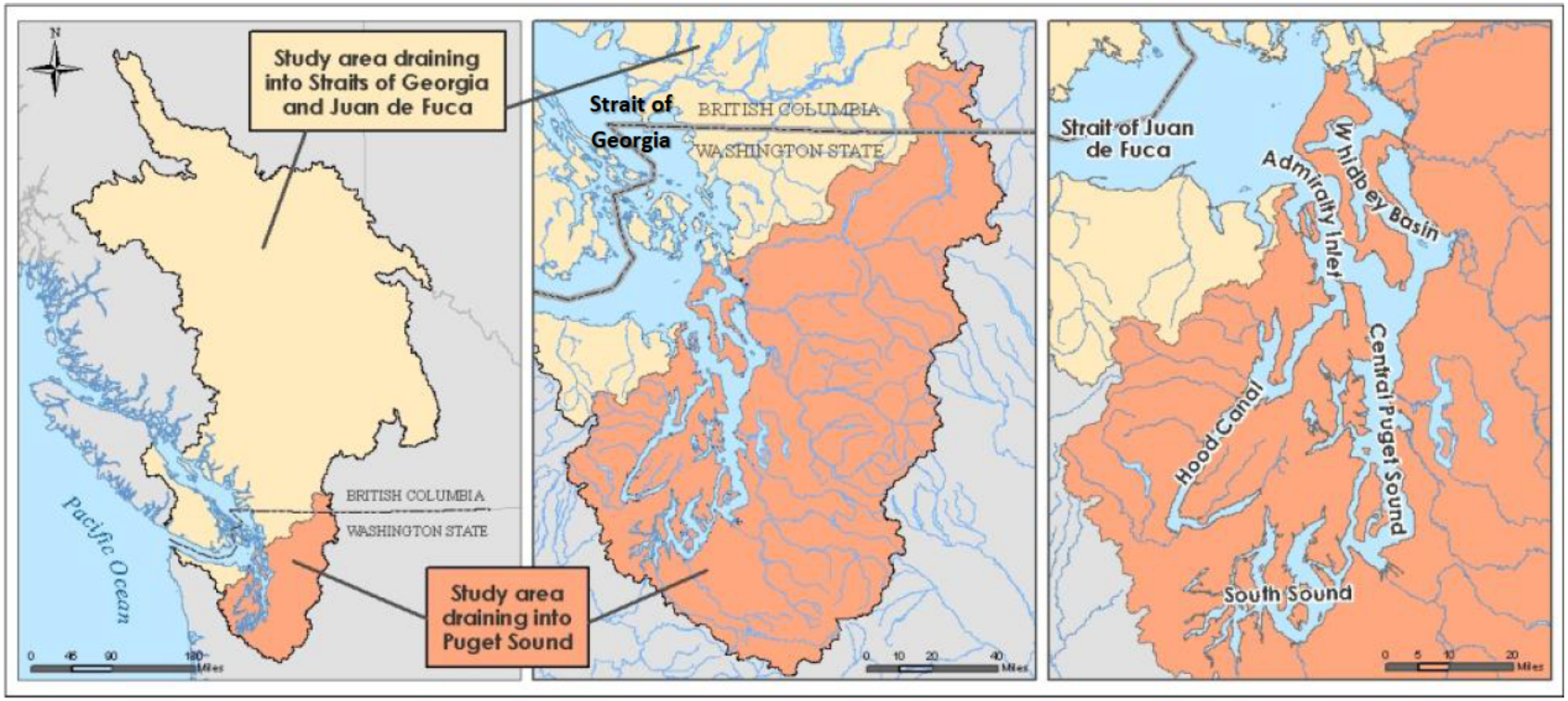

Figure 1. Salish Sea (Puget Sound, Strait of Georgia, Strait of Juan de Fuca) with land areas discharging to marine waters within the model domain.

Source: Long et al., 2014; Mohamedali et al., 2011.

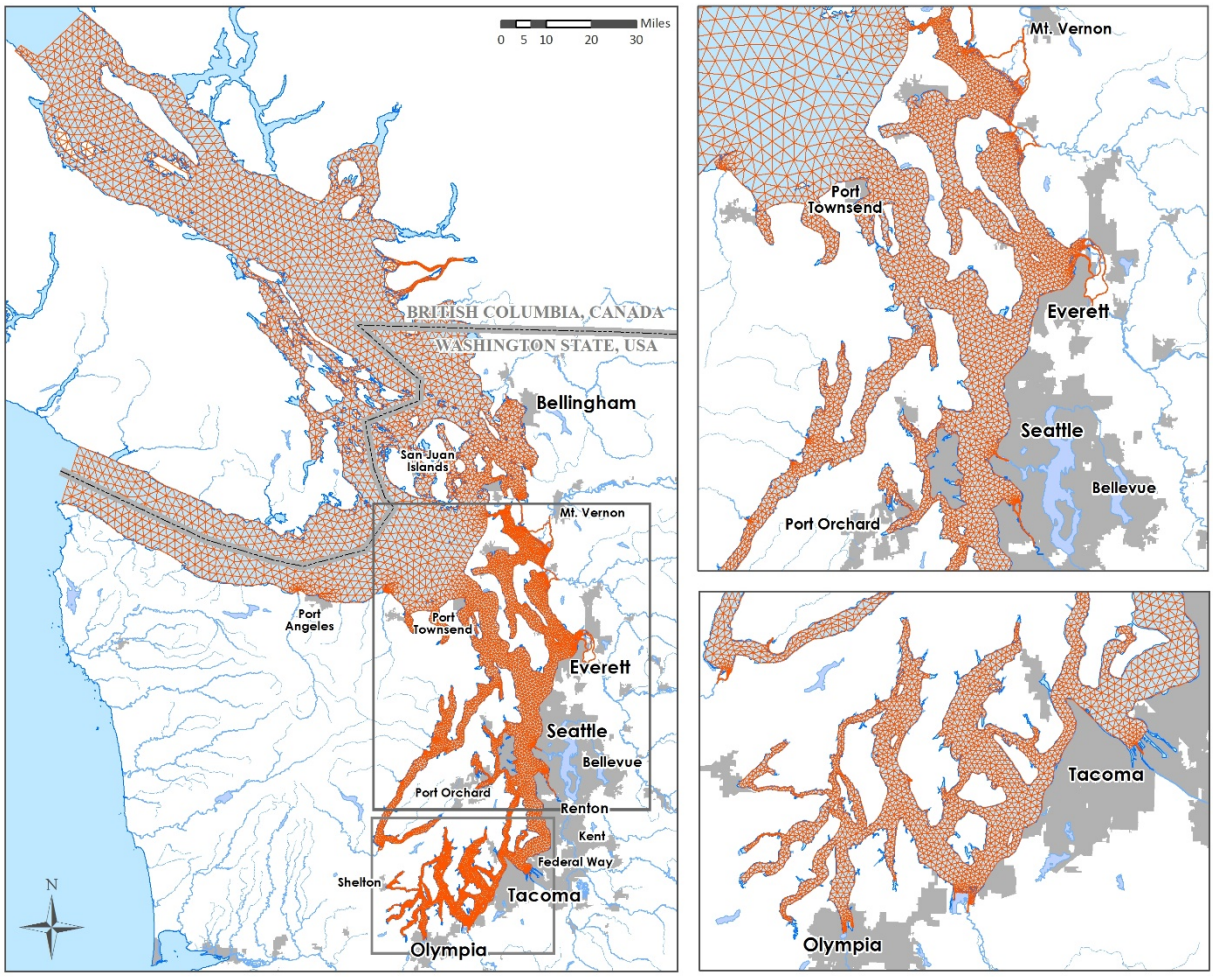

Figure 2. Salish Sea Model (SSM) computational grid.

Estuarine waters exhibit highly complex circulation patterns. These reflect the intricate horizontal shape of the Salish Sea as well as the bathymetry. Shallow sills occur at the entrances to various basins, including Hood Canal, Admiralty Inlet, and the Tacoma Narrows. Shallow water depths coupled with large tidal exchanges result in strong currents and vertical mixing. Stratification affects vertical mixing throughout the Salish Sea as well. The unstructured grid fits the model grid smoothly to the complex boundaries of Salish Sea shoreline (Yang et al., 2010).

History of study area

Sackmann (2009) detailed the history of the study area. In summary, low dissolved oxygen (DO) has been measured in several locations within the Salish Sea. A fundamental question is whether human contributions are responsible for, or contributing to, declines in oxygen levels. This project enhances the capability of the model for future work to address this question.

Banas et al. (2015) conducted a particle-based analysis of the circulatory patterns within the Salish Sea to map the area of influence of rivers and their nutrient loadings. The Salish Sea Model (referred to in past reports as the Puget Sound Dissolved Oxygen Model, as well as the

Puget Sound/Georgia Basin model) was jointly developed by Ecology/PNNL. This modeling effort provides additional insights into the relative nutrient loading contributions and impacts of local sources, the Pacific Ocean, and changing climate.

The time line of studies and reports related to this model to date is outlined below:

Year	Studies	Reference
2009	Quality Assurance Project Plan for Puget Sound Dissolved Oxygen Modeling Study	Sackmann (2009)
2010	Development of hydrodynamic model of the Salish Sea	Yang et al. (2010)
2011	Development of nutrient loading estimates from point and nonpoint sources into the Salish Sea	Mohamedali et al. (2011), Khangaonkar et al. (2011)
2012	Development of water quality model of the Salish Sea	Khangaonkar et al. (2012a,b)
2014	Scenarios Report: Application of Salish Sea dissolved oxygen model to current and future scenario	Roberts et al. (2014)
2017	Addition of Sediment Diagenesis Module to the Salish Sea Model	This report
2017	Addition of Ocean Acidification Module to the Salish Sea Model	Pelletier et al. (2017)

Parameters of concern

Dissolved oxygen (DO) is the primary parameter of concern, and it is important in the biogeochemical cycling of carbon and nitrogen. Nutrients from local natural and human sources, the Pacific Ocean, and atmospheric sources stimulate phytoplankton growth, producing organic matter containing carbon and nitrogen. As a fraction of the phytoplankton die and sink to the bottom, oxygen is consumed during oxidation of the decomposing organic matter, and some of the organic nitrogen is re-mineralized and released back into the water. Therefore, nitrogen and carbon contributions to organic matter processing are the primary contaminants of concern. Circulation patterns that tend to increase water residence times (Ahmed et al., 2017) exacerbate DO depletion.

Results of previous studies

Pacific Northwest National Laboratory (PNNL), in collaboration with Ecology, developed a predictive ocean-modeling tool for coastal estuarine research, restoration planning, water-quality management, and assessment of response to future conditions (Khangaonkar et al., 2011, 2012a,b) for the Salish Sea. The Salish Sea Model (SSM) was developed using an unstructured grid framework specifically to function efficiently in a region dominated by the complex shorelines and fjord-like features (Figure 2). The model simulates hydrodynamics (tides, salinity, temperature) and water quality (biogeochemical variables such as algal biomass, nutrients, carbon, DO, and pH) including annual biogeochemical cycles.

In 2014, Ecology completed an analysis of the relative influences of human nutrient sources and Pacific Ocean influences on DO concentrations in the Salish Sea. This analysis involved

applying the model to a series of scenarios to isolate the influence on DO of different sources, both now and into the future (Roberts et al., 2014). Results indicated that human nitrogen contributions from the U.S. and Canada have the greatest impacts on DO in South and Central Puget Sound. Marine point sources cause greater decreases in DO than watershed inflows compared with reference conditions (also referred to as natural conditions in previous Ecology publications related to this work).

Separately, Ecology developed a different three-dimensional circulation and water quality model of South and Central Puget Sound with an external boundary at Edmonds. The calibrated model was applied to a series of scenarios to isolate the effects of different sources, including local human nutrient sources (Ahmed et al., 2014). We used the SSM to assess the change in water quality at the Edmonds boundary that would result from eliminating human sources in the Salish Sea under natural conditions. The relationship was then used to adjust the boundary condition at Edmonds to account for different external load scenarios. To assess sediment-water exchanges under different load scenarios, we calculated scalars (scaling factors) from a mass balance of external loads to the region south of Whidbey Island where the majority of the U.S. human sources originate. However, these scalars reflected total loads of nitrogen and were not specific to an individual source. We applied the sediment scalars to the entire region and were unable to develop spatially heterogeneous sediment fluxes.

Very little is known about sediment fluxes in Puget Sound (Sheibley and Paulson, 2014) due to limited observations. Most available information focuses on shallow regions of Puget Sound in the late summer, but those express a wide range of magnitudes. The Budd Inlet Scientific Study (Aura Nova Consultants et al., 1998) provided the most complete year-round assessment of fluxes. The study found that fluxes generally peak in the late summer months but display high variability.

Both of the efforts detailed above involved the use of the SSM which was previously calibrated by specifying constant sediment-water exchanges of nitrogen and oxygen (Khangaonkar et al., 2012a,b). The modeling team recognized that dynamic computations of the fluxes would result in a more robust representation of the biochemical processes, as described below.

Project Description

Prior to this study, the SSM externally specified the sediment fluxes of nitrogen and oxygen (Khangaonkar et al., 2012a,b). These were linearly scaled in proportion to DIN loading from watershed inflows, marine point sources, and atmospheric deposition (Roberts et al., 2014) to account for changes in external nutrient loading while evaluating alternative natural, current, and future loads (Roberts et al., 2014). Higher loads would cause additional phytoplankton growth, higher particulate deposition to the sediments, and higher exchanges of nitrogen and oxygen.

Roberts et al. (2014) recommended adding the capability to dynamically simulate sediment-water exchanges to the SSM via incorporation of a Sediment Diagenesis Module. This report describes the integration of sediment process algorithms into the model so that calculations occur dynamically in response to changing loads and hydrodynamic conditions. This revised version of the model will next be applied to scenarios in ongoing modeling studies.

Sediment diagenesis

Sediment diagenesis is the process where biogeochemical processes transform the nutrients delivered to the sediments from particles settling from the water column and release a portion of the nutrients back into the water column (Figure 3). The process also consumes oxygen. A portion of the nutrients are buried as well, where they are permanently lost from the active system.

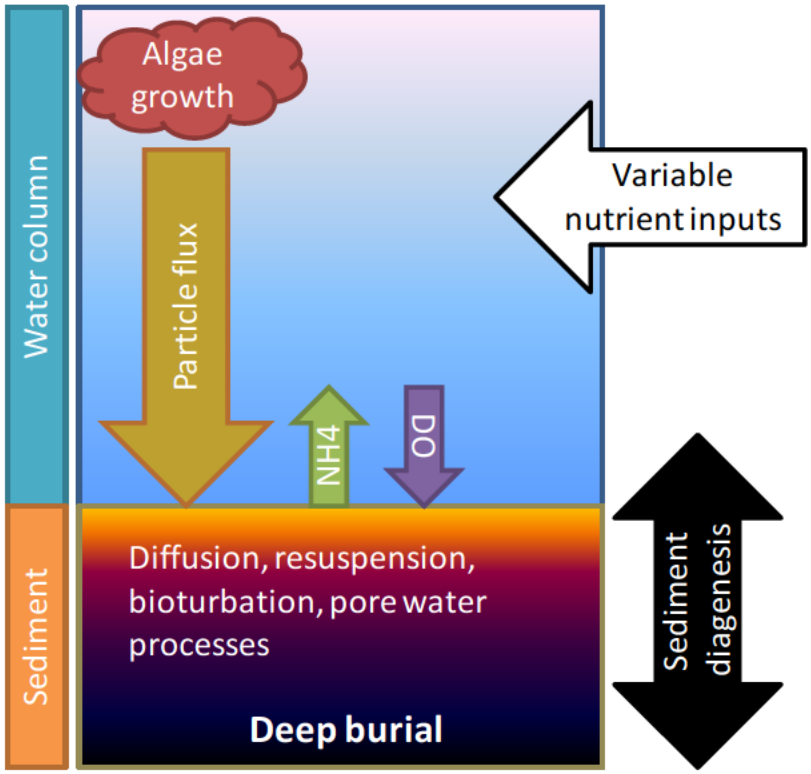

Figure 3. Sediment diagenesis schematic.

The Pacific Ocean, natural sources, and human activities are sources of nutrients to the Salish Sea. Nutrients that reach the euphotic zone, where there is sufficient light, spur phytoplankton growth. These nutrients include a combination of inputs from rivers, atmospheric deposition, and the surface waters of incoming tides, as well as deeper sources of nutrients from deep discharges and the bottom waters of incoming tides that are mixed up into the water column. This vertical mixing is especially important across shallow sills, such as the Tacoma Narrows and Admiralty Inlet. These processes can also mix deeper nutrients into surface waters.

As the algae bloom, they transform dissolved material into particulate matter. As the algae die, a fraction settles to the bottom. Zooplankton that feed on the algae also produce wastes that settle to the bottom as a flux of particles. These combined fluxes fuel processes within the sediments.

A variety of physical and biogeochemical processes act on the organic matter in the sediments. Microbes decompose the organic matter in the sediment which consumes oxygen. Plants and animals physically rework the sediments in a process known as bioturbation. Decomposition and

oxidation of organic matter transforms nutrients and release them back to the water column. Sediment oxygen levels decline from bottom water concentrations to near zero within a few millimeters to centimeters of the water surface, which produces strong gradients. These gradients contribute to diffusion into the sediments as oxygen is used to fuel decomposition of organic matter. This exerts a sediment oxygen demand (SOD) on the water column. The decomposition of organic nitrogen generates ammonium and also creates a gradient that pushes ammonium out of the sediments and into the water column.

Project goals

The overall modeling goal is to improve the performance of the SSM by incorporating sediment diagenesis to better identify and quantify factors and processes that influence DO. In addition to developing and implementing the code changes needed to simulate this process, this project also extensively tested the revised code to verify the correct model connections and behavior under idealized conditions. The revised model was then applied to the calibration period. This report does not include re-evaluating the scenarios previously completed or running new scenarios.

Project objectives

The project objectives were to:

- Successfully integrate a Sediment Diagenesis Module with the SSM.
- Evaluate the overall performance of the upgraded model.
- Improve the model's ability to: assess oxygen levels under natural conditions including the influences of sediments, distinguish relative impacts of current sources, and project future oxygen conditions that reflect sediment processes.

Project tasks

This project included several tasks:

- Implement software changes to connect sediment-water interactions to model code.
- Test software changes on idealized systems with analytical solutions.
- Apply updated code to Salish Sea system and confirm against monitoring data.
- Recalibrate the model for DO and other relevant water quality parameters.
- Document findings.

Methods

Model Selection

Sackmann et al. (2009) describes the model selection, approach for the set up, and application of the Salish Sea circulation and DO model. We considered several needs in the initial model selection, including the ability to simulate:

- Complex horizontal shapes, including branching basins and inlets.
- Highly variable bathymetry, with deep basins >200 meters, shallow inlets <20 meters, and shallow sills that divide the region into basins.
- Large tidal amplitudes that produce very high velocities in constricted regions.
- Regions that are dry at low tide but that contribute to biogeochemical processes.
- Time-varying river inputs and human sources.
- Physical, chemical, and biological processes that affect DO.

We selected the Finite-Volume Coastal Ocean Model (FVCOM; Chen et al., 2003) to simulate three-dimensional circulation in the Salish Sea using an unstructured grid. FVCOM can simulate wetting and drying and uses a sigma grid system where the vertical layer thickness changes to simulate sea surface height. PNNL developed the linked FVCOM-ICM (Integrated Compartment Model) based on the kinetic equations of CE-QUAL-ICM (Cerco and Cole, 1995). Yang et al. (2010) and Khangaonkar et al. (2011) describe the circulation calibration, and Khangaonkar et al. (2012a,b) describes the water quality model calibration.

Several modeling efforts have included sediment diagenesis in freshwater or marine environments. Frameworks considered for the sediment diagenesis component include Di Toro et al. (1990), Martin and Wool (2013), and Morse and Eldridge (2007).

Sediment flux models (SFMs) range from simple empirical relationships (Fennel et al., 2006) to complex process simulations with time-varying state variables (Boudreau, 1997). Simple representations include assigning constant fluxes of SOD or nutrients (Scully, 2010) or using simple relationships with overlying water concentrations (Imteaz and Asaeda, 2000; Fennel et al., 2006; Hetland and DiMarco, 2008). More complex models may simulate one or two layers, each representing a particular chemical environment (Di Toro, 2001; Emerson et al., 1984; Gypens et al., 2008; Slomp et al., 1998; Vanderborght et al., 1977). SFMs may also be resolved into numerous layers (Morse and Eldridge, 2007; Boudreau, 1997; Dhakar and Burdige, 1996; Cai et al., 2010). Multi-layer models have been found to fit observations better than two-layer models with some data sets (Wilson et al., 2013). However, depth resolution entails higher computational demand (Gypens et al., 2008) than two-layer models. Therefore two-layer models are often used as a compromise between computational efficiency and depth-resolution, while providing acceptable accuracy (Testa et al., 2013; Brady et al., 2013).

Di Toro et al. (1990 and 2001) developed a model of SOD that has gained wide adoption in estuarine modeling frameworks such as those of Cerco and Cole (1995), Chapra (1997), and Martin and Wool (2013). Di Toro's approach (Di Toro, 2001) calculates SOD and the release of nitrogen and phosphorus as functions of the downward flux of carbon, nitrogen, and phosphorus from the water column. This approach, well founded in diagenetic theory and supported by field and laboratory measurements, was an important advancement in the field of sediment-water interactions.

Water Analysis Simulation Program (WASP) incorporates a Sediment Diagenesis Module (Martin and Wool, 2013) and uses the two-layer methods of Di Toro (2001). WASP is one of the most widely used water quality models in the U.S. and throughout the world. Because of the model's capabilities of handling multiple pollutant types, it has been widely applied in the development of Total Maximum Daily Loads (TMDLs).

We selected the WASP sediment diagenesis routines because they (1) have been found to provide an acceptable level of complexity with sufficient accuracy, (2) are well documented, (3) have been applied to a wide range of freshwater and marine water systems, and (4) are broadly vetted by the modeling community. These routines also represent a compromise between computational efficiency and depth-resolution, while providing acceptable accuracy.

Model Theory

Sediment Diagenesis Module (SDM) overview

The SDM is based on the well-documented WASP modeling framework developed by EPA (Martin and Wool 2013).

The structure for the SDM integrates four processes illustrated in Figure 4:

1. Deposition of particulate organic carbon (C) and nitrogen (N), collectively referred to as particulate organic matter (POM), from the water column into the sediment. (Phosphorus and silicate were not included because they are not simulated in the present version of the SSM). This includes all forms of POM from phytoplankton and detritus.
2. Decomposition of POM in the sediment, producing dissolved forms of C and N in the sediment pore water. The process of decomposition of POM is called diagenesis.
3. The solutes formed by diagenesis react and are (1) transported between a thin aerobic layer at the surface of the sediment and a thicker anaerobic layer below the aerobic layer, or (2) released as gases (methane and nitrogen gas).
4. Solute forms of C and N are returned to the overlying water, and DO from the overlying water is transferred from the overlying water into the sediment to supply the oxidation of solutes (dissolved organic C and ammonium) in the aerobic sediment layer.

The SDM numerically integrates the mass balance equations for chemical constituents in two layers of sediment (Figure 4):

- Layer 1: A relatively thin aerobic layer at the sediment water interface with variable thickness that is dynamically calculated.
- Layer 2: A thicker anaerobic layer with thickness equal to the total sediment depth of 10 cm[1] (Di Toro, 2001) minus the depth of the aerobic layer.

POM initially decomposes rapidly in the sediments, but then slows down as the more labile fraction is consumed (Burdige, 2007). In order to capture this process, the settled POM is fractioned to one of three "G classes" based on overall reactivity (Figure 1 in Di Toro, 2001). The three G classes represent a relatively rapidly decomposing labile class (G1), a more refractory form (G2), and a relatively inert form (G3). The decomposition of the three G classes of POM occurs in layer 2. These and other parameter values were selected based on published values in Di Toro's (2001) Table 15.5. More recent published values by Testa et al. (2013) and others were also used for guidance to constrain parameter values.

The mass balance equations are solved for the concentration at the present time step during the numerical integration using information from the previous time step and the new deposition of POM during the present time step. Once the concentrations at the present time step are computed, the diagenesis source terms for reactions and transfers are computed. Diagenesis source terms are computed for C and N from the sum of the product of the chemical-specific reaction velocities and computed concentrations in each of the three G classes.

[1] Di Toro (2001) identifies the bioturbation depth as the depth of the active layer because that is the depth to which sediment solids are mixed, leading to greater homogeneity in this region. Boudreau (1994) found that the worldwide mean from 200 cores in estuarine and marine sediment had bioturbation zone thickness of 9.8 +/- 4.5 cm. Carpenter et al. (1985) found that the thickness of the bioturbated upper layers in sediment cores from the main basin ranged from about 4 to 18 cm. Lavelle et al. (1986) reported that the bioturbated upper layers in Puget Sound ranged from about 5 to 40 cm. The median thickness of the upper bioturbated layer of sediment from 63 cores in these two studies was 12 cm with inter-quartile range of 10 to 30 cm.

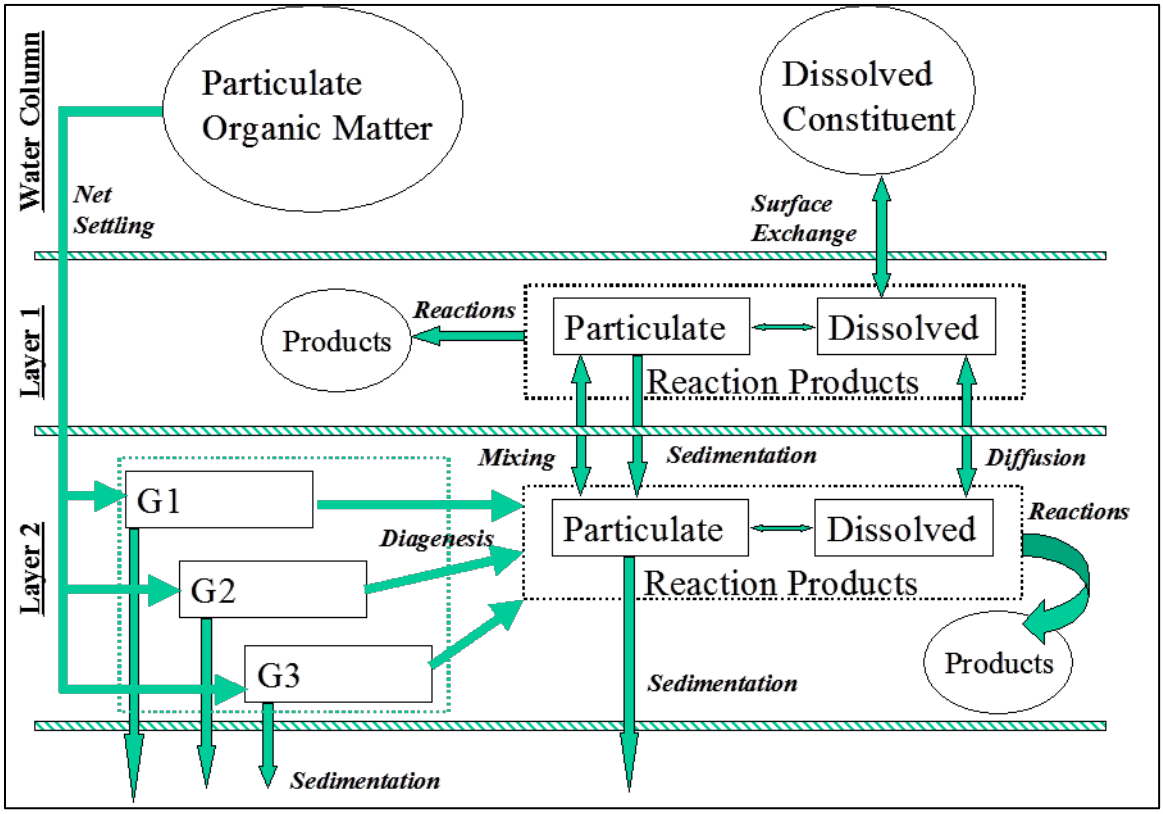

Figure 4. Basic structure of the Sediment Diagenesis Module (SDM).
(Martin and Wool, 2013)

Once the sediment POM (C and N) concentrations and source terms are computed for the present time step, the reactions and transfers are computed. Concentrations of ammonia, nitrates, methane, and sulfide in sediment layers are computed and then used to compute fluxes to the overlying water column, including SOD from the water by the sediments. The total chemical (C, N) concentrations are computed from mass balance relationships for each of the two sediment layers. The equations are conveniently solved for the new concentrations using a matrix solution stepwise procedure described in Appendix A.

There are two choices for estimating the initial conditions of concentrations of constituents in the sediment layers:

- Option 1: The initial conditions may be specified by the user as an input to the SDM. Specified initial conditions would ideally be derived from field measurements of POM subdivided into G classes. In practice, the lack of field data and/or accepted analytical procedures from fractionating G classes makes this difficult.
- Option 2: The SDM can compute the initial conditions assuming the sediment is at steady-state (Appendix A) with the initial depositional fluxes of POM to the sediment layer (based on initial settling fluxes).

Option 2 is the method that was selected for this application of the SDM in the Salish Sea.

A detailed description of the model theory and all of the equations in the SDM are provided in Appendix A, excerpted from Martin and Wool (2013). Major assumptions related to the new diagenesis element of the SSM can be found in Martin and Wool (2013) and Di Toro (2001).

Input arguments from FVCOM-ICM to the SDM subroutine for each time step during the numerical integration in FVCOM-ICM include the following:

- SStateIC = 1 for using steady state solution based on overlying water column concentration and fluxes for initializing the first time step; SStateIC = 0 for reading initial sediment state variables from input or continuous time-variable simulation.
- DLTS = calculation time step (days) used for time variable model (if SStateIC = 0)
- Jcin = flux to sediments from settling organic carbon from phytoplankton and detritus in oxygen equivalent units (g-O_2/m^2/d) (NOTE: g-O_2/m^2/d = g-C/m^2/d * 2.67 g-O_2/g-C)
- Jnin = nitrogen flux in settling phytoplankton and detritus (g-N/m^2/d)
- Jpin = phosphorus flux in settling phytoplankton and detritus (g-P/m^2/d)
- Jsin = silicate flux in settling phytoplankton and detritus (g-Si/m^2/d)
- O20 = dissolved oxygen in water overlying the sediment (mg-O_2/L)
- depth = total water depth overlying the sediment (m) (used to calculate methane saturation concentration at in situ pressure)
- Tw = temperature in water overlying the sediment (deg C)
- NH30 = ammonia N in water overlying the sediment (mg-N/L)
- NO30 = nitrate N in water overlying the sediment (mg-N/L)
- PO40 = phosphate P in water overlying the sediment (mg-P/L)
- CH40 = overlying water column methane concentration (gO2/m3) (assumed zero, for water column model did not include methane as state variable)
- SALw = salinity in the water overlying the sediment (ppt)

Outputs from the SDM to FVCOM-ICM during each time step are the following:

- Output sediment concentrations – For time-variable model: these are inputs at the beginning of time step and outputs at the end of the time step (values are initialized on the first calculation step using the steady-state model).
  - NH42 = sediment dissolved ammonia concentration in layer 2 (mg-N/L)
  - NH41 = sediment dissolved ammonia concentration in layer 1 (mg-N/L)
  - NO32 = sediment dissolved nitrate concentration in layer 2 (mg-N/L)
  - NO31 = sediment dissolved nitrate concentration in layer 1 (mg-N/L)
  - PO42 = sediment dissolved phosphate concentration in layer 2 (mg-P/L)
  - PO41 = sediment dissolved phosphate concentration in layer 1 (mg-P/L)

- SI2 = sediment dissolved silicate concentration in layer 2 (mg-Si/L)
- CH42 = dissolved methane concentration in layer 2 (mgO2/L)
- HS2 = dissolved hydrogen sulfide concentration in layer 2 (mgO2/L)
- POC1 = G1 particulate organic carbon in layer 2 (mgO2/L)
- POC2 = G2 particulate organic carbon in layer 2 (mgO2/L)
- POC3 = G3 particulate organic carbon in layer 2 (mgO2/L)
- PON1 = G1 particulate organic nitrogen in layer 2 (mg-N/L)
- PON2 = G2 particulate organic nitrogen in layer 2 (mg-N/L)
- PON3 = G3 particulate organic nitrogen in layer 2 (mg-N/L)
- POP1 = G1 particulate organic phosphorus in layer 2 (mg-N/L)
- POP2 = G2 particulate organic phosphorus in layer 2 (mg-N/L)
- POP3 = G3 particulate organic phosphorus in layer 2 (mg-N/L)
- PSISED = particulate biogenic silicate in sediment layer 2 (mg-Si/L)
- BENSTR = accumulated benthic stress on organisms living in the aerobic sediment layer due to low dissolved O_2 (dimensionless)

- Output sediment/water fluxes and layer 1 thickness – Steady-state and time-variable models:
  - JPOC = total particulate organic carbon flux into sediments from water column (gO2/ m^2/day)
  - JPON = total particulate organic nitrogen flux into sediments from water column (gN/ m^2/day)
  - JPOP = total particulate organic phosphorus flux into sediments from water column (gP/ m^2/day)
  - JPOS = total particulate organic silicate flux into sediments from water column (gSi/ m^2/day)
  - SOD = sediment oxygen demand (gO2/ m^2/day)
  - JNO3 = sediment to water column nitrate flux (gN/ m^2/day)
  - JNH4 = sediment to water column ammonia flux (gN/ m^2/day)
  - JCH4 = sediment to water column dissolved methane flux (gO2/ m^2/day)
  - JCH4g = sediment to water column gas-phase methane flux (gO2/ m^2/day)
  - JHS = sediment to water column hydrogen sulfide flux (gO2/ m^2/day)
  - JSI = sediment to water column silicate flux (gSi/ m^2/day)
  - H1 = thickness of the aerobic sediment layer (cm) (typically 1 cm to 10 cm)

Derivatives for the following existing state variables in the FVCOM-ICM model were modified to include the source/sink terms for exchanges between the bottom layer of the water column and the sediment:

- Phytoplankton groups (sinking loss from water column and source of Jcin, Jnin, and Jpin to sediment)
- Particulate organic C (sinking loss from water column and source of Jcin to sediment)
- Particulate organic N (sinking loss from water column and source of Jnin to sediment)
- Particulate organic P (sinking loss from water column and source of Jpin to sediment)
- Dissolved oxygen (loss from water column for SOD)
- Ammonium (gain to water column from sediment flux)
- Nitrate+nitrite (loss/gain from water column from sediment flux)
- Phosphate (loss/gain from water column from sediment flux)
- Fast reacting DOC/CBOD (gain/loss from water column from sediment flux)

Links between FVCOM-ICM and the SDM are described in Appendix A. The following implementation/modification steps were completed:

Modularization of current code - Sediment diagenesis fluxes are connected with overlying water settling POM. A clean separation of these modules is important for stepwise testing purposes and better code management.

Input and output control - The CE-QUAL-ICM format of inputs and outputs were retained for the most part. We incorporated a new option to read the SDM control variables using a simplified FORTRAN name list method. The inputs include the following:

- Geometry, time step
- Reaction rates and temperature control
- Mixing rates, diffusion rates, settling rates
- Fractions of G1,G2,G3, partitioning coefficients
- Flags for various scenarios (steady state vs. time-dependent)
- Initial conditions for time-dependent simulation
- Output frequency and variable selection (station time-series, history)

Coupling with other components of the model - The fluxes are connected to the water column. In this step, we ensure that data transfer between these different modules are clearly defined and well organized with switches to turn on or off each connection. The focus was on coupling SDM with the water column eutrophication model in this project. The code was designed to ensure that submerged aquatic vegetation **(**SAV), benthic algae, suspension feeder, and deposition feeder modules may be added in the future.

Parallelization - The FVCOM-ICM code was improved for parallelized operation by PNNL. Parallelization is needed for the master processor to distribute and collect information on model inputs and outputs to allow faster runs through the use of multiple processors. Once the SDM code was incorporated into FVCOM-ICM, the code with SDM was parallelized.

Processes and parameters considered but not included

We also considered several processes and parameters but did not implement them at this time. These include:

Submerged aquatic vegetation (SAV) – While the ICM code has considered these, we do not have spatial information on the biomass of SAV around the Salish Sea. We also lack rate process information governing interactions between SAV and water quality. We anticipate that while this could be locally important in regions with extensive eelgrass areas such as Padilla Bay, we do not know if SAV significantly affects sediment diagenesis or DO throughout the system.

Shellfish – While the ICM code has considered shellfish, we lack fundamental information on shellfish interactions with water quality such as standing stock and rate processes governing native species (Konrad, 2014). More information is available on the Pacific oyster as a commercially valuable species, but this information may not be applicable to native shellfish populations. We anticipate shellfish may be locally important in regions with extensive shellfish biomass.

Phosphorus – ICM includes the capability of simulating soluble reactive phosphorus but does not currently include organic phosphorus. Calibration of phosphorus was not pursued at this stage because significant resources would be needed to calibrate this state variable and we do not anticipate that phosphorus significantly limits primary productivity within the model domain.

Silica – ICM includes the capability of simulating silica, but this capability has not been implemented or calibrated. Calibration of silica was not pursued at this stage because significant resources would be needed to calibrate this state variable and we do not anticipate that silica significantly limits primary productivity (e.g., Mauger et al., 2015). Silica may be locally important but is not likely a major influence throughout the system.

Model Development and Testing

Sackmann et al. (2009) described the objectives of the original DO model study and the procedures for model development and testing, including both the circulation and water quality model components. Information includes ocean boundary conditions, meteorology, river inputs, marine discharges from WWTPs, and marine profiles and time-series for model skill assessment. Khangaonkar et al. (2012a,b) and Roberts et al. (2014) describe the final information used to calibrate the linked models and to apply the tools to several current and future water quality scenarios. Roberts et al. (2014) describes the method used to adjust sediment fluxes to account for changes in external loading prior to interactively computed fluxes through sediment diagenesis in the SDM.

The SDM developed for the EPA WASP model has previously undergone rigorous review and testing (Martin, 2002). Professor James Martin at Mississippi State University developed a stand-alone testing tool called SED_JLM.FOR that provides identical results compared with the WASP SFM. Ecology, in collaboration with Dr. Martin, also developed an Excel VBA version of the SDM called 'SedFlux.xlsm' that predicts nearly identical results (same within ±0.001%) compared with the SED_JLM.FOR (Ecology, 2013). Appendix B presents a comparison of results of Ecology's SedFlux.xlsm with Martin's SED_JLM.FOR testing tool.

Implementation and testing of the SDM into the FVCOM-ICM model of the Salish Sea was conducted in the following steps:

1. A Fortran version of the SDM code was first developed for testing and implementation into FVCOM-ICM. The code was based on the SDM from CE-QUAL-ICM modified for equivalency with WASP SFM and SedFlux.xlsm.
2. The results of this SDM subroutine were compared with SedFlux.xlsm for hypothetical conditions for a single model cell under the following tests:
    a. Steady-state solution of constant deposition of POM and constant overlying water quality.
    b. Time-variable solution using assumed initial conditions for G classes of POM and assumed constant deposition of POM and constant overlying water quality.
    c. Time-variable solution using assumed initial conditions for G classes of POM and assumed time-variable deposition of POM and time-variable overlying water quality.
    d. Time-variable solution using initial conditions computed assuming steady state with assumed constant deposition of POM and constant overlying water quality.
    e. Time-variable solution using initial conditions computed assuming steady state with assumed time-variable deposition of POM and time-variable overlying water quality.
3. Once step 2 was completed, we linked the SDM subroutine with the FVCOM-ICM model of the Salish Sea. The results of the linked model for a one-year simulation of existing conditions during 2006 were compared with SedFlux.xlsm at a location in the model domain.

Results of the testing steps described above are summarized in Appendix C. The median relative percent differences (RPDs) comparing FVCOM-ICM-SDM with Ecology's SedFlux.xlsm were within +/- 0.1% and considered to be acceptable.

Results

Model Procedure and Calibration

We used 2006 during the integration of the SDM for consistency with the previous calibration of the SSM DO model. Measurements collected in 2006 include salinity, temperature, nutrients, phytoplankton, and DO. Unfortunately, sediment flux data are not available for 2006. Sediment flux data are relatively sparse, and methodologies used to collect these data have inherent limitations.

In general, 2006 late-summer DO levels represented somewhat average conditions over the past 10 years (Krembs, 2011). Examination of data from winters of 2005 and 2006 showed that the water column was relatively homogeneous and fully mixed. At first, data from the Puget Sound Main Basin station PSB003 from 2005 were used to initialize the model throughout the domain. Nutrients (inorganic N and P), chlorophyll-a (converted to carbon using a carbon-to-chlorophyll-a ratio of 50 per Appendix E model calibration parameters), and DO specified as initial conditions are listed in Khangaonkar et al. (2012). Due to limited availability of data, initial conditions for the remaining constituents were set to zero.

For simplicity, uniform initial conditions were chosen. This approach assumes that, during the winter, biological activity is low and, by the time spring bloom occurs, the remaining constituents are internally updated via boundary fluxes and transformation from the other pools. Results at the end of one year were treated as preconditioning spin-up and were then used to re-initialize the model. The simulation for 2006 was then repeated for second year. The results of the second year were then used as the predicted conditions for 2006.

A detailed description of the procedure for running the hydrodynamics and water quality models is as follows:

- **Hydrodynamics (FVCOM)**
  1. First, a cold start hydrodynamic model run for a year was completed assuming a constant domain-wide initial condition for temperature, salinity, and currents. At the end of the year, a restart file for domain-wide conditions for temperature, salinity, and currents was saved. The output from this model run was saved at 20-second intervals in netcdf format. This was named cold-start-hydrodynamics-yr1.
  2. Second, a hot start hydrodynamic model run for a year was completed using the restart file (generated in step 1) for initial conditions. The output from this model run was also saved at 20-second interval in netcdf format. This was named hot-start-hydrodynamics-yr2.
- **Water Quality (FVCOM-ICM)**
  3. First, a cold start water quality model run for a year was completed assuming constant domain-wide uniform concentrations for water quality constituents with linkage to the cold-start-hydrodynamics-yr1. At the end of the model run, a restart file was saved that contained domain-wide variable concentrations for water quality constituents.

4. Second, a hot start water quality run for a year was completed using the water quality restart file (generated in step 3 above) for initial water quality conditions and linkage to hot-start-hydrodynamics-yr2.

A water quality netcdf file was created from the output of second year of the ICM model run (hot start run in step 4 above) for post processing of output data.

Initial values for model calibration parameters were set to the same values as the previous model version (Khangaonkar et al., 2012). Parameter values for the additional rates and constants for the new SDM were set to default values recommended by DiToro (2001) and Testa et al. (2013).

The most significant parameter adjustment for re-calibration of the water quality model was an iterative procedure that was used to re-calibrate the model by trial of different values for the WSSNET model parameter in the ICM module. The WSSNET parameter is the settling velocity of suspended particles from the bottom layer of the model grid into the sediment (Cerco and Cole, 1995). Decreasing the value of WSLNET and WSRNET, which are net settling velocities of the labile and refractory particulate organic matter (POM) to the sediments, has the effect of maintaining higher concentrations of suspended particles in the water column. The previous calibration of the model assumed net settling rates of 5 m/d. Recalibration of the current version adjusted the value of WSLNET and WSRNET to 2 m/d by trial to improve model skill. The settling velocities used in the SSM are generally within the range of the literature (e.g., EPA, 1985).

Graphical comparisons of predicted and observed water quality variables at all of the sentinel stations described by Khangaonkar et al. (2012b) are presented in Appendix D.

The final values selected for each of the kinetics rates and constants parameters of the water quality model are presented in Appendix E.

Model skill compared with the previous version of the model

A comparison of the model-predicted concentrations of water quality variables with observed data is presented in Figure 5 for the previous calibration of the model (old version, without sediment diagenesis) compared with the current re-calibrated model from this study (new version, with sediment diagenesis). The root mean squared error (RMSE) for the new version was considered to be acceptable. The RMSE in the new version for DO, nitrate (NO3), temperature, and chlorophyll-a (Chl) is marginally higher but still acceptable compared with the old version. Visual comparisons of scatter plots showed that model skill for DO and other variables with increased RMSE were as good as, or better than, the old version (Figure 5). For example, the RMSE for DO increased from 1.26 mg/l in the old version to 1.37 mg/l in the new version, but the scatter plot for DO shows that the new version of the model calibration improved the model skill at low DO (Figure 5).

A comparison of the time-series of model-predicted concentrations of DO, Chl, NO3, and ammonia (NH4) for the surface and bottom layers at the selected stations (described by Khangaonkar et al., 2012b) with observed data is presented in Figures 6, 7, 8, and 9 for the previous calibration of the model (old version) compared with the current re-calibrated model

from this study (new version). In general, the new version of the calibration performed as well as the old version in terms of representation of seasonal patterns.

In some cases, the new version performed better than the old version (e.g., bottom DO in Saratoga Passage at station SAR003 and Hood Canal HCB010). In other cases. the new version did not perform as well as the old version but still reproduced seasonal patterns of low DO fairly well (e.g., Commencement Bay station CMB003).

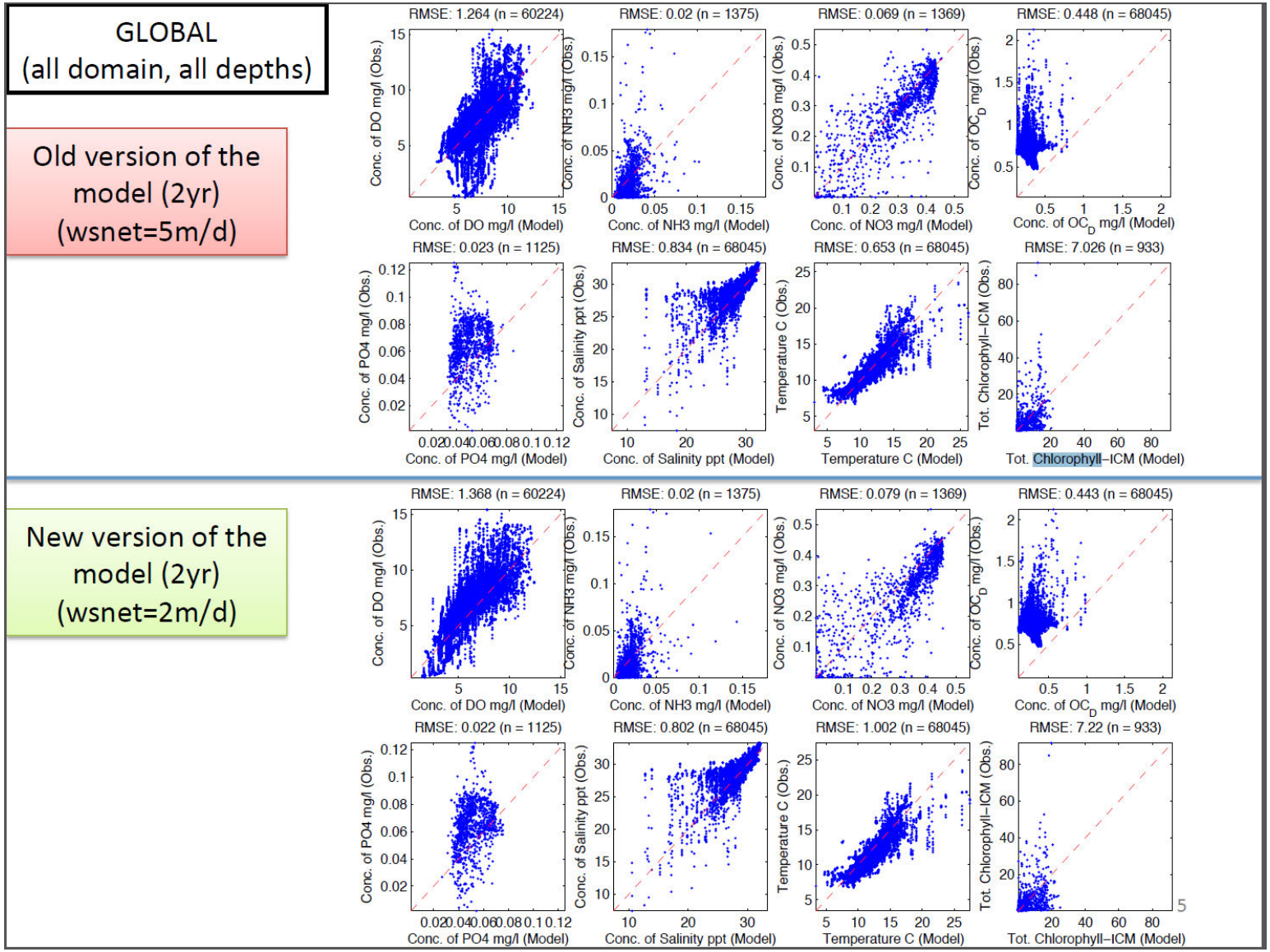

Figure 5. Comparison of model-predicted concentrations (Model) of water quality variables with observed data (Obs).

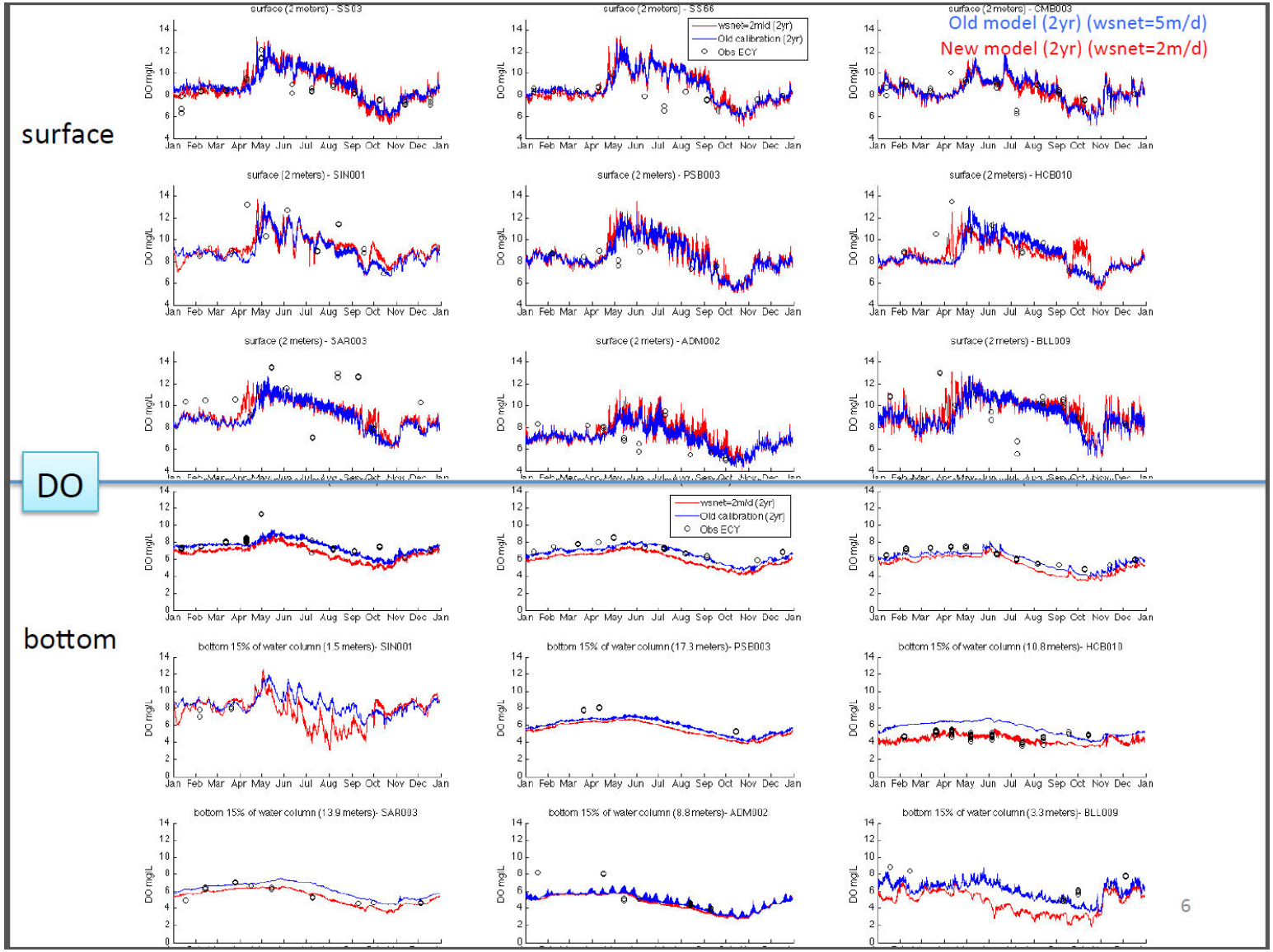

Figure 6. Comparison of time-series of model-predicted concentrations (old and new model calibration) of dissolved oxygen (DO) with observed data (Obs) for the surface layer and bottom layer of selected stations.

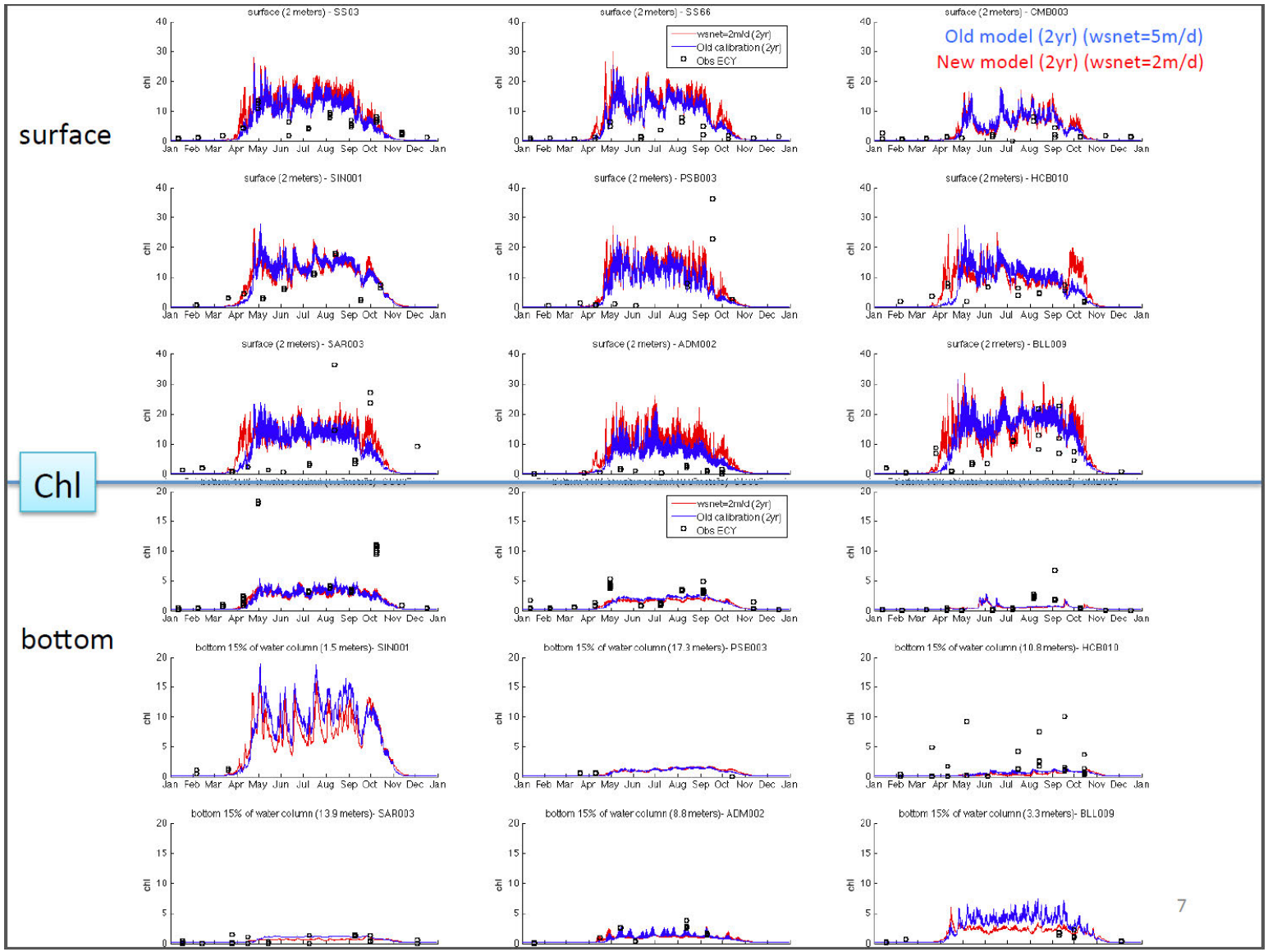

Figure 7. Comparison of time-series of model-predicted concentrations (old and new model calibration) of chlorophyll-a (Chl) with observed data (Obs) for the surface layer and bottom layer of selected stations.

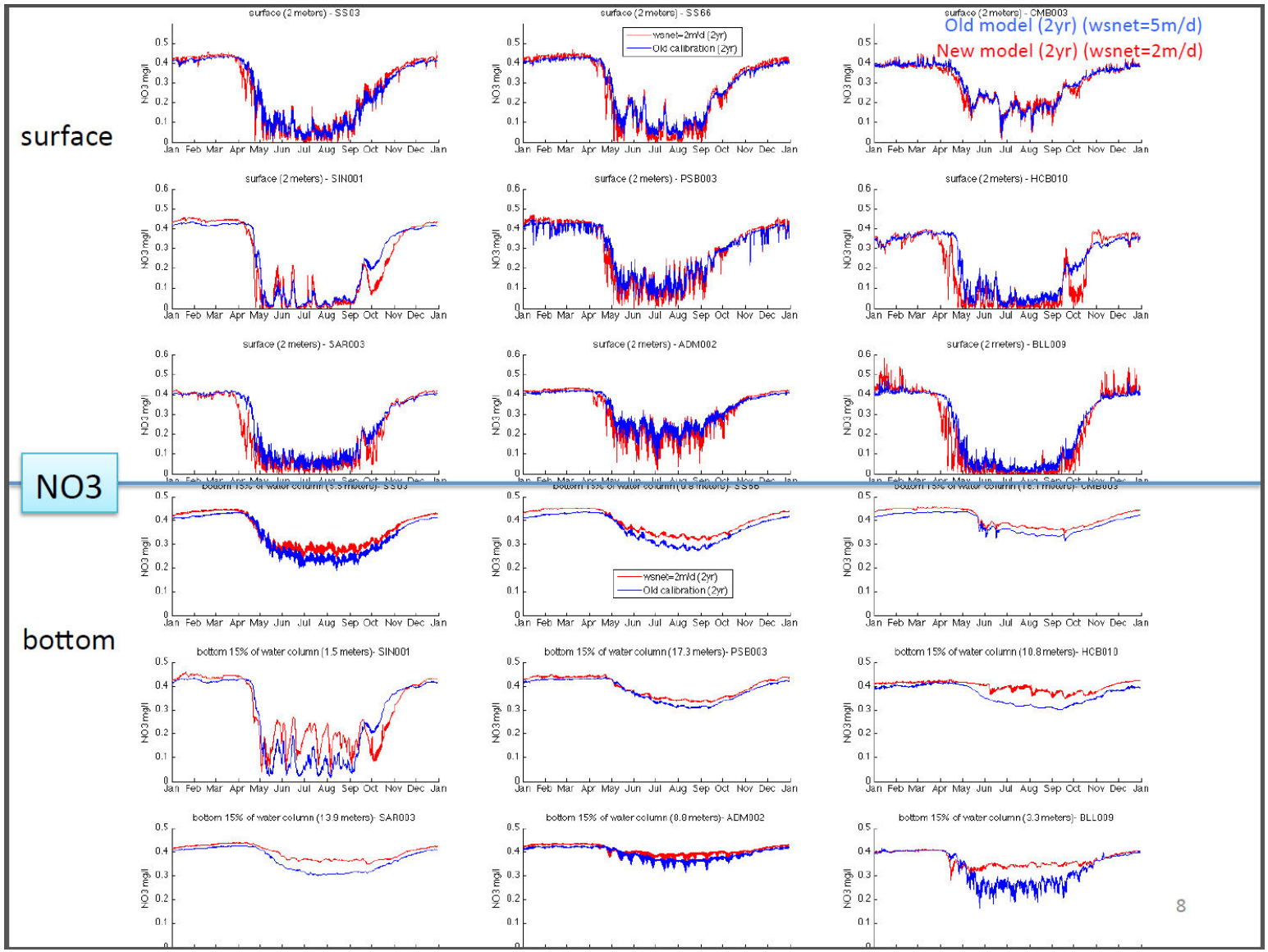

Figure 8. Comparison of time-series of model-predicted concentrations (old and new model calibration) of nitrate (NO3) for the surface layer and bottom layer of selected stations. *Comparisons with observed data are in Appendix D.*

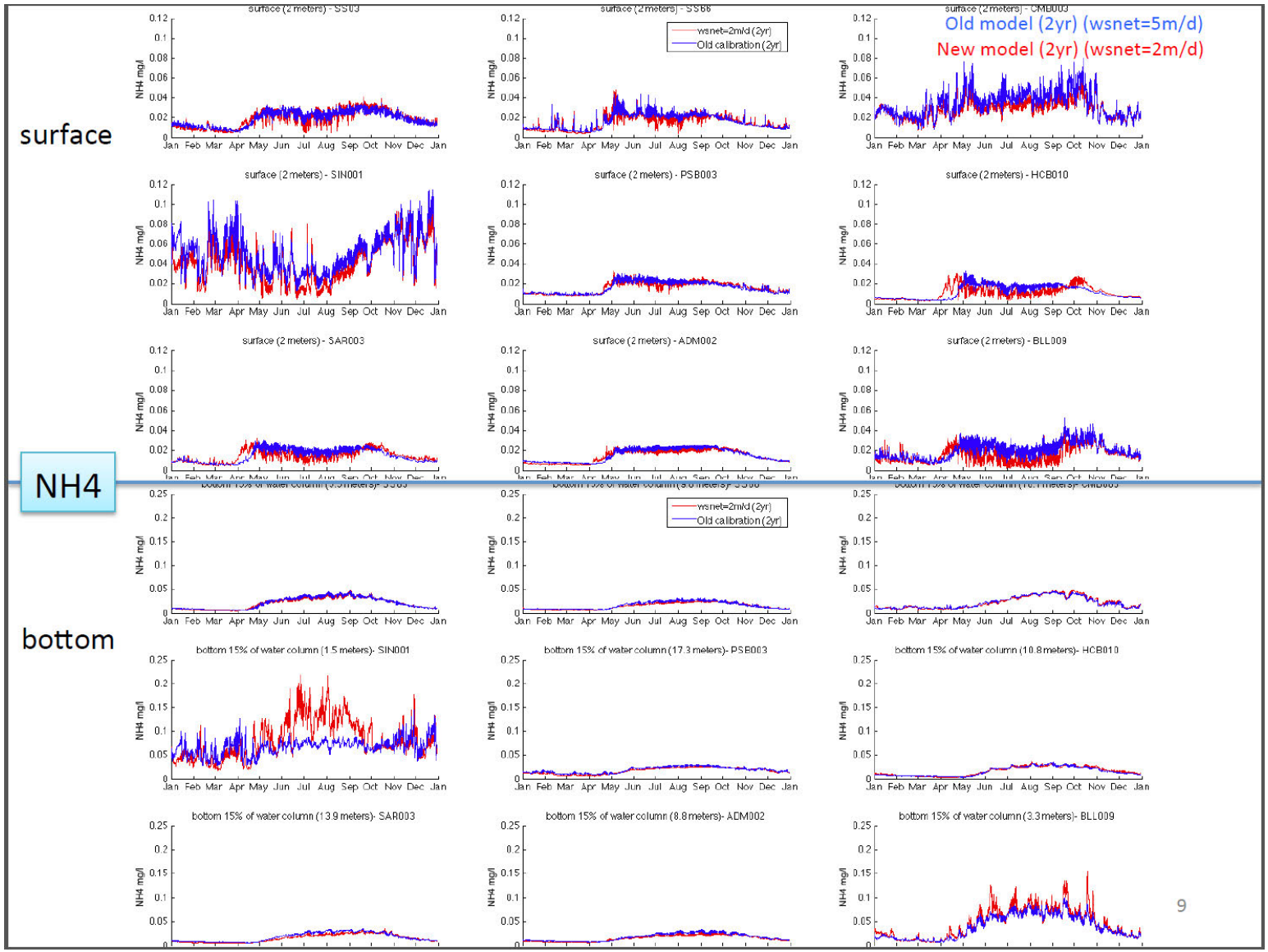

Figure 9. Comparison of time-series of model-predicted concentrations (old and new model calibration) of ammonia (NH4) for the surface layer and bottom layer of selected stations. *Comparisons with observed data are in Appendix D.*

Comparison of predicted and observed sediment fluxes

Sheibley and Paulson (2014) compiled available sediment flux data for Puget Sound from various sources (Table 1). In the present study, we compared the model-predicted sediment fluxes from the 2006 simulation with the limited available observed data from various years. Since model predictions and observed data are from different years, an exact match is not expected for various sediment flux parameters. The model-predicted sediment oxygen demand (SOD), ammonia (Jnh4), and nitrate+nitrite (Jno3) were reasonably close to the observed fluxes as described below.

Table 1. General information for benthic chamber sites in Puget Sound.
(Sheibley and Paulson, 2014)

Station/site identifier	Date sampled	Depth (meters)	Study details	Reference
Carkeek pelagic site (PS17)	June 8–9, 1982	175	Single site, measured once	Murray (1982)
Carkeek pelagic site	Unknown	200	Single site, measured once	Grundmanis (1989)
Holmes Harbor	August 1993	50–70	Three sites, measured once	Brandes and Devol (1997)
Dabob Bay	January 1987–January 1988	110	Single site, measured 20 times during the year	Colbert and others, unpub. data (2010)
Budd Inlet	September 1996–September 1997	5–15	Four sites measured 17–19 times during the year	Aura Nova Consultants and others (1998)
Case Inlet	September–October 2007	5–25	Three depths measured 3 times	Roberts and others (2008)
Carr Inlet	September–October 2007	5–25	Three depths measured 3 times	Roberts and others (2008)
Eld Inlet	September–October 2007	5–25	Three depths measured 3 times	Roberts and others (2008)
Budd Inlet	September–October 2007	3–25	Three depths measured 3 times	Roberts and others (2008)
Quartermaster Harbor	September 1–2, 2010	4–17	Five sites measured once	King County (2012)

Sediment oxygen demand (SOD)

The model-predicted SOD is compared with observed data in Table 2. The RMSE comparing predicted and observed SOD is 0.73 $gO_2/m^2/d$. For comparison, Brady et al. (2013) reported a similar RMSE of 0.64 $gO_2/m^2/d$ in a similar application of a SFM in Chesapeake Bay.

Model-predicted SOD tended to be higher than observed SOD, but this could be an artifact of the chamber method that was used to measure observed SOD. The *in-situ* incubation chambers that were used in the various studies in Puget Sound may underestimate the actual SOD because of lower circulation within the chamber compared with the ambient current velocity. Ambient water velocities above the sediment are likely significantly greater than the near-zero current velocities within the chambers. Stagnant conditions at low velocity tend to reduce the gradient of concentrations between the sediment and the overlying water, and thereby reduces the rate of fluxes between the water and sediment. Higher velocity tends to mix the overlying water and increase the concentration gradients between the sediment and water, and thereby increase the rate of fluxes between the water and sediment.

Mackenthun and Stefan (1995) showed that increasing current velocities increase the SOD. Increases in SOD due to increased velocity are significant at low ambient velocities typical in lakes, where velocity-related increases in SOD of an order of magnitude have been reported at low velocities (Cerco et al., 1992). SOD values measured in chambers increase significantly

with increased mixing inside the chamber, but there is no standardized method of introducing circulation in a sediment flux chamber (Cerco et al., 1992).

The fairly close agreement between the RMSE of predicted and observed SOD compared with Brady et al. (2013) suggest that the model skill for prediction of SOD is reasonably accurate.

Table 2. Comparison of model-predicted and observed sediment oxygen demand (SOD)[1]

		Model predictions (gO2/m^2/d)				**Observed data (gO2/m^2/d)**			
Stations	Node	Year	Mean	Min	Max	Year (Month)	Mean	Min	Max
BUDD05	8615	2006	1.60	0.93	2.00	2007 (Sep-Oct)	0.44	0.08	0.99
BUDD15	8374	2006	1.54	0.95	1.89	2007 (Sep-Oct)	0.82	0.63	1.13
BUDD25	8372	2006	1.43	0.91	1.75	2007 (Sep-Oct)	0.62	0.50	0.70
CARR05	8016	2006	1.01	0.73	1.33	2007 (Sep-Oct)	0.51	0.33	0.79
CARR15	7950	2006	1.05	0.82	1.37	2007 (Sep-Oct)	0.69	0.64	0.77
CARR25	7846	2006	1.26	1.06	1.45	2007 (Sep-Oct)	0.25	0.21	0.27
CASE05	8858	2006	0.88	0.59	1.07	2007 (Sep-Oct)	0.33	-0.03	0.69
CASE15	8756	2006	1.08	0.73	1.29	2007 (Sep-Oct)	0.53	0.39	0.62
CASE25	8656	2006	1.28	0.84	1.54	2007 (Sep-Oct)	0.70	0.49	1.03
ELD05	8741	2006	1.34	0.66	1.89	2007 (Sep-Oct)	1.49	1.23	1.71
ELD15	8579	2006	1.48	0.78	2.01	2007 (Sep-Oct)	0.94	0.89	1.02
ELD25	8397	2006	1.60	1.00	1.99	2007 (Sep-Oct)	0.74	0.22	1.08
QMH_A	6817	2006	1.30	0.94	1.69	2010 (Sep)	1.72	1.72	1.72
QMH_B	6783	2006	1.19	0.89	1.44	2010 (Sep)	0.72	0.72	0.72
QMH_C	6684	2006	1.16	0.97	1.29	2010 (Sep)	0.64	0.64	0.64
QMH_D	6645	2006	1.14	0.99	1.25	2010 (Sep)	0.95	0.95	0.95
QMH_E	6574	2006	1.20	1.05	1.27	2010 (Sep)	0.16	0.16	0.16
BD-2	8374	2006	1.03	0.36	1.96	1996-7 (Sep-Sep)	0.57	0.26	0.92
LOON-1	8492	2006	1.03	0.41	1.87	1996-7 (Sep-Sep)	0.59	0.36	1.01
BA-1	8615	2006	1.24	0.54	2.24	1996-7 (Sep-Sep)	0.57	0.32	0.87
BI-5	8775	2006	2.37	1.26	4.41	1996-7 (Sep-Sep)	0.58	0.17	1.14
DABOB	5380	2006	0.61	0.32	0.97	1981-2 (Jan-Jan)	0.17	0.07	0.36
HOLMES	4786	2006	0.95	0.94	0.97	1993 (Aug)	0.14	0.12	0.16
CARKEEK	4276	2006	0.64	0.52	0.74	1982 (Jun)	0.17	0.17	0.17
All stations mean, min, or max			1.23	0.32	4.41		0.63	-0.03	1.72

[1] The stations in this table are located in:
Budd Inlet (BUDD05, BUDD15, BUDD25, BD-2, LOON-1, BA-1, BI-5)
Carr Inlet (CARR05, CARR15, CARR25)
Case Inlet (CASE05, CASE15, CASE25)
Eld Inlet (ELD05, ELD15, ELD25)
Quartermaster Harbor (QMH_A, QMH_B, QMH_C, QMH_D, QMH_E)
Dabob Bay (DABOB)
Holmes Harbor (HOLMES)
Near Carkeek (CARKEEK)

Sediment flux of ammonia

The model-predicted sediment flux of ammonia (Jnh4) is compared with observed data in Table 3. The RMSE comparing predicted and observed Jnh4 is 38 mgN/m^2/d. For comparison, Brady et al. (2013) reported a similar RMSE ranging from 22 to 50 mgN/m^2/d at various sampling locations.

The fairly close agreement between the RMSE of predicted and observed Jnh4 compared with Brady et al. (2013) suggest that the model skill for prediction of Jnh4 is reasonably accurate.

Table 3. Comparison of model-predicted and observed flux of ammonia (Jnh4).

		Model predictions (mgN/m^2/d)				**Observed data (mgN/m^2/d)**			
Stations	Nodes	Year	Mean	Min	Max	Year (Month)	Mean	Min	Max
BUDD05	8615	2006	77	38	97	2007 (Sep-Oct)	31	6	78
BUDD15	8374	2006	79	42	102	2007 (Sep-Oct)	54	38	69
BUDD25	8372	2006	72	40	91	2007 (Sep-Oct)	66	50	90
CARR05	8016	2006	52	29	66	2007 (Sep-Oct)	20	12	31
CARR15	7950	2006	58	35	69	2007 (Sep-Oct)	77	56	104
CARR25	7846	2006	76	55	86	2007 (Sep-Oct)	41	30	49
CASE05	8858	2006	40	17	57	2007 (Sep-Oct)	19	2	30
CASE15	8756	2006	56	28	73	2007 (Sep-Oct)	88	51	153
CASE25	8656	2006	71	36	91	2007 (Sep-Oct)	99	35	153
ELD05	8741	2006	56	23	82	2007 (Sep-Oct)	135	122	156
ELD15	8579	2006	71	30	98	2007 (Sep-Oct)	123	95	140
ELD25	8397	2006	85	45	108	2007 (Sep-Oct)	87	4	143
QMH_A	6817	2006	68	41	84	2010 (Sep)	155	155	155
QMH_B	6783	2006	62	40	71	2010 (Sep)	60	60	60
QMH_C	6684	2006	60	49	64	2010 (Sep)	50	50	50
QMH_D	6645	2006	59	52	63	2010 (Sep)	0	0	0
QMH_E	6574	2006	63	57	66	2010 (Sep)	0	0	0
BD-2	8374	2006	43	0	102	1996-7 (Sep-Sep)	40	7	110
LOON-1	8492	2006	40	0	87	1996-7 (Sep-Sep)	53	19	122
BA-1	8615	2006	50	0	101	1996-7 (Sep-Sep)	41	-1	138
BI-5	8775	2006	102	0	180	1996-7 (Sep-Sep)	90	9	189
DABOB	5380	2006	25	0	49	1981-2 (Jan-Jan)	8	-4	28
HOLMES	4786	2006	44	42	47	1993 (Aug)	6	4	9
CARKEEK	4276	2006	20	12	27	1982 (Jun)	4	4	4
All stations mean, min, or max			60	0	180		56	-4	189

Sediment flux of nitrate+nitrite

The model-predicted sediment flux of nitrate+nitrite (Jno3) is compared with observed data in Table 4. The RMSE comparing predicted and observed Jno3 is 14 mgN/m^2/d. The model predictions and the observed data show that the average flux of nitrate+nitrite is from the water into the sediment.

Table 4. Comparison of model-predicted and observed flux of nitrate+nitrite (Jno3).

		Model predictions (mgN/m^2/d)				**Observed data (mgN/m^2/d)**			
Stations	Nodes	Year	Mean	Min	Max	Year (Month)	Mean	Min	Max
BUDD05	8615	2006	-11	-16	3	2007 (Sep-Oct)	3	-3	14
BUDD15	8374	2006	-14	-17	-9	2007 (Sep-Oct)	-38	-81	-12
BUDD25	8372	2006	-14	-17	-10	2007 (Sep-Oct)	-12	-17	-5
CARR05	8016	2006	-17	-21	-1	2007 (Sep-Oct)	12	4	20
CARR15	7950	2006	-18	-21	-3	2007 (Sep-Oct)	-27	-36	-18
CARR25	7846	2006	-20	-21	-17	2007 (Sep-Oct)	-10	-11	-7
CASE05	8858	2006	-17	-19	-8	2007 (Sep-Oct)	10	2	21
CASE15	8756	2006	-18	-19	-12	2007 (Sep-Oct)	-18	-21	-14
CASE25	8656	2006	-18	-19	-14	2007 (Sep-Oct)	-20	-29	-11
ELD05	8741	2006	0	-12	8	2007 (Sep-Oct)	-14	-32	-3
ELD15	8579	2006	-7	-14	1	2007 (Sep-Oct)	-18	-27	-14
ELD25	8397	2006	-13	-16	-7	2007 (Sep-Oct)	-8	-24	1
QMH_A	6817	2006	-15	-19	-3	2010 (Sep)	-5	-5	-5
QMH_B	6783	2006	-16	-19	-6	2010 (Sep)	0	0	0
QMH_C	6684	2006	-18	-19	-15	2010 (Sep)	0	0	0
QMH_D	6645	2006	-18	-19	-17	2010 (Sep)	10	10	10
QMH_E	6574	2006	-18	-19	-17	2010 (Sep)	-10	-10	-10
BD-2	8374	2006	-13	-18	0	1996-7 (Sep-Sep)	-11	-22	1
LOON-1	8492	2006	-12	-19	2	1996-7 (Sep-Sep)	-8	-19	3
BA-1	8615	2006	-11	-20	5	1996-7 (Sep-Sep)	-13	-63	9
BI-5	8775	2006	-12	-25	5	1996-7 (Sep-Sep)	-13	-67	1
DABOB	5380	2006	-18	-21	0	1981-2 (Jan-Jan)	-12	-26	3
HOLMES	4786	2006	-18	-19	-17	1993 (Aug)	-8	-11	-6
CARKEEK	4276	2006	--	--	--	1982 (Jun)	--	--	--
All stations mean, min, or max			-15	-25	8		-9	-81	21

Final model calibration parameter values

Final values for the *kinetics rates* and *constants* parameters for the water quality model are presented in Appendix E.

Predicted Sediment Fluxes during 2006

Average sediment oxygen demand (SOD) during 2006 ranges from about 0.4 to 1.3 $gO_2/m^2/d$ (Figure 10). The highest average SOD tends to occur at the landward ends of inlets and bays (e.g., South Puget Sound, Commencement Bay, East Passage, Sinclair/Dyes Inlets, Whidbey basin, and Bellingham Bay).

Average sediment flux of ammonia (Jnh4) during 2006 ranges from about 12 to 47 $mgN/m^2/d$ (Figure 11). The highest average Jnh4 tends to occur in similar locations as the highest average SOD, at the landward ends of inlets and bays (e.g., South Puget Sound, Commencement Bay, East Passage, Sinclair/Dyes Inlets, Whidbey basin, and Bellingham Bay).

Average sediment flux of nitrate+nitrite (Jno3) during 2006 ranges from about -5 to -18 $mgN/m^2/d$ (Figure 12). Negative values of Jno3 indicate that the average flux of nitrate+nitrite is from the water to the sediment throughout Puget Sound because of denitrification that occurs in the sediment. Areas with the most negative values of Jno3, and most likely the greatest denitrification, include the deeper areas of East Passage, Hood Canal, and Port Susan.

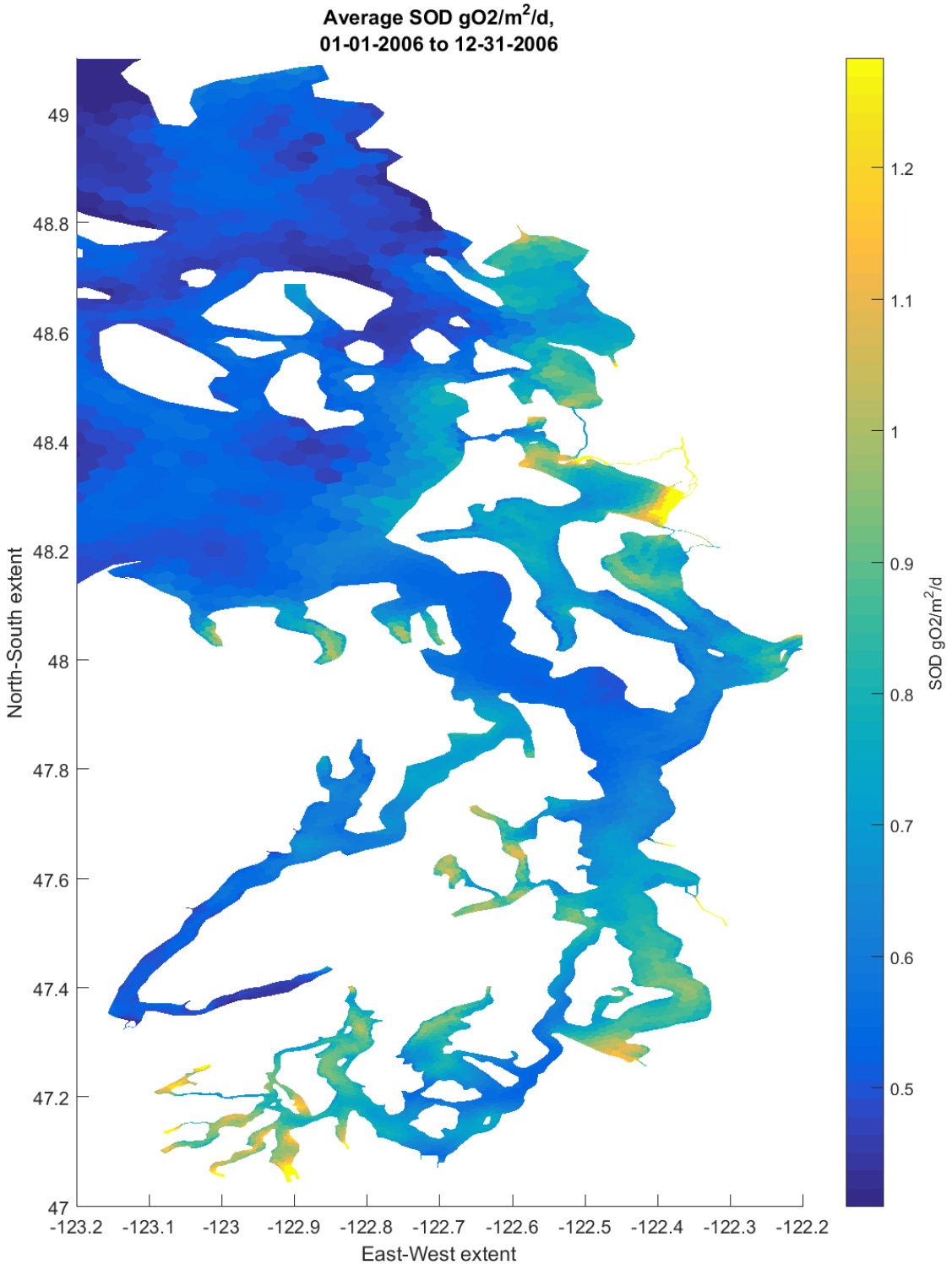

Figure 10. Average sediment oxygen demand (SOD) during 2006.

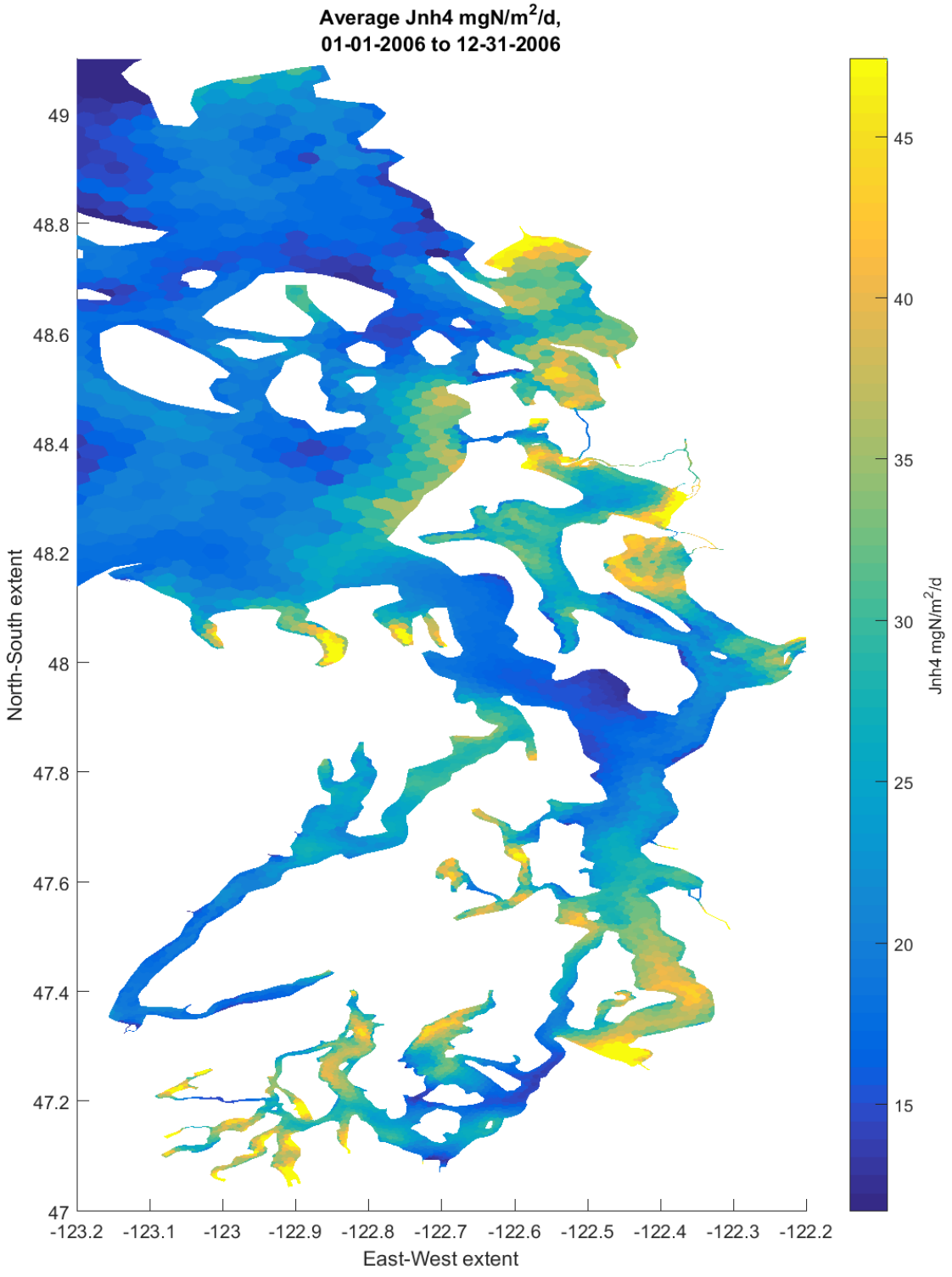

Figure 11. Average sediment flux of ammonia (Jnh4) during 2006.
Positive values indicate flux of ammonia from the sediment to the water.

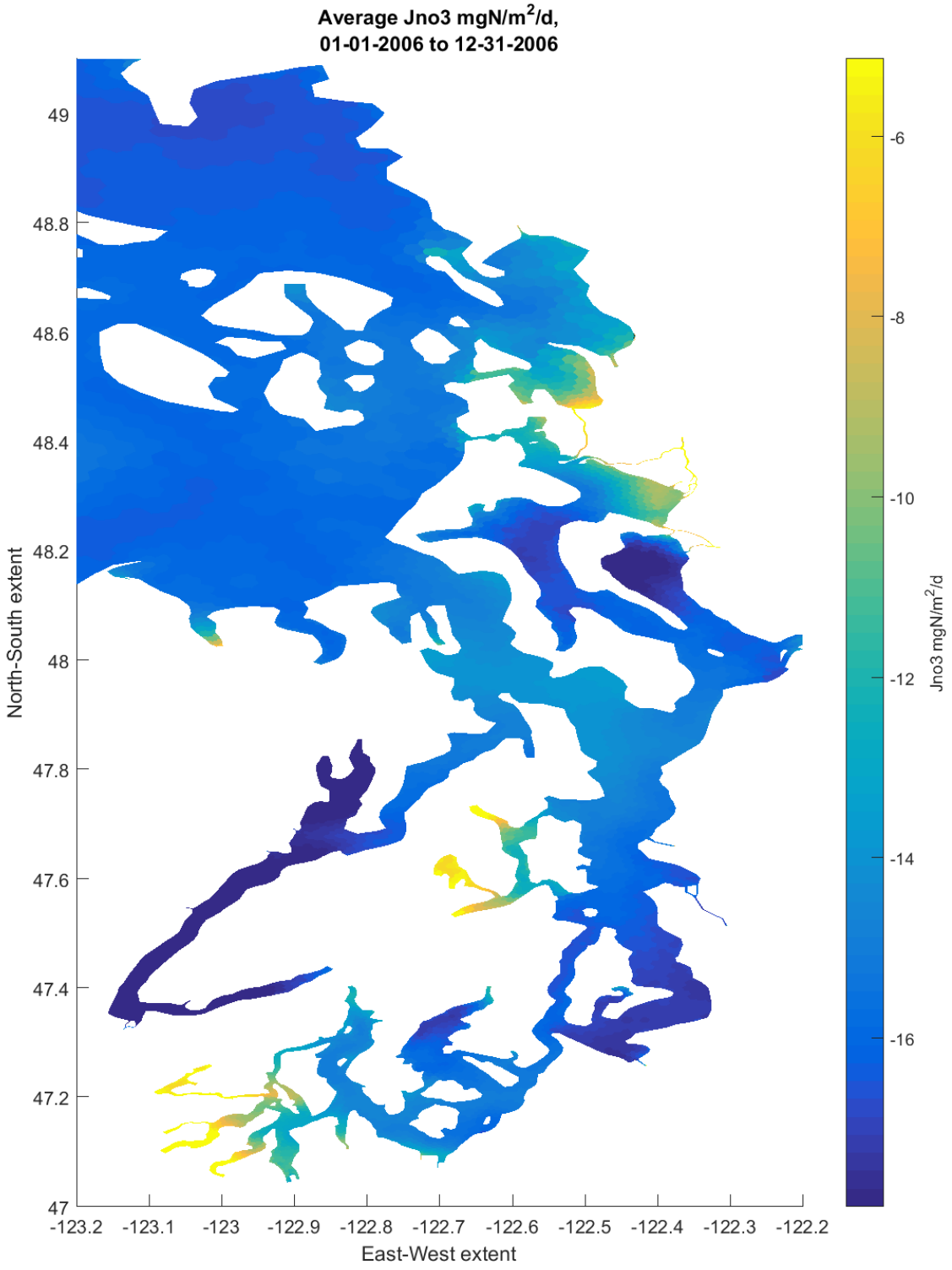

Figure 12. Average sediment flux of nitrate+nitrite (Jno3) during 2006.
Negative values indicate flux of nitrate from the water to the sediment.

Discussion

With this study, we aimed to improve the Salish Sea Model's ability to compute dissolved oxygen (DO) concentrations throughout the water column with the integration of a Sediment Diagenesis Module (SDM), thus simulating sediment-water interactions which strongly influence oxygen levels. Previous modeling studies externally specified the sediment-water exchanges and adjustments were made regionally to account for changes in external nutrient loading. That approach could not distinguish between the loading and sediment flux effects of individual nutrient sources.

We selected a sediment diagenesis algorithm that the water quality modeling community has vetted and thus is applied widely in Total Maximum Daily Load (TMDL) studies. In addition, the algorithm provides an acceptable level of complexity, representing a compromise between computational efficiency and depth-resolution, while providing acceptable accuracy. We set up and tested the model code to ensure that sediment-water exchanges were incorporated appropriately, and then applied the revised model to the Salish Sea and compared against monitoring data to assess the model skill. This report documents the final values selected for each of the kinetics rates and constants parameters of the water quality model during calibration (Appendix E).

The SDM simulates material fluxes to the sediment from the water column. These fluxes fuel biogeochemical processes that release some of the nutrients back to the water column and consume oxygen in the process. As a result, we see improvements in the model's ability to simulate low levels of DO (Figure 5), though the overall RMSE statistics did not change significantly.

Sediment oxygen demand (SOD) flux data collected over time are limited and highly variable (Table 2). Salish Sea Model estimates for SOD tend to be higher than observed SOD, but monitoring SOD has challenges. Also these observed data may not be representative of the full range of temporal and spatial conditions represented by the model. Nonetheless, the modeled RMSE for SOD (0.73 gO2/m2/day) is close to Brady et al.'s (2013) reported RMSE derived from measurements (0.64 gO2/m2/day).

Similarly, the model-predicted RMSE for sediment flux of ammonia (38 $mgN/m^2/d$) compares well with Brady et al.'s (2013) reported RMSE ranging from 22 to 50 $mgN/m^2/d$ at various sampling locations. In terms of the sediment flux of nitrate+nitrite (Jno3), the model-predicted values fall within a similar range as the measured values (Table 4). Thus, we are encouraged by indications that the model's error falls within measurement error ranges. In addition, following the modest recalibration of the Salish Sea Model after incorporating the SDM, predictions of water column DO and other water quality parameters are within reasonable and acceptable ranges compared to observed data.

The magnitudes of estimated fluxes resulting from sediment diagenesis are highly sensitive to specification of net settling rates of particulate organic matter (POM). Net settling rates are the resultant depositional rates estimated as difference between particle settling and resuspension. These rates are high in depositional areas such as coves and bays that are basins with relatively

low tidal currents. Conversely, net deposition rates would be relatively low in high energy regions with flushing where high currents would re-suspend deposited material and flush it away. In the present model configuration, net settling rates were specified as a uniform quantity over the entire domain. The uniform rates were adjusted as part model calibration and provide overall reasonable performance. This is a model limitation which may be addressed through incorporation of dynamic spatially varying settling rates.

We plan to continue evaluating performance of the Salish Sea Model as we produce model runs for a series of years. Our next steps are to use the revised model for future studies to reevaluate scenarios which will help us evaluate the relative influences of climate effects, local human nutrient sources, and the Pacific Ocean on DO.

Conclusions and Recommendations

Conclusions

Results of this study support the following conclusions.

- A Sediment Diagenesis Module (SDM) was successfully added to the Salish Sea Model (SSM).
- The updated SSM, including simulation of sediment diagenesis and fluxes of oxygen and nitrogen between the water and sediment, was re-calibrated to the observed data. The model skill with the new SDM was comparable to the previous version of the SSM, with improvement in skill for simulating dissolved oxygen (DO) levels in the lower ranges.
- The updated SSM performed well for predicting water quality and sediment flux variables.

Recommendations

Results of this study support the following recommendations.

- The updated SSM, including simulation of sediment diagenesis and fluxes between the water and sediment, should be used in future studies to reevaluate scenarios to identify the relative influences of climate effects, local human nutrient sources, and the Pacific Ocean on DO.
- Additional years should be simulated to explore relationships between inter-annual variations in the important drivers such as river flows and upwelling on DO levels in the Salish Sea.
- Increased emphasis on acquiring and improving methodologies for sediment flux observations will allow for better model evaluation.
- The use of dynamic spatially varying resuspension rates and net settling rates of particulate organic matter (POM) could allow better representation of spatial variations in high and low energy environments. This could be accomplished by internally calculating settling and resuspension as a function of simulated bed shear stress over the entire domain at each time step.
- Confirmation with measured sediment deposition rates is recommended as the next SSM improvement step. This would follow incorporation of dynamic spatially varying settling rates, including consideration of settling rates in the water column and deep burial.

References

Ahmed, A., G. Pelletier, M. Roberts, and A. Kolosseus. 2014. South Puget Sound Dissolved Oxygen Study: Water Quality Model Calibration and Scenarios. Washington State Department of Ecology, Olympia, WA. Publication No. 14-03-004. https://fortress.wa.gov/ecy/publications/summarypages/1403004.html.

Ahmed, A., G. Pelletier, and M. Roberts. 2017. South Puget Sound flushing and residual flows. Estuarine, Coastal and Shelf Science. 187(2017) 9-21. http://dx.doi.org/10.1016/j.ecss.2016.12.027

Aura Nova Consultants, L. W. M. P. 1998. Budd Inlet scientific study final report, Olympia, WA: Lacy, Olympia, Tumwater, and Thurston County (LOTT) Wastewater Management Partnership.

Baker, E.T., R.A. Feely, M.R. Landry, and M. Lamb. 1985. Temporal variations in the concentration and settling flux of carbon and phytoplankton pigments in a deep fjordlike estuary. Estuarine, Coastal and Shelf Science 21:859-877.

Baker, E.T. 1982. Suspended Particulate Matter in Elliott Bay. NOAA Technical Report ERL 417-PMEL 35. Pacific Marine Environmental Laboratory, Seattle, WA.

Banas, N.S., Conway-Cranos, L., Sutherland, D.A. Patterns of River Influence and Connectivity Among Subbasins of Puget Sound, with Application to Bacterial and Nutrient Loading Estuaries and Coasts (2015) 38: 735.

Booz Allen Hamilton. 2013. Chesapeake Center for Collaborative Computing Concept of Operations, Version 0.7. Prepared for the Chesapeake Bay Program.

Boudreau, B.P. 1997. Diagenetic models and their implementation. Springer.

Boudreau, B.P. 1994. Is burial velocity a master parameter for bioturbation? Geochimica et Cosmochimica Acta.58(4)1243-1249

Brady, D.C., J.M. Testa, D.M. Di Toro, W.R. Boynton, W.M. Kemp. 2013. Sediment flux modeling: Calibration and application for coastal systems. Estuarine, Coastal and Shelf Systems. 117:107-124. http://dx.doi.org/10.1016/j.ecss.2012.11.003

Brandes, J.A. and Devol, A.H. 1997. Isotopic fractionation of oxygen and nitrogen in coastal marine sediments: Geochimica et Cosmochimica Acta, v. 61, no. 9, p. 1793–1801, doi: 10.1016/S0016-7037(97)00041-0.

Brown, Sharon. 2014. Environmental Engineer with Toxics Cleanup Program. Personal communication by email, August.

Burdige, D.J. 2007. Preservation of Organic Matter in Marine Sediments: Controls, Mechanisms, and an Imbalance in Sediment Organic Carbon Budgets? Chemical Reviews 107:467-485.

Cai, W.-J. G.W. Luther III, J.C. Cornwell, A.E. Giblin. 2010. Carbon cycling and the coupling between proton and electron transfer reactions in aquatic sediments in Lake Champlain. Aquatic Geochemistry. 16:421-446.

Carpenter, R., M.L. Peterson, and J.T. Bennett. 1985. 210Pb-derived sediment accumulation and mixing rates for the greater Puget Sound region. Marine Geology. 64(1985)291-312.

Cerco, C., D. Gunnison, and C.B. Price. 1992. Proceedings, US Army Corps of Engineers workshop on sediment oxygen demand: Providence, Rhode Island 21-22 August 1990. USAE Water Quality Research Program Miscellaneous Paper W-92-1.

Cerco, C.F. and T.M. Cole. 1995. User's Guide to the CE-QUAL-ICM Three-Dimensional Eutrophication Model, Release Version 1.0. U.S. Army Corps of Engineers, Washington, DC. 320 pp.

Chen, C., H. Liu, R.C. Beardsley. 2003. An unstructured, finite-volume, three-dimensional primitive equation ocean model: Application to coastal ocean and estuaries. Journal of Atmospheric and Oceanic Technology 20:159-186.

Dhakar, S.P. and D.J. Burdige. 1996. Coupled, non-linear, steady state model for early diagenetic processes in pelagic sediments. Journal of American Science. 296:296-330.

Di Toro, D.M. 2001. Sediment Flux Modeling. Wiley Interscience. John Wiley & Sons, Inc.
Ecology. 2013. SedFlux – An Excel/VBA model of sediment nutrient fluxes and sediment oxygen demand (SOD). Washington State Department of Ecology, Olympia WA. http://www.ecy.wa.gov/programs/eap/models.html.

Di Toro, D.M., Paquin, P.R., Subburamu, K., and Gruber D.A. 1990. Sediment oxygen demand model: Methane and ammonia oxidation. Journal of Environmental Engineering 116 (5), 945–986.

Emerson, S. R. Jahnke, D. Heggie. 1984. Sediment water exchange in shallow water estuarine sediments. Journal of Marine Systems. 42:709-730.

EPA. 1985. Rates, constants, and kinetics formulations in surface water quality modeling (second edition). EPA/600/3-85/040. U.S. Environmental Protection Agency. Environmental Research Laboratory. Athens, GA.

EPA Council on Regulatory Environmental Modeling. 2009. Guidance on the Development, Evaluation, and Application of Environmental Models. Council for Regulatory Environmental Models, Washington DC. www.epa.gov/crem/library/cred_guidance_0309.pdf.

Fennel, K. J. Wilkin, J Levin, J. Moisan, J. O'Reilly, D. Haidvogel. 2006. Nitrogen cycling in the Middle Atlantic Bight: results from a three-dimensional model and implications for the North Atlantic nitrogen budget. Global Biogeochemical Cycles. 20. http://dx.doi.org/10.1029/2005GB002456

Greengrove, C. 2005. Surficial total organic carbon concentration from Puget Sound and the Straits (unpublished data).

Gries, T. and D. Osterberg. 2011. Control of Toxic Chemicals in Puget Sound: Characterization of Toxic Chemicals in Puget Sound and Major Tributaries, 2009-10. Washington State Department of Ecology, Olympia, WA. Publication No. 11-03-008. https://fortress.wa.gov/ecy/publications/summarypages/1103008.html.

Grundmanis, V., 1989. A study of the oxidation of organic matter in pelagic and near shore sedimentary environments: Seattle, Washington, University of Washington, Ph.D. dissertation, 561 p.

Gypens, N. C. Lancelot, K. Soetaert. 2008. Simple parameterisations for describing N and P diagenetic processes: application in the North Sea. Progress in Oceanography. 76: 89-110.

Hetland, R.D., S.F. DiMarco. 2008. How does the character of oxygen demand control the structure of hypoxia on the Texas-Louisiana continental shelf? Journal of Marine Systems. 70:49-62.

Imteaz, M.A., T. Asaeda. 2000. Artificial mixing of lake water by bubble plume and effects of bubbling operations on algal bloom. Water Research. 34:1919-1929.

Khangaonkar, T., B. Sackmann, W. Long, T. Mohamedali, and M. Roberts. 2012 a. Simulation of annual biogeochemical cycles of nutrient balance, phytoplankton bloom(s), and DO in Puget Sound using an unstructured grid model. Ocean Dynamics. (2012) 62:1353–1379.doi: 10.1007/s10236-012-0562-4.

Khangaonkar, T., W. Long, B. Sackmann, T. Mohamedali, and M. Roberts. 2012 b. Puget Sound Dissolved Oxygen Modeling Study: Development of an Intermediate Scale Water Quality Model. U.S. Department of Energy, Pacific Northwest National Laboratory and Washington State Department of Ecology. Ecology Publication No. 12-03-049. https://fortress.wa.gov/ecy/publications/summarypages/1203049.html

Khangaonkar, Tarang, Zhaoqing Yang, Taeyun Kim, and Mindy Roberts. 2011. Tidally averaged circulation in Puget Sound sub-basins: Comparison of historical data, analytical model, and numerical model. Estuarine, Coastal and Shelf Science, 93:305-319.

King County, 2012, Quartermaster Harbor benthic flux study: Prepared by Curtis DeGasperi, Seattle, Washington, King County, Water and Land Resources Division, 34 p. http://your.kingcounty.gov/dnrp/library/2012/kcr2320.pdf.

Konrad, C.P. 2014. Approaches for evaluating the effects of bivalve filter feeding on nutrient dynamics in Puget Sound, Washington: U.S. Geological Survey Scientific Investigations Report 2013–5237, 22 p. http://dx.doi.org/10.3133/sir20135237.

Krause, D., D.P. Boyle, and F. Base. 2005. Comparison of different efficiency criteria for hydrological model assessment. Advances in Geoscience 5:89-97.

Lavelle, J.W. G.J. Massoth, and E.A. Crecelius. 1986. Accumulation rates of recent sediment in Puget Sound, WA. Marine Geology. 72(1986)59-70.

Long, W., T. Khangaonkar, M. Roberts, and G. Pelletier. 2014. Approach for Simulating Acidification and the Carbon Cycle in the Salish Sea to Distinguish Regional Source Impacts. Washington State Department of Ecology, Olympia, WA. Publication No. 14-03-002. https://fortress.wa.gov/ecy/publications/SummaryPages/1403002.html.

Mackas, D. and P. Harrison, 1997. Nitrogenous Nutrient Sources and Sinks in the Juan de Fuca Strait/Strait of Georgia/Puget Sound Estuarine System: Assessing the Potential for Eutrophication. Estuarine, Coastal and Shelf Science. 44:1-21.

Mackenthun, A.A. and H.G. Stefan. 1995. Effect of flow velocity on sediment oxygen demand: experimental results. University of Minnesota, St. Anthony Falls Hydraulic Laboratory, Project Report No. 371. Prepared for US Environmental Protection Agency, Environmental Research Laboratory, Duluth Minnesota.

Martin, J.L. 2002. A review and evaluation of sediment diagenesis routines for potential incorporation into the Water Analysis Simulation Program (WASP). For Tetra Tech, Inc. Prepared by J.L. Martin, Mississippi State University, Department of Civil and Environmental Engineering.

Martin, J.L. and T.A. Wool. 2013. Supplement to Water Analysis Simulation Program User Documentation. WASP Sediment diagenesis Routines: Model Theory and Users Guide. U.S. Environmental Protection Agency, Region 4, Atlanta GA.

Mauger, G.S., J.H. Casola, H.A. Morgan, R.L. Strauch, B. Jones, B. Curry, T.M. Busch Isaksen, L. Whitely Binder, M.B. Krosby, and A.K. Snover. 2015. State of Knowledge: Climate Change in Puget Sound. Report prepared for the Puget Sound Partnership and the National Oceanic and Atmospheric Administration. Climate Impacts Group, University of Washington, Seattle. DOI:10.7915/CIG93777D

Morse, John W. and Peter M. Eldridge. 2007. A non-steady state diagenetic model for changes in sediment biogeochemistry in response to seasonally hypoxic/anoxic conditions in the “dead zone” of the Louisiana shelf. Marine Chemistry 106:239-255.

Murray, J.W., 1982, Bioturbation and irrigation in Puget Sound sediments: Seattle, Washington, University of Washington.

Norton, D. 2009. Sediment Trap Monitoring in Four Inlets of South Puget Sound. Washington State Department of Ecology, Olympia, WA. Publication No. 09-03-006. https://fortress.wa.gov/ecy/publications/SummaryPages/0903006.html.

Paulson, A.J., E.T. Baker, R.A. Feely, T.S. Bates, P. Murphy, H.C. Curl Jr., D. Tennant, S. Walker, J.F. Gendron, M.F. Lamb, E.A. Crecelius. 1991. Puget Sound Sediment Trap Data: 1980-1985. NOAA Data Report ERL PMEL-37. Pacific Marine Environmental Laboratory, Seattle, WA.

Pelletier, G. and T. Mohamedali. 2009. Control of toxic chemicals in Puget Sound Phase 2: Development of simple numerical models. The long-term fate and bioaccumulation of polychlorinated biphenyls in Puget Sound. Washington State Department of Ecology, Olympia, WA. Publication No. 09-03-015. https://fortress.wa.gov/ecy/publications/SummaryPages/0903015.html

Pelletier, G.J., L. Bianucci, W. Long, T. Khangaonkar, T. Mohamedali, A. Ahmed, and C. Figueroa-Kaminsky. 2017. Salish Sea Model, Ocean Acidification Module and the Response to Regional Anthropogenic Sources. Washington State Department of Ecology, Olympia, WA. Publication No. 17-03-009. https://fortress.wa.gov/ecy/publications/SummaryPages/1703009.html

Press, W.H., S.A. Teukolsky, W.T. Vetterling, and B.P. Flannery. 1992. Numerical recipes in C. The art of scientific computing. Second edition. Cambridge University Press.

RETEC Group, Inc. 2006. Supplemental Remedial Investigation & Feasibility Study, Volume 1: RI Report, Whatcom Waterway Site, Bellingham, Washington. Prepared for Port of Bellingham. https://fortress.wa.gov/ecy/gsp/CleanupSiteDocuments.aspx?csid=219.

Roberts, M.L., Bos, J., and Albertson, S.L. 2008. South Puget Sound dissolved oxygen study: Olympia, Washington, Interim Data Report. Washington State Department of Ecology, Olympia, WA. Publication No. 08-03-037, 191 p. https://fortress.wa.gov/ecy/publications/SummaryPages/0803037.html

Roberts, M., T. Mohamedali, B. Sackmann, T. Khangaonkar, and W. Long. 2014. Puget Sound and the Straits Dissolved Oxygen Assessment: Impacts of Current and Future Human Nitrogen Sources and Climate Change through 2070. Washington State Department of Ecology, Olympia, WA. Publication No. 14-03-007. https://fortress.wa.gov/ecy/publications/SummaryPages/1403007.html

Roberts, M., A. Ahmed, G. Pelletier, and D. Osterberg. 2012. Deschutes River, Capitol Lake, and Budd Inlet Temperature, Fecal Coliform Bacteria, Dissolved Oxygen, pH, and Fine Sediment Total Maximum Daily Load Technical Report: Water Quality Study Findings. Washington State Department of Ecology, Olympia, WA. Publication No. 12-03-008. https://fortress.wa.gov/ecy/publications/SummaryPages/1203008.html

Roberts, M., J. Bos, and S. Albertson. 2008. South Puget Sound Dissolved Oxygen Study: Interim Data Report. Washington State Department of Ecology, Olympia, WA. Publication No. 08-03-037. https://fortress.wa.gov/ecy/publications/SummaryPages/0803037.html

Sackmann, B. 2009. Quality Assurance Project Plan: Puget Sound Dissolved Oxygen Modeling Study: Intermediate-scale Model Development. Washington State Department of Ecology, Olympia, WA. Publication No. 09-03-110. https://fortress.wa.gov/ecy/publications/summarypages/0903110.html.

Sackmann, B. 2011. Addendum #1 to Quality Assurance Project Plan. Puget Sound Dissolved Oxygen Modeling Study: Intermediate-scale Model Development. Washington State Department of Ecology, Olympia, WA. Publication No. 09-03-110Addendum1. https://fortress.wa.gov/ecy/publications/summarypages/0903110Addendum1.html

Scully, M.E. 2010. The importance of climate variability to wind-driven modulation of hypoxia in Chesapeake Bay. Journal of Physical Oceanography. 40:1435-1440.

Sheibley, R.W. and A.J. Paulson. 2014. Quantifying benthic nitrogen fluxes in Puget Sound, Washington—A review of available data: U.S. Geological Survey Scientific Investigations Report 2014-5033, 44 p., http://dx.doi.org/10.3133/sir20145033.

Slomp, C.P., J.F.P Malschaert, W. van Raaphorst. 1998. The role of adsorption in sediment-water exchange of phosphate in North Sea continental margin sediments. Limnology and Oceanography. 43-832-846.

Testa, J.M., D.C. Brady, D.M. Di Toro, W.R. Boynton, J.C. Cornwell, and W.M Kemp. 2013. Sediment flux modeling: simulating nitrogen, phosphorus, and silica cycles. Estuarine, Coastal, and Shelf Science. 2013), http://www.sciencedirect.com/science/article/pii/S0272771413002928.

Toxics Cleanup Program. 2012. Partial Remedial Investigation and Feasibility Study for Port Gamble Bay, WA. Washington State Department of Ecology, Olympia, WA. https://fortress.wa.gov/ecy/gsp/Sitepage.aspx?csid=3444.

Vanderborght, J.-P., R Wollast, G. Billen. 1977. Kinetic-models of diagenesis in disturbed sediments. Part 2. Nitrogen diagenesis. Limnology and Oceanography. 22:787-793.

WAC 173-201A. Water Quality Standards for Surface Waters in the State of Washington Washington State Department of Ecology, Olympia, WA. www.ecy.wa.gov/laws-rules/ecywac.html

Wilson, R.F., K. Fennel, and J.P. Mattern. 2013. Simulating sediment-water exchange of nutrients and oxygen: A comparative assessment of models against mesocosm observations. Continental Shelf Research 63:69-84.

Yang, Z., T. Khangaonkar, R. Labiosa, and T. Kim. 2010. Puget Sound Dissolved Oxygen Modeling Study: Development of an Intermediate-Scale Hydrodynamic Model. Pacific Northwest National Laboratory Publication No. PNNL-18484.

Appendices

Appendix A. Detailed Description of the Sediment Diagenesis Module (SDM)

Introduction

The basic framework of the SDM consists of two well-mixed sediment layers, underlying each surface water column segment: a thin upper sediment layer (the aerobic layer) and a thicker active (anaerobic) layer (Figure 4). In WASP, the thickness of the active layer is specified by the user (input) and assumed constant among all sediment columns. Three major processes included in the sediment model are:

- Fluxes of particulate organic matter (POM) from the water column to the sediments. (Note that since the upper sediment layer is assumed to have a negligible thickness, the fluxes are deposited directly into the second, or anaerobic, layer.)
- Mineralization (or diagenesis) of the POM.
- Reactions and transfers (between sediment layers, to the water column and deep inactive sediments) of the reaction products.

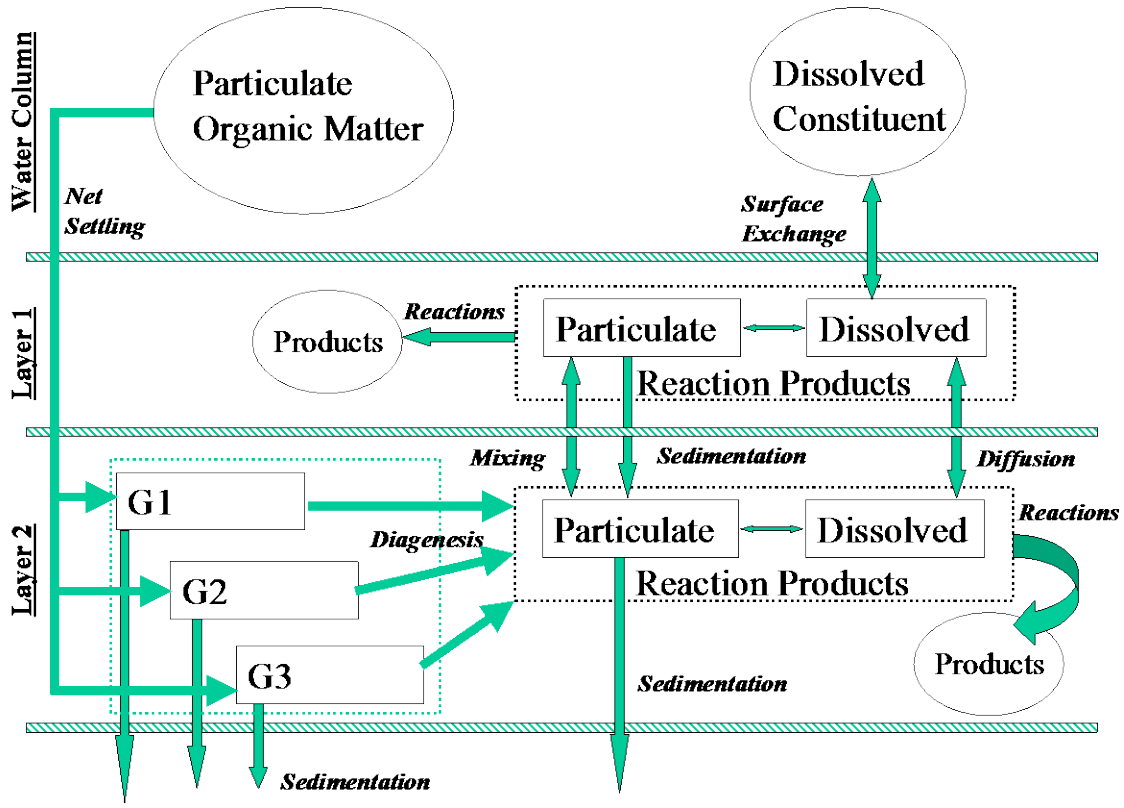

Figure A-1. Sediment Diagenesis Module (SDM) framework.

Particulate Organic Matter (POM) Fluxes (Deposition)

Fluxes of POM from the water column represent a source term for the sediments. The POM fluxes are subdivided into particulate organic carbon (C, in oxygen equivalents), nitrogen (N), and phosphorus forms (POC, PON, and POP) and then into separate forms (G classes) based on their reactivity.

The flux of POM from the water column to the sediments is computed using the standard WASP transport conventions for the following state variables: CBOD, algae, organic nitrogen, and organic phosphorus. In WASP, settling fluxes for these state variables are computed based on the specified fraction dissolved (which can vary by segment and state variable), specified particulate transport field (for the state variable), and the specified rates of solids transport (flow fields 1 to 3). The particulate organic carbon, in the diagenesis model, is in oxygen equivalent units (CBOD) as opposed to carbon units in similar models. The flux of algae to the sediment model is subdivided into carbon (oxygen equivalents), nitrogen, and phosphorus, using specified stoichiometric constants.

Internal sediment state variables for diagenesis are based on the multi-class G model, in which the organic forms are divided based on their reactivity into reactive (G1), refractory (G2), and inert (G3) forms (Figure A-1). Therefore, the fluxes of particulate organic carbon (oxygen equivalents), nitrogen, and phosphorus are subdivided into G-class fractions, based on user specified ratios. Due to the negligible thickness of the upper layer, deposition (as described later) is assumed to proceed directly from the water column to the lower (anoxic) sediment layer.

Diagenesis

Diagenesis reactions are assumed to occur in the second (anaerobic) sediment layer. The diagenesis equations are solved for each form of POM (forms for N, P, and C where C is in oxygen equivalents) and for each G class (1-3) using the same basic formulation. In order to compute the time-varying diagenesis for each modeled variable, a mass balance equation is written as:

Equation 1

$$\frac{\partial C_{T2}}{\partial t} = \frac{J_2}{H_2} - \frac{W_2}{H_2} C_{T2}^{t+\Delta t} - K_2 C_{T2}^{t+\Delta t} \approx \frac{C_{T2}^{t+\Delta t} - C_{T2}^{t}}{\Delta t}$$

where
$C_{T2}^{t+\Delta t}$ = total concentration in layer 2 at time $t+\Delta t$
C_{T2}^{t} = total concentration in layer 2 at time t (from initial conditions or computed value from previous time step)

Δt = time step (from the water quality model converted to internal units)
J_2 = flux from the water column
H_2 = thickness of the active sediment layer (input variable)
K_2 = reaction velocity (specific to chemical and G class, temperature corrected)
W_2 = net sedimentation velocity (input variable)

The mass balance equation is solved algebraically for the concentration at the present time step, as:

Equation 2

$$C_{T2}^{t+\Delta t} = \frac{J_2 \frac{\Delta t}{H_2} + C_{T2}^{t}}{1 + K_2 H_2 \frac{\Delta t}{H_2} + W_2 \frac{\Delta t}{H_2}}$$

Once the concentrations at the present time step are computed, the diagenesis source terms for reactions and transfers ($J_{T2}^{t+\Delta t}$) are computed. Diagenesis source terms are computed for C, N, and P from the sum of the product of the chemical-specific reaction velocities (K_2) and computed concentrations in each of the three G classes. For example:

Equation 3

$$J_{T2}^{t+\Delta t} = \sum_{i=1}^{3} K_{2,i} C_{T2,i}^{t+\Delta t} \quad \text{H2}$$

where

$J_{T2}^{t+\Delta t}$ = source term for total chemical in layer 2 at time $t+\Delta t$

K2,I = reaction velocity for total chemical in G class i

$C_{T2,i}^{t+\Delta t}$ = total chemical concentration for G class i

The WASP diagenesis model also contains an option for steady-state computations for use in computing the initial conditions for the model. The steady-state computations involve an iterative solution for kinetic reactions, as discussed in a following section. That is, an initial guess for the solution is specified (the initial conditions) and the computations iterated until the solution converges. The maximum number of allowable iterations and convergence criteria are specified in input. For POM diagenesis, the steady-state solution to Equation 1 is given by:

Equation 4

$$C_{T2} = \frac{\frac{J_2}{H_2}}{K_2 + \frac{W_2}{H_2}}$$

Reactions and Transfers

Overview

Once the sediment POM (C, N, and P) concentrations and source terms are computed for the present time step, as described above, the reactions and transfers are computed. Concentrations of ammonia, nitrates, methane, sulfides, silica, and phosphorus are computed and then used to compute fluxes to the overlying water column.

The total chemical concentrations are computed from mass balance relationships for each of the two sediment layers. Since the surface layer is thin (on the order of 0.1 cm) compared to the active anaerobic layer (on the order of 10 cm), it is assumed that layer 1 can be considered at steady-state in comparison to the slower processes occurring in layer 2. From Di Toro (2001; Equations 13.28 and 13.30), the two equations solved are:

Layer 1

Equation 5

$$\mathbf{0} = -s\left(f_{d1}C_{T1}^{t+\Delta t} - C_{dO}^{t+\Delta t}\right) + \omega_{12}\left(f_{p2}C_{T2}^{t+\Delta t} - f_{p1}C_{T1}^{t+\Delta t}\right) + K_{L12}\left(f_{d2}C_{T2}^{t+\Delta t} - f_{d1}C_{T1}^{t+\Delta t}\right)$$
$$-\omega_2\left(C_{T1}^{t+\Delta t} - \frac{\kappa_1^2}{s}C_{T1}^{t+\Delta t} + J_{T1}^{t+\Delta t} + C_{T2}^{t+\Delta t}\dot{H}_1^{+} - C_{T1}^{t+\Delta t}\left(\dot{H}_1 + \dot{H}_1^{-}\right)\right)$$

Layer 2

Equation 6

$$\mathbf{0} = -\omega_{12}\left(f_{p2}C_{T2}^{t+\Delta t} - f_{p1}C_{T1}^{t+\Delta t}\right) - K_{L12}\left(f_{d2}C_{T2}^{t+\Delta t} - f_{d1}C_{T1}^{t+\Delta t}\right) - \kappa_2 C_{T2}^{t+\Delta t} + \omega_2\left(C_{T1}^{t+\Delta t} - C_{T2}^{t+\Delta t}\right)$$
$$-\frac{H_2 C_{T2}^{t+\Delta t}}{\Delta t} + J_{T2}^{t+\Delta t} + \frac{H_2 C_{T2}^{t}}{\Delta t} + C_{T2}^{t+\Delta t}\dot{H}_1^{+} - C_{T2}^{t+\Delta t}\left(\dot{H}_2 + \dot{H}_1^{+}\right)$$

s = surface transfer rate; SOD/[$O_2(0)$], where SOD=SOD rate and $O_2(0)$ is the overlying water concentration
f_{d1} = fraction dissolved in layer 1
f_{d2} = fraction dissolved in layer 2
f_{p1} = fraction particulate in layer 1
f_{p2} = fraction particulate in layer 2
$C_{T1}^{t+\Delta t}$ = total concentration in layer 1 at time t+Δt
$C_{T2}^{t+\Delta t}$ = total concentration in layer 2 at time t+Δt
C_{T2}^{t} = total concentration in layer 2 at time t
$C_{dO}^{t+\Delta t}$ = concentration in overlying water column
K_{L12} = mass transfer coefficient via diffusion
ω_{12} = particle mixing coefficient between layers 1 and 2
ω_2 = sedimentation velocity for layer 2
$J_{T1}^{t+\Delta t}$ = source term for total chemical in layer 1 at time t+Δt
$J_{T2}^{t+\Delta t}$ = source term for total chemical in layer 2 at time t+Δt
κ_1^2 = square of reaction velocity in layer 1

κ_2 = reaction velocity in layer 2

$\dot{H}_1^-$ = time derivative for H in layer 1 (*not used*)

$\dot{H}_1^+$ = time derivative for H in layer 1 (*not used*)

$\dot{H}_1$ = time derivative for H in layer 1 (*not used*)

$\dot{H}_2$ = time derivative for H in layer 2 (*not used*)

H_2 = thickness of layer 2

Δt = time step

The two equations and two unknowns can be written in the form:

Equation 7

$$a_{11}x_1 + a_{12}x_2 = b_1$$

Equation 8

$$a_{21}x_1 + a_{22}x_2 = b_2$$

The equations are solved for the new concentrations ($C_{T1}^{t+\Delta t}$ and $C_{T2}^{t+\Delta t}$) using a matrix. The solution to this system of equations is (Chapra and Canale, 1998) as follows:

$$x_1 = \frac{a_{22}b_1 - a_{12}b_2}{a_{11}a_{22} - a_{12}a_{21}}$$

$$x_2 = \frac{a_{11}b_2 - a_{21}b_1}{a_{11}a_{22} - a_{12}a_{21}}$$

where the elements of the matrix are:

Equation 9

$$a_{11} = -s\left(f_{d1}\right) - \omega_{12}\left(f_{p1}\right) - K_{L12}\left(f_{d1}\right) - \omega_2 - \frac{\kappa_1^2}{s}$$

Equation 10

$$a_{21} = +\omega_{12}\left(f_{p1}\right) + K_{L12}\left(f_{d1}\right) + \omega_2$$

Equation 11

$$a_{12} = +\omega_{12}\left(f_{p2}\right) + K_{L12}\left(f_{d2}\right)$$

Equation 12

$$a_{22} = -\omega_{12}\left(f_{p2}\right) - K_{L12}\left(f_{d2}\right) - \kappa_2 - \omega_2 - \frac{H_2}{\Delta t}$$

Equation 13

$$b_1 = -J_{T1}^{t+\Delta t} = \text{-s} f_{do}\, C_{T0}^{t+\Delta t}$$

Equation 14

$$b_2 = -J_{T2}^{t+\Delta t} - \frac{H_2 C_{T2}^{t}}{\Delta t}$$

For the steady-state solution, an option in WASP used to compute the initial conditions, the elements of the matrix are modified as follows:

Equation 15

$$a_{22} = -\omega_{12}\left(f_{p2}\right) - K_{L12}\left(f_{d2}\right) - \kappa_2 - \omega_2$$

Equation 16

$$b_2 = -J_{T2}^{t+\Delta t}$$

The fraction dissolved and particulate in the two layers are computed from:

Equation 17

$$f_{d,1} = \frac{1}{1+\pi_{C1} S_1};\ f_{p,1} = \frac{\pi_{C1} S_1}{1+\pi_{C1} S_1}$$

$$f_{d,2} = \frac{1}{1+\pi_{C2} S_2};\ f_{p,2} = \frac{\pi_{C2} S_2}{1+\pi_{C2} S_2}$$

where
π_{C1} = partition coefficient for total chemical in layer 1
π_{C2} = partition coefficient for total chemical in layer 2
S1 = solids concentration in layer 1
S2 = solids concentration in layer 2

The equations are conveniently solved for the new concentrations ($C_{T1}^{t+\Delta t}$ and $C_{T2}^{t+\Delta t}$) using the matrix solution. Once the concentrations have been updated, the flux of the material to the overlying water column (J) can be computed from:

Equation 18

$$J = s\left(f_{d1} C_{T1}^{t+\Delta t} - C_{dO}^{t+\Delta t}\right)$$

The surface transfer rate(s) quantifies the mixing between layer 1 and the overlying water column, which can be related to sediment oxygen demand (SOD) by Di Toro (2001).

Equation 19

$$SOD = D\left.\frac{d[O_2]}{dz}\right|_{z=0} \approx D\frac{[O_2(0) - O_2(H_1)]}{H_1} = \frac{D}{H_1}[O_2(0)]$$

where
D = rate of oxygen diffusion
$O_2(0)$ = oxygen concentration of the overlying water
$O_2(H_1)$ = oxygen concentration at the depth H_1

assuming a straight line approximation of the derivative, so that the mass transfer coefficient ($K_{L,O2}$) may be estimated from Di Toro (2001).

Equation 20

$$K_{L,O2} = \frac{D}{H_1} = \frac{SOD}{[O_2(o)]} = s$$

The reaction rate in the aerobic layer is formulated as a first order rate (K_1), where the term in the layer 1 equation is K_1H_1. The depth of the aerobic zone follows the definition of the surface mass transfer coefficient ($s=D/H_1$) so that $K_1H_1=K_1D_1/s$, resulting in the following:

Equation 21

$$\kappa_1 = \sqrt{DK_1}$$

and

Equation 22

$$K_1H_1 = \frac{\kappa_1^2}{s}$$

which is the term applied to the total chemical in the equation for layer 1 (Equation 5).
The rate of mixing of the sediment by macrobenthos (bioturbation, w_{12}) is estimated by an apparent particle diffusion coefficient (D_p), temperature corrected that varies with the biomass of the benthos. Assuming that the mass of the benthos is proportional to the labile carbon in the sediment ($C^t_{POC,1}$, or POC, in oxygen equivalents in layer 2 in G class 1),

Equation 23

$$w^*_{12} = D_P\frac{\Theta^{(T-20)}}{H_2/2}\frac{C^t_{POC,1}}{C_{POC,R}}$$

where w_{12}^{*} is a particle mixing coefficient that is further modified as discussed below, and $C_{POC,R}$ is a reference POC concentration. Note that in the above equation and elsewhere, POC in the WASP code is in units of oxygen equivalents. Also note that the ICM code and Equation 13.1 of Di Toro (2001) use H_2 in denominator, rather than $H_2/2$, so that the user should use caution in providing the appropriate value for D_p when comparing model codes or inputs.

An additional impact is that if anoxia occurs for periods of time, the benthic population is ultimately reduced or eliminated, so that bioturbation is consequently reduced or eliminated. To include this effect, Di Toro (2001) computes the stress that low dissolved oxygen conditions (benthic stress, S) impose on the population, assuming that the stress accumulates as:

Equation 24

$$\frac{\partial S}{\partial t} = -k_s S^{t+\Delta t} + \frac{K_{M,D_p}}{K_{M,D_p} + [O_2(0)]} \approx \frac{S^{t+\Delta t} - S^t}{\Delta t}$$

where
ks = decay constant for benthic stress
$K_{M,Dp}$ = particle mixing half-saturation concentration for oxygen

which can be solved for:

Equation 25

$$S^{t+\Delta t} = \frac{S^t + \frac{K_{M,D_p}}{K_{M,D_p} + [O_2(0)]}\Delta t}{1 + k_s \Delta t}$$

As $[O_2(0)]$ approaches zero, then $(1-k_sS)$ approaches zero, so that the particle mixing coefficient is similarly reduced, as:

Equation 26

$$w_{12} = w_{12}^{*}\left(1 - k_s S^{t+\Delta t}\right)$$

The stress is continued at the minimum value for the year to conform to the observation that once the benthic population has been reduced by low dissolved oxygen, it does not recover until the next year (Di Toro, 2001).

The dissolved phase mixing coefficient between layers 1 and 2 (K_{L12}) is due to passive molecular diffusion that is enhanced by the action of organisms (bio-irrigation). The mixing coefficient is computed from Equation 13.6 (Di Toro, 2001).

Equation 27

$$K_{L12} = \frac{D_D}{H_2/2}\Theta^{(T-20)}$$

where
D_D = pore-water diffusion coefficient
$K_{L,B}$ = ratio of bio-irrigation to bio-particle mixing

Note that the ICM code uses H_2 in denominator, rather than $H_2/2$, so the user should use caution in providing the appropriate value for D_D when comparing model codes or inputs. The sediment temperature is assumed equal to the temperature of the overlying water column.

The solution of the reaction and transfer equations comprises the bulk of the computations of the diagenesis model. Part of the complexity results from the relationship of the surface transfer coefficient (s) to the sediment oxygen demand (SOD) and dissolved oxygen concentration in the overlying water column $\{O_2(0); s=SOD/[O_2(0)]\}$. Since the SOD is a function of the computed ammonia, nitrate (denitrification), sulfide (salt water), or methane (freshwater) concentrations, an iterative solution is required for those constituents. The procedure for the solution is:

1. Start with an initial estimate of the SOD
2. Solve layer 1 and 2 equations for ammonia, nitrate, sulfide and methane
    a. Solve for the ammonia flux by establishing the chemical-specific conditions
    b. Compute the oxygen consumed by nitrification (NCOD)
    c. Solve for the nitrate flux by establishing the chemical specific conditions
    d. Compute methane (freshwater) or sulfide (salt water) oxidation
        i. For salt water, compute sulfide reaction terms and compute SOD due to hydrogen sulfide
        ii. For freshwater, compute methane flux by establishing the chemical specific
            1. Compare computed and saturation concentrations and correct
            2. Calculate the CSOD due to methane
    a. Compute the total CSOD due to sulfides or methane
    b. Compute flux terms
    c. Compute the total SOD due to the sulfide or methane, adding term for NCOD
    d. Refine the estimate of SOD. A root finding method is used to make the new estimate
3. Go to step (2) if no convergence

Once the SOD is determined, then the layer 1 and 2 equations for phosphate and silica can be solved and the flux rates determined.

Computation of SOD and related reactions

As discussed above, the SOD is computed iteratively using a function Zbrent from Numerical Recipes (Press et al., 1992), which finds the root of a function without knowing the derivative. The SOD related terms are solved for each iteration, until convergence is attained. The computations require the solution of equations for ammonia, nitrate, nitrite, sulfide (salt water) or methane (freshwater) reactions, along with the carbonaceous and nitrogenous SOD. The computation of each of these terms is briefly presented below.

Ammonia

The two-layer mass balance equations for ammonia are:

Layer 1

Equation 28

$$\mathbf{0} = -s\left(f_{d1}C_{NH4T,1}^{t+\Delta t} - C_{NH4T,O}^{t+\Delta t}\right) + \omega_{12}\left(f_{p2}C_{NH4T,2}^{t+\Delta t} - f_{p1}C_{NH4T,1}^{t+\Delta t}\right)$$

$$+K_{L12}\left(f_{d2}C_{NH4T,2}^{t+\Delta t} - f_{d1}C_{NH4T,1}^{t+\Delta t}\right) - \omega_2\ C_{NH4T,1}^{t+\Delta t} - \frac{\kappa_{NH4,1}^2\theta^{T-20}}{s} f_O f_{NH4}\ f_{d1}C_{NH4T,1}^{t+\Delta t}$$

Layer 2

Equation 29

$$\mathbf{0} = -\omega_{12}\left(f_{p2}C_{NH4T,2}^{t+\Delta t} - f_{p1}C_{NH4T,1}^{t+\Delta t}\right) - K_{L12}\left(f_{d2}C_{NH4T,2}^{t+\Delta t} - f_{d1}C_{NH4T,1}^{t+\Delta t}\right)$$

$$+\omega_2(C_{NH4T,1}^{t+\Delta t} - C_{NH4T,2}^{t+\Delta t}) - \frac{H_2C_{NH4T,2}^{t+\Delta t}}{\Delta t} + J_{NH4T,2}^{t+\Delta t} + \frac{H_2C_{NH4T,2}^{t}}{\Delta t}$$

where all terms have been previously defined, with the exception of two terms for the surface layer (f_{NH4}, f_O). Note that the primary difference between the general equations presented previously and the ammonia equations are that the square of the reaction velocity in layer 1 (nitrification) is applied only to the dissolved fraction and is modified by functions based on the oxygen and ammonia concentrations. Note also that there are two separate reaction velocities that may be specified for layer 1 in the diagenesis code ($\kappa_{NH4,1}$), for fresh and salt waters respectively, with the one used based on the salinity (SAL) of the overlying water column as compared to a salinity switch (input). In addition, the reaction velocity for layer 2 is zero. The source term for ammonia in layer 2 is equal to the flux from the diagenesis of PON.

Based on the two-layer mass balance equations above, the elements in the solution matrix then become:

Equation 30

$$a_{11} = -\left(f_{d1}\right)K_{L12} - \left(f_{p1}\right)\omega_{12} - \frac{\kappa_{NH4}^2\theta^{\mathrm{T\text{-}20}}}{s}\mathbf{f_O}\ \mathbf{f_{NH4}}\ f_{d1} - \left(f_{d1}\right)s - \omega_2$$

Equation 31

$$a_{21} = +\omega_{12}\left(f_{p1}\right) + K_{L12}\left(f_{d1}\right) + \omega_2$$

Equation 32

$$a_{12} = +\omega_{12}\left(f_{p2}\right) + K_{L12}\left(f_{d2}\right)$$

Equation 33

$$a_{22} = -\omega_{12}\left(f_{p2}\right) - K_{L12}\left(f_{d2}\right) - \omega_2 - \frac{H_2}{\Delta t}$$

Equation 34

$$b_1 = -s\, C_{NH4T,O}^{t+\Delta t}$$

Equation 35

$$b_2 = -J_{NH4T,2}^{t+\Delta t} - \frac{H_2 C_{NH4T,2}^{t}}{\Delta t}$$

For the steady-state solution, an option in WASP used to compute the initial conditions, the elements of the matrix are modified as follows:

Equation 36

$$a_{22} = -\omega_{12}\left(f_{p2}\right) - K_{L12}\left(f_{d2}\right) - \omega_2$$

Equation 37

$$b_2 = -J_{NH4T,2}^{t+\Delta t}$$

The fraction dissolved and particulate in the two layers are computed from:

Equation 38

$$f_{d1} = \frac{1}{1 + \pi_{NH4} S_1}; \; f_{p1} = \frac{\pi_{NH4} S_1}{1 + \pi_{NH4} S_1}$$

$$f_{d2} = \frac{1}{1 + \pi_{NH4} S_2}; \; f_{p1} = \frac{\pi_{NH4} S_2}{1 + \pi_{NH4} S_2}$$

where
π_{NH4} = partition coefficient for ammonia
S1 = solids concentration in layer 1
S2 = solids concentration in layer 2

The modification of the nitrification reaction for dissolved oxygen is computed from:

Equation 39

$$f_O = \frac{O_{2,0}}{O_{2,0} + K_{NH4,O2}}$$

where
$O_{2,0}$ = dissolved oxygen concentration in the overlying water column
$K_{NH4,O2}$ = half-saturation concentration of dissolved oxygen in the nitrification reaction

The modification for ammonia concentrations is computed by:

Equation 40

$$f_{NH4} = \frac{K_{NH4}}{C^{t}_{NH4,1} + K_{NH4}}$$

where
$C^{t}_{NH4,1}$ = ammonia concentration from the previous time step
K_{NH4} = half-saturation concentration of ammonia in the nitrification reaction

Note that if K_{NH4} is specified in input, the f_{NH4} is computed as above. Otherwise f_{NH4}=1.

Once the ammonia concentrations have been updated, the flux to the water column is computed from:

Equation 41

$$J_{NH4} = s\left(C^{t+\Delta t}_{NH4,1} - C_{NH4,0}\right)$$

where
J_{NH4} is the flux to the water column.

In order to compute the oxygen consumption due to the oxidation of ammonia in the aerobic layer, the two-stage reaction can be represented by Chapra (1997) and Di Toro (2001)

Equation 42

$$NH_4^+ + \mathbf{1.5}O_2 \rightarrow \mathbf{2}H^+ + NO_2^- + H_2O$$

so that the consumption of oxygen during the process can be represented by Chapra (1997, Equation 23.3)

Equation 43

$$a_{no} = \frac{\mathbf{1.5(32)}}{\mathbf{14}} = \mathbf{3.43}\ \ gO\ \ gN^{-1}$$

Therefore, the contribution of the oxidation of ammonia to SOD can be estimated from:

Equation 44

$$NSOD_{NH_4} = a_{no}\frac{\kappa^{2}_{NH4,1}\theta^{T-20}}{s} f_O f_{NH4}\ f_{d1} C^{t+\Delta t}_{NH_4,1}$$

Nitrite

The two-layer mass balance equations for nitrite are:

Layer 1

Equation 45

$$\mathbf{0} = -s\left(C_{NO2,1}^{t+\Delta t} - C_{NO2,O}^{t+\Delta t}\right) + K_{L12}\left(C_{NO2,2}^{t+\Delta t} - C_{NO2,1}^{t+\Delta t}\right) - \boldsymbol{\omega}_2\ C_{NO2T,1}^{t+\Delta t}$$
$$-\frac{\boldsymbol{\kappa}_{N02,1}^2\boldsymbol{\theta}^{T-20}}{s} f_O C_{NO2,1}^{t+\Delta t} + \frac{\boldsymbol{\kappa}_{NH4,1}^2\boldsymbol{\theta}^{T-20}}{s} f_O f_{NH4}\ f_{d1} C_{NH_4,1}^{t+\Delta t}$$

Layer 2

Equation 46

$$\mathbf{0} = -K_{L12}\left(C_{NO2,2}^{t+\Delta t} - C_{NO2,1}^{t+\Delta t}\right)$$
$$+\boldsymbol{\omega}_2(C_{NO2,1}^{t+\Delta t} - C_{NO2,2}^{t+\Delta t}) - \frac{H_2 C_{NO2,2}^{t+\Delta t}}{\Delta t} + \frac{H_2 C_{NO2,2}^{t}}{\Delta t}$$

where all terms have been previously defined. Note that the primary difference between the general equations presented previously and the nitrite equations are that:

- The reaction velocity for nitrite is modified by the dissolved oxygen concentration in the overlying water column (factor f_O).
- All nitrite is assumed dissolved; therefore, the fraction particulate is zero and the rate of particle mixing zero.
- The first-stage nitrification loss from layer 1 becomes a source term for nitrite.
- The reaction velocity for layer 2 is zero.

Note also that unlike reaction rates for ammonia and nitrate-nitrogen, the reaction velocity for nitrite is assumed to not vary between fresh and salt water systems. Note also that this model assumes that the only reaction of NO_2 is nitrification to NO3. However, Wetzel (2001, pp. 217 and 513) indicates that denitrification occurs through NO_2. Any error is assumed small due to the typically small concentration of NO_2.

Based on the two-layer mass balance equations above, the elements in the solution matrix then become:

Equation 47

$$a_{11} = -K_{L12} - \frac{\boldsymbol{\kappa}_{NO2}^2\boldsymbol{\theta}^{\mathrm{T\text{-}20}}}{s}\mathbf{f_O} - s - \boldsymbol{\omega}_2$$

Equation 48

$$a_{21} = K_{L12} + \boldsymbol{\omega}_2$$

Equation 49

$$a_{12} = K_{L12}$$

Equation 50

$$a_{22} = -K_{L12} - \omega_2 - \frac{H_2}{\Delta t}$$

Equation 51

$$b_1 = -s\, C_{NO2,O}^{t+\Delta t} - \frac{\kappa_{NH4,1}^2 \theta^{T-20}}{s} f_O\, f_{NH4}\; f_{d1} C_{NH_4,1}^{t+\Delta t}$$

Equation 52

$$b_2 = -\frac{H_2 C_{NO2,2}^t}{\Delta t}$$

For the steady-state solution, an option in WASP used to compute the initial conditions, the elements of the matrix are modified as follows:

Equation 53

$$a_{22} = -K_{L12} - \omega_2$$

Equation 54

$$b_2 = 0$$

The modification of the second-stage nitrification reaction by dissolved oxygen is computed from:

Equation 55

$$f_O = \frac{O_{2,0}}{O_{2,0} + K_{NO2,O2}}$$

where
$O_{2,0}$ = dissolved oxygen concentration in the overlying water column
$K_{NO2,O2}$ = half-saturation concentration of dissolved oxygen in the second-stage nitrification reaction

Once the nitrite-concentrations have been updated, the flux to the water column is computed from:

Equation 56

$$J_{NO2} = s\left(C_{NO2,1}^{t+\Delta t} - C_{NO2,0}\right)$$

where
J_{NO2} is the nitrite flux to the water column. Note that in WASP, nitrite is not a state variable and the water column concentration is assumed to equal zero.

In order to compute the oxygen consumption due to the oxidation of ammonia in the aerobic layer, the second state of the nitrification reaction can be represented by Chapra (1997).

Equation 57

$$NO_2^- + \mathbf{0.5}O_2 \rightarrow NO_3^-$$

so that the consumption of oxygen during the process can be represented by Chapra (1997, Equation 23.4).

Equation 58

$$a_{no2} = \frac{\mathbf{0.5(32)}}{\mathbf{14}} = \mathbf{1.14}\ \ gO\ \ gN^{-1}$$

Therefore, the contribution of the oxidation of ammonia to SOD can be estimated from:

Equation 59

$$NSOD_{NO2} = a_{no2}\frac{\kappa_{NO2,1}^2\theta^{T-20}}{s} f_O C_{NO2,1}^{t+\Delta t}$$

Nitrate

The two-layer mass balance equations for nitrate are:

Layer 1

Equation 60

$$\mathbf{0} = -s\left(C_{NO3,1}^{t+\Delta t} - C_{NO3,O}^{t+\Delta t}\right) + K_{L12}\left(C_{NO3,2}^{t+\Delta t} - C_{NO3,1}^{t+\Delta t}\right) - \omega_2\ C_{NO3,1}^{t+\Delta t} - \frac{\kappa_{NO3,1}^2}{s} C_{NO3,1}^{t+\Delta t}$$
$$+ \frac{\kappa_{N02,1}^2\theta^{T-20}}{s} f_O C_{NO2,1}^{t+\Delta t}$$

Layer 2

Equation 61

$$\mathbf{0} = -K_{L12}\left(C_{NO3,2}^{t+\Delta t} - C_{NO3,1}^{t+\Delta t}\right) + \omega_2(C_{NO3,1}^{t+\Delta t} - C_{NO3,2}^{t+\Delta t}) - \frac{H_2 C_{NO3,2}^{t+\Delta t}}{\Delta t}$$

$$-\kappa_{NO3,2} C_{NO3,2}^{t+\Delta t} + \frac{H_2 C_{NO3,2}^{t}}{\Delta t}$$

where all terms have been previously defined. Note that the primary difference between the general and nitrate equations is that there is no sorption so the total and dissolved concentrations are equal. For nitrate, there is a reaction velocity due to denitrification for both layers 1 and 2.

The second-stage nitrification rate becomes a source term for layer 1. Note also that there are two separate denitrification reaction velocities specified for each layer ($\kappa_{NO3,1}$ and $\kappa_{NO3,2}$), for fresh and salt waters with the one used based on the salinity (SAL) as compared to a salinity switch (SALTND, input).

Based on the two-layer mass balance equations above, the elements in the solution matrix then become:

Equation 62

$$a_{11} = -K_{L12} - \frac{\kappa_{NO3,1}^2 \theta^{\text{T-20}}}{s} - s - \omega_2$$

Equation 63

$$a_{21} = K_{L12} + \omega_2$$

Equation 64

$$a_{12} = K_{L12}$$

Equation 65

$$a_{22} = -K_{L12} - \kappa_{NO3,2}\theta^{\text{T-20}} - \omega_2 - \frac{H_2}{\Delta t}$$

Equation 66

$$b_1 = -s\, C_{NO3,O}^{t+\Delta t} - \frac{\kappa_{NO3,1}^2 \theta^{T-20}}{s} f_O C_{NO2,1}^{t+\Delta t}$$

Equation 67

$$b_2 = -\frac{H_2 C^t_{NO3,2}}{\Delta t}$$

For the steady-state solution, an option in WASP used to compute the initial conditions, the elements of the matrix are modified as follows:

Equation 68

$$a_{22} = -K_{L12} - \kappa_{NO3,2}\theta^{\mathrm{T-20}} - \omega_2$$

Equation 69

$$b_2 = \mathbf{0}$$

Once the nitrate concentrations have been updated, the flux to the water column is computed from:

Equation 70

$$J_{NO3} = s\left(C^{t+\Delta t}_{NO3,1} - C_{NO3,0}\right)$$

where
J_{NO3} is the flux to the water column

The process of denitrification requires a carbon source as indicated by Di Toro (2001, Equation 9.16)

Equation 71

$$\frac{10}{8}CH_2O + H^+ + NO_3^- \rightarrow \frac{10}{8}CO_2 + \frac{1}{2}N_2 + \frac{7}{4}H_2O$$

so that the carbon to nitrogen stoichiometric coefficient (a_{cn}) is 1.071 gC gN^{-1}. The oxidation of methane in the aerobic zone may be represented by:

Equation 72

$$\frac{1}{2}CH_4 + O_2 \rightarrow \frac{1}{2}CO_2 + H_2O$$

so the oxygen to carbon stoichiometric coefficient (a_{oc}) is 2.67 g O g C^{-1}.

If all of the carbon produced by the diagenesis reaction was converted to methane and fully oxidized, the maximum SOD that could be produced would be:

Equation 73

$$J_{O_2,C} = J_{C,2}^{t+\Delta t}$$

where in WASP, J_c is in oxygen equivalents.

However, this maximum is reduced by the carbon utilized during denitrification, so that the maximum oxygen utilization becomes:

Equation 74

$$J_{O_2,C} = J_{C,2}^{t+\Delta t} - a_{oc}a_{cn}\left[\frac{\kappa_{NO3,1}\Theta^{T-20}C_{NO3,1}^{t+\Delta t}}{S} + \kappa_{NO3,2}\Theta^{T-20}C_{NO3,2}^{t+\Delta t}\right]$$

where $a_{oc}a_{cn}$ is 2.857.

Sulfides

Note that sulfide reactions are only computed in the WASP model for salt water systems (salinity greater than a salt switch, SALTSW). The two-layer mass balance equations for sulfide are:

Layer 1

Equation 75

$$\mathbf{0} = -s\left(f_{d1}C_{H2S,1}^{t+\Delta t} - C_{H2S,O}^{t+\Delta t}\right) + \omega_{12}\left(f_{p2}C_{H2S,2}^{t+\Delta t} - f_{p1}C_{H2S,1}^{t+\Delta t}\right) + K_{L12}\left(f_{d2}C_{H2S,2}^{t+\Delta t} - f_{d1}C_{H2S,1}^{t+\Delta t}\right)$$
$$-\omega_2\, C_{H2S,1}^{t+\Delta t} - f_O\left[\frac{\kappa_{D,H2S,1}^2}{S} f_{d1} + \frac{\kappa_{P,H2S,1}^2}{S} f_{p1}\right]C_{H2S,1}^{t+\Delta t}$$

Layer 2

Equation 76

$$\mathbf{0} = -\omega_{12}\left(f_{p2}C_{H2S,2}^{t+\Delta t} - f_{p1}C_{H2S,1}^{t+\Delta t}\right) - K_{L12}\left(f_{d2}C_{H2S,2}^{t+\Delta t} - f_{d1}C_{H2S,1}^{t+\Delta t}\right) + \omega_2(C_{H2S,1}^{t+\Delta t} - C_{H2S,2}^{t+\Delta t})$$
$$-\frac{H_2C_{HS,2}^{t+\Delta t}}{\Delta t} + J_{HS,2}^{t+\Delta t} + \frac{H_2C_{HS,2}^{t}}{\Delta t}$$

where all terms have been previously defined. Note that the primary difference between the ammonia and sulfide equations is that there are separate reaction velocities in layer 1 for the dissolved and particulate forms.

Based on the two-layer mass balance equations above, the elements in the solution matrix then become:

Equation 77

$$a_{11} = -\left(f_{d1}\right) K_{L12} - \left(f_{p1}\right)\omega_{12} - \frac{\left(\kappa^2_{HS,D} f_{D,1} + \kappa^2_{HS,P} f_{P,1}\right)\theta^{\text{T-20}}}{s} \mathbf{f_O} - \left(f_{d1}\right) s - \omega_2$$

Equation 78

$$a_{21} = +\omega_{12}\left(f_{p1}\right) + K_{L12}\left(f_{d1}\right) + \omega_2$$

Equation 79

$$a_{12} = +\omega_{12}\left(f_{p2}\right) + K_{L12}\left(f_{d2}\right)$$

Equation 80

$$a_{22} = -\omega_{12}\left(f_{p2}\right) - K_{L12}\left(f_{d2}\right) - \omega_2 - \frac{H_2}{\Delta t}$$

Equation 81

$$b_1 = \mathbf{0}$$

Equation 82

$$b_2 = -J_{OC} - \frac{H_2 C^t_{HS,2}}{\Delta t}$$

where the $J_{HS,2}$ flux (Equation 76) is expressed as an oxygen equivalent flux (J_{OC}) computed from Equation 74.

For the steady-state solution, an option in WASP used to compute the initial conditions, the elements of the matrix are modified as follows:

Equation 83

$$a_{22} = -\omega_{12}\left(f_{p2}\right) - K_{L12}\left(f_{d2}\right) - \omega_2$$

Equation 84

$$b_2 = -J_{OC}$$

The fraction dissolved and particulate in the two layers are computed from:

Equation 85

$$f_{d1} = \frac{1}{1 + \pi_{HS,1} S_1}; \; f_{p1} = \frac{\pi_{HS,1} S_1}{1 + \pi_{HS,1} S_1}$$

$$f_{d2} = \frac{1}{1 + \pi_{HS,2} S_2}; \; f_{p1} = \frac{\pi_{HS,2} S_2}{1 + \pi_{HS,2} S_2}$$

where
$\pi_{HS,1}$ = partition coefficient for sulfides in layer 1
$\pi_{HS,2}$ = partition coefficient for sulfides in layer 2
S1 = solids concentration in layer 1
S2 = solids concentration in layer 2

The dissolved oxygen correction to the surface reaction is computed from (with KMHSO2 being the sulfide oxidation normalization constant):

Equation 86

$$f_O = \frac{O_{2,0}}{K_{MHS,O2}}$$

The primary other difference is that partition coefficients are specified separately for the two layers, so that:

Equation 87

$$f_{d,1} = \frac{1}{1 + \pi_{H2S,1} S_1}; \; f_{p,1} = \frac{\pi_{H2S,1} S_1}{1 + \pi_{H2S,1} S_1}$$

Equation 88

$$f_{d,2} = \frac{1}{1 + \pi_{H2S,2} S_2}; \; f_{p,1} = \frac{\pi_{H2S,2} S_2}{1 + \pi_{H2S,2} S_2}$$

where
$\pi_{H2S,1}$ = partition coefficient for sulfide in layer 1
$\pi_{H2S,2}$ = partition coefficient for sulfide in layer 2
S1 = solids concentration in layer 1
S2 = solids concentration in layer 2

There is no external source term for sulfides in layer 1. The source term for layer 2 is computed from the carbon diagenesis term (Equation 74), in oxygen equivalents and corrected for denitrification, since denitrification requires a carbon source and is a sink for carbon. Once the sulfide concentrations have been updated, the flux to the water column is computed from:

Equation 89

$$J_{H2S} = s\ f_{D1} C_{H2S,1}^{t+\Delta t}$$

where
J_{H2S} is the flux to the water column.

The SOD due to carbonaceous demand is then computed from:

Equation 90

$$CSOD_{HS} = \frac{\left(\kappa_{HS,D}^2 f_{D,1} + \kappa_{HS,P}^2 f_{P,1}\right)\theta^{T-20}}{s} \mathbf{f_O}\ C_{H2S,1}^{t+\Delta t}$$

Methane

In WASP, methane fluxes are only computed for freshwater systems (where the salinity (SAL) is less than a specified quantity (SALTSW). The first consideration in the computation of methane fluxes is that the maximum methane production, in oxygen equivalents, is related to the carbon diagenesis (J_{OC}), corrected for denitrification (Equation 74). Assuming complete oxidation, the maximum carbonaceous SOD that can be exerted is (Chapra, 2000; Di Toro, 2001):

Equation 91

$$CSOD_{max} = \sqrt{2 K_{L12} C_S J_{O2}}$$

or (for computed $CSOD_{max} > J_{O2}$)

Equation 92

$$CSOD_{max} = J_{O2}$$

where K_{L12} was defined previously and C_s the saturation methane concentration, computed from (Di Toro, 2001, Equation 10.51)

Equation 93

$$\mathbf{C_{CH4,SAT} = 100\left(1 + \frac{H_O}{10}\right)1.024^{(20-T)}}$$

where H_o is the depth of the water column over the sediment. As indicated, if the computed $CSOD_{max}$ exceeds the available carbon flux (J_{OC} in oxygen equivalents and corrected for denitrification), then $CSOD_{max}$ is set equal to that flux ($CSOD_{max}=J_{OC}$).

The flux of dissolved methane at the sediment water interface can be computed from (Chapra 2000, Eq. 25.43; Di Toro, 2001 Eq. 10.32):

Equation 94

$$J_{out} = CSOD_{\max}\ Sech(\lambda_c H_1)$$

where (Di Toro, 2001, Equation 10.39)

Equation 95

$$\lambda_c H_1 = \frac{\kappa_{CH4,1}\theta^{(T-20)/2}}{s})$$

Note that the temperature correction in the above equation is reflected in the ICM code (Cerco and Cole, 1995) and elsewhere. The hyperbolic secant (Sech) is computed as:

Equation 96

$$Sech(x) = \frac{2}{e^x + e^{-x}}$$

Methane may be oxidized, producing sediment oxygen demand (SOD), or exchanged with the water column in either gaseous or dissolved form. The carbonaceous SOD can be computed from:

Equation 97

$$CSOD_{CH4} = CSOD_{\max}(1 - Sech(\lambda_c H_1))$$

and the fluxes of dissolved and gaseous methane can be computed from:

Equation 98

$$J[CH_4(aq)] = CSOD_{\max} - CSOD_{CH4}; \quad J[CH_4(g)] = J_{OC} - J[CH_4(aq)] - CSOD_{CH4}$$

SOD

Once the concentrations of materials affecting oxygen are computed, and the stoichiometric relationships described above applied, the SOD is computed from:

Equation 99

$$SOD = CSOD_{HS} + CSOD_{NH4} + CSOD_{NO2}$$

for salt water systems or

Equation 100

$$SOD = CSOD_{CH4} + CSOD_{NH4} + CSOD_{NO2}$$

for freshwater systems, where the oxygen demands due to sulfide (Equation 90), methane (Equation 97), and nitrification (Equation 44 and Equation 59) were defined previously. Note that in the iterative solution for s, the SOD computed for this computational step is compared to that from the previous iteration and, as discussed above, if it differs by more than a specified amount, a new value of s is computed and the solution iterated.

Computation of silica and phosphate

As discussed above, the SOD is computed iteratively in order to determine the value of s (the surface sediment transfer rate). Once completed, the concentrations of phosphate and ammonia, which do not affect SOD, are computed. The computations for silica and phosphate are similar to those described above and briefly presented below.

Silica

The two-layer mass balance equations for silica are:

Layer 1

Equation 101

$$\mathbf{0} = -s\left(f_{d1}C_{Si,1}^{t+\Delta t} - C_{Si,O}^{t+\Delta t}\right) + \omega_{12}\left(f_{p2}C_{Si,2}^{t+\Delta t} - f_{p1}C_{Si,1}^{t+\Delta t}\right)$$
$$+K_{L12}\left(f_{d2}C_{Si,2}^{t+\Delta t} - f_{d1}C_{Si,1}^{t+\Delta t}\right) - \omega_2\ C_{Si,1}^{t+\Delta t}$$

Layer 2

Equation 102

$$\mathbf{0} = -\omega_{12}\left(f_{p2}C_{Si,2}^{t+\Delta t} - f_{p1}C_{Si,1}^{t+\Delta t}\right) - K_{L12}\left(f_{d2}C_{Si,2}^{t+\Delta t} - f_{d1}C_{Si,1}^{t+\Delta t}\right) + \omega_2(C_{Si,1}^{t+\Delta t} - C_{Si4,2}^{t+\Delta t})$$
$$-\kappa_3 C_{Si,2}^{t+\Delta t} - \frac{H_2 C_{Si,2}^{t+\Delta t}}{\Delta t} + J_{Si,2}^{t+\Delta t} + \frac{H_2 C_{Si,2}^{t}}{\Delta t}$$

where all terms have been previously defined. Note that the primary difference between the general equations presented previously and the silica equations is that there are no silica source terms or reactions in the aerobic layer. In the anaerobic layer (layer 2), the reaction rate is applied only to the dissolved fraction.

Based upon the two-layer mass balance equations above, the elements in the solution matrix then become:

Equation 103

$$a_{11} = -\left(f_{d1}\right)K_{L12} - \left(f_{p1}\right)\omega_{12} - \omega_2$$

Equation 104

$$a_{21} = +\omega_{12}\left(f_{p1}\right) + K_{L12}\left(f_{d1}\right) + \omega_2$$

Equation 105

$$a_{12} = +\omega_{12}\left(f_{p2}\right) + K_{L12}\left(f_{d2}\right)$$

Equation 106

$$a_{22} = -\omega_{12}\left(f_{p2}\right) - K_{L12}\left(f_{d2}\right) - \omega_2 - \kappa_3 - \frac{H_2}{\Delta t}$$

Equation 107

$$b_1 = -s\, C_{Si,O}^{t+\Delta t}$$

Equation 108

$$b_2 = -J_{Si}^{t+\Delta t} - \frac{H_2 C_{Si,2}^{t}}{\Delta t}$$

For the steady-state solution, an option in WASP used to compute the initial conditions, the elements of the matrix are modified as follows:

Equation 109

$$a_{22} = -\omega_{12}\left(f_{p2}\right) - K_{L12}\left(f_{d2}\right) - \omega_2 - \kappa_3$$

Equation 110

$$b_2 = -J_{Si,2}^{t+\Delta t}$$

The fraction dissolved and particulate in the two layers are computed from:

Equation 111

$$f_{d1} = \frac{1}{1 + \pi_{Si,1} S_1};\ f_{p1} = \frac{\pi_{Si,1} S_1}{1 + \pi_{Si,1} S_1}$$

$$f_{d2} = \frac{1}{1 + \pi_{Si,2} S_2};\ f_{p1} = \frac{\pi_{Si,2} S_2}{1 + \pi_{Si,2} S_2}$$

where
$\pi_{Si,1}$ = partition coefficient for Silica in layer 1
$\pi_{Si,1}$ = partition coefficient for Silica in layer 2

S1 = solids concentration in layer 1
S2 = solids concentration in layer 2

The partition coefficient in the anaerobic layer is set to an input value. For layer 1, the aerobic layer, if the oxygen concentration in the overlying water column exceeds a critical concentration (specified in input), then the partition coefficient is increased to represent the trapping of silica, or sorption onto iron oxyhydroxide. If the dissolved oxygen is below the critical value, then the sorption coefficient in layer 1 goes to zero as in (Di Toro, 2001, Eq. 7.18)

Equation 112

$$\pi_{Si,1} = \pi_{Si,2}\left(\Delta\pi_{Si,1}\right) \; for \left[O_2(0)\right] > \left[O_2(0)\right]_{crit,Si}$$

and

Equation 113

$$\pi_{Si,1} = \pi_{Si,2}\left(\Delta\pi_{Si,1}\right)^{\beta_{Si}} \; for \left[O_2(0)\right] \le \left[O_2(0)\right]_{crit,Si}$$

where $\beta_{PO4} = \dfrac{\left[O_2(0)\right]}{\left[O_2(0)\right]_{crit,PO4}}$

and $\Delta\pi_{Si}$ is a specified incremental change.

The expression for silica dissolution in the anaerobic layer, modified by the Michaelis-Menton dependency of the dissolution rate on particulate silica, is given by (Di Toro, 2001, Eq. 7.16):

Equation 114

$$S_{Si} = k_{Si}\Theta^{(T-20)}\frac{P_{Si}}{P_{Si}+K_{m,PSi}}\left(C_{Si,sat} - f_{d,2}C_{si,2}^{t+\Delta t}\right)$$

where
P_{Si} = the biogenic silica diagenesis flux to which detrital silica was added
$K_{m,Psi}$ = half saturation constant (KMPSI)
k_{Si} = rate of silica dissolution (KADSA from water quality model)
$C_{Si,sat}$ = saturation concentration for silica ($C_{SI,sat}$, an input value)

Based on Equation 114, the loss term (κ_3) and source term for the sediments ($J_{Si,2}^{t+\Delta t}$) are then specified as:

Equation 115

$$\kappa_3 = k_{Si}\Theta^{(T-20)} f_{d,2}\frac{P_{Si}}{P_{Si}+K_{m,PSi}}$$

and

Equation 116

$$J_{Si,2}^{t+\Delta t} = k_{Si}\Theta^{(T-20)}\frac{P_{Si}}{P_{Si}+K_{m,PSi}}C_{Si,sat}$$

Once the silica concentrations have been updated, the flux to the water column is computed from:

Equation 117

$$J_{Si} = s\left(C_{Si,1}^{t+\Delta t} - C_{Si,0}\right)$$

where J_{Si} is the flux to the water column.

Phosphate

The two-layer mass balance equations for phosphate are:

Layer 1

Equation 118

$$\mathbf{0} = -s\left(f_{d1}C_{PO4,1}^{t+\Delta t} - C_{PO4,O}^{t+\Delta t}\right) + \omega_{12}\left(f_{p2}C_{PO4,2}^{t+\Delta t} - f_{p1}C_{PO4,1}^{t+\Delta t}\right)$$
$$+K_{L12}\left(f_{d2}C_{PO4,2}^{t+\Delta t} - f_{d1}C_{PO4,1}^{t+\Delta t}\right) - \omega_2 C_{PO4,1}^{t+\Delta t}$$

Layer 2

Equation 119

$$\mathbf{0} = -\omega_{12}\left(f_{p2}C_{PO4,2}^{t+\Delta t} - f_{p1}C_{PO4,1}^{t+\Delta t}\right) - K_{L12}\left(f_{d2}C_{PO4,2}^{t+\Delta t} - f_{d1}C_{PO4,1}^{t+\Delta t}\right) + \omega_2(C_{PO4,1}^{t+\Delta t} - C_{PO44,2}^{t+\Delta t})$$
$$-\frac{H_2 C_{PO4,2}^{t+\Delta t}}{\Delta t} + J_{PO4,2}^{t+\Delta t} + \frac{H_2 C_{PO4,2}^{t}}{\Delta t}$$

where all terms have been previously defined. Note that the primary difference between the general equations presented previously and the phosphate equations is that there are no reactions in either layer.

Based on the two-layer mass balance equations above, the elements in the solution matrix then become:

Equation 120

$$a_{11} = -\left(f_{d1}\right)K_{L12} - \left(f_{p1}\right)\omega_{12} - (f_{d1})s - \omega_2$$

Equation 121

$$a_{21} = +\omega_{12}\left(f_{p1}\right) + K_{L12}\left(f_{d1}\right) + \omega_2$$

Equation 122

$$a_{12} = +\omega_{12}\left(f_{p2}\right) + K_{L12}\left(f_{d2}\right)$$

Equation 123

$$a_{22} = -\omega_{12}\left(f_{p2}\right) - K_{L12}\left(f_{d2}\right) - \omega_2 - \frac{H_2}{\Delta t}$$

Equation 124

$$b_1 = -s\, C_{PO4,O}^{t+\Delta t}$$

Equation 125

$$b_2 = -J_{PO4,2}^{t+\Delta t} - \frac{H_2 C_{PO4,2}^{t}}{\Delta t}$$

For the steady-state solution, an option in WASP used to compute the initial conditions, the elements of the matrix are modified as follows:

Equation 126

$$a_{22} = -\omega_{12}\left(f_{p2}\right) - K_{L12}\left(f_{d2}\right) - \omega_2$$

Equation 127

$$b_2 = -J_{PO4,2}^{t+\Delta t}$$

The fraction dissolved and particulate in the two layers are computed from:

Equation 128

$$f_{d,1} = \frac{1}{1 + \pi_{PO4,1} S_1}; \; f_{p,1} = \frac{\pi_{PO4,1} S_1}{1 + \pi_{PO4,1} S_1}$$

$$f_{d,2} = \frac{1}{1 + \pi_{PO4,2} S_2}; \; f_{p,1} = \frac{\pi_{PO4,2} S_2}{1 + \pi_{PO4,2} S_2}$$

where

$\pi_{PO4,i}$ = partition coefficient for silica in layer i (PIE2)
S1 = solids concentration in layer 1 (M1)
S2 = solids concentration in layer 2 (M2)

The partition coefficient in the anaerobic layer is set to an input value. For layer 1, the aerobic layer, if the oxygen concentration in the overlying water column exceeds a critical concentration (O2CRIT, specified in input), then the partition coefficient is increased to represent the trapping of phosphates, or sorption onto iron oxyhydroxide. If the dissolved oxygen is below the critical value, then the sorption coefficient in layer 1 goes to zero as in (Di Toro, 2001, Eq. 6.19).

Equation 129

$$\pi_{PO4,1} = \pi_{PO4,2}\left(\Delta\pi_{PO4,1}\right) \; for \left[O_2(0)\right] > \left[O_2(0)\right]_{crit}$$

and

$$\pi_{PO4,1} = \pi_{PO4,2}\left(\Delta\pi_{PO4,1}\right)^{\beta_{PO4}} \; for \left[O_2(0)\right] \le \left[O_2(0)\right]_{crit}$$

where $\beta_{PO4} = \dfrac{\left[O_2(0)\right]}{\left[O_2(0)\right]_{crit,PO4}}$

and $\Delta\pi_{PO4}$ is a specified incremental change (which is set to either a freshwater or salt water input value).

The source term for layer 2 is a result of the phosphate produced by sediment diagenesis to which is added the flux of inorganic phosphorus from the water column. Once the phosphate concentrations have been updated, the flux to the water column is computed from:

Equation 130

$$J_{PO4} = s\left(C^{t+\Delta t}_{PO4,1} - C_{PO4,0}\right)$$

Links with FVCOM-ICM

Khangaonkar et al. (2012a,b) describes the previous development, testing, and calibration of the water quality model. In summary, FVCOM is used to develop temperature, salinity, free surface heights and elevations, velocity components, and boundary fluxes. These outputs are then used to drive the ICM kinetic equations. ICM uses 19 state variables, including two species of algae, dissolved and particulate carbon, and nutrients to simulate the carbon cycle accounting for algal production and decay and the impact on DO. Phytoplankton primary productivity, inorganic and organic carbon fluxes, and nitrogen sources and sinks are computed and compared with measured data during model calibration (Khangaonkar et al., 2012b).

We modified the following subroutines and processes to couple the bottom water layer with the surface sediment layer:

- SED_READ - Subroutine to read control information for the Sediment Diagenesis Module (SDM).
- SED_INIT - Subroutine to initiate SDM variables and parameters.
- SED_ALLOC - Subroutine to allocate arrays related to SDM.

- SED_DEALLOC - Subroutine to de-allocate arrays related to SDM.
- SED_CALC - Subroutine to carry out SDM calculations by solving time-dependent, two-layer sediment concentration equations for each cell. A new subroutine was created to handle output of sediment fluxes to output files.
- SEDTSFNL - Subroutine to solve 2x2 set time varying equations for the two sediment layers.
- SEDSSFNL - Subroutine to solve 2x2 set steady-state equations for the two sediment layers (mainly for methane generation in the system, where a 3-layer redox process can be reduced to 2-layer under assumption of steady state).
- MODULE FILE_INFO - Module that defines water column constituents and SDM variables. The SFM arrays were moved to SFM module and subroutine SED_INIT.
- INIT_FILE_INFO - Subroutine within Module FILE_INFO which defines water column and SFM constituents as well as file units for input and output. We expect to move file units and variables related to SDM to SED_INIT.
- PARWQM - Main program of FVCOM-ICM water quality model which issues the call to SFM module when it is activated, and also moves de-allocation of sediment variables into SED_DEALLOC.
- ALLOC_WQM - Subroutine used for allocating both water-column water quality variables and variables related to SDM. We moved all SDM variables to SED_ALLOC.
- INPUTS - Subroutine for reading model input files. This file was modified to call SED_READ for reading SDM related input files.
- NITROG - Subroutine for water column nitrogen calculation, where nitrate (NO3) and ammonia (NH4) source terms include contributions from sediment flux of nitrate and ammonia, respectively, from the SDM.
- OXYGEN - Subroutine for water column oxygen calculation, where oxygen sink terms include contribution from SDM.
- SED_INIT_ICI - Subroutine to read sediment initial condition if not using steady state solution to initialize SDM.
- SED_INIT2 - Subroutine to calculate some of the total concentrations and initialize temperature-dependent rates based on dissolved constituents as initial condition and temperature related parameters.
- POM_ACCMUL - Subroutine to calculate accumulation of particulate organic matter (POM) through settling of phytoplankton, zooplankton, and detritus from water column.

References for Appendix A

Cerco, C.F. and T. Cole. 1993. Three-dimensional eutrophication model of Chesapeake Bay. *Journal of Environmental Engineering. 119*:1006-1025.

Cerco, C.F. and T.M. Cole. 1991. "Thirty year simulation of Chesapeake Bay Dissolved Oxygen," in *Environmental Hydraulics*, J.H. Lee and Y.K. Cheung, eds. Balkema, Rotterdam, 771-776.

Cerco, C.F. and T.M. Cole. 1992. "Thirty year simulation of Chesapeake Bay eutrophication," In Estuarine and Coastal Modeling, M. L. Spaulding, K. Bedford, A. Blumberg, R. Chen, and C. Swanson, eds. ASCE, 116-126.

Cerco, C.F. 1995. "Response of Chesapeake Bay to nutrient load reductions," ASCE J. Environmental Engineering Div. 121(8), 549-557.

Cerco, C.F. and T.M. Cole. 1995. "User documentation for Release Version 1.0 of the CE-QUAL-ICM Three Dimensional Eutrophication Model," Technical Report EL-95-1, U.S. Army Corps of Engineers, Waterways Experiment Station, Vicksburg, MS.

Chapra, S.C. 1997. *Surface Water-Quality Modeling*, McGraw-Hill, New York, New York, 844 pp.

Di Toro, D.M. 2001. *Sediment Flux Modeling*, Wiley-Interscience, New York, New York. 624 pp.

Di Toro, D.M., Paquin, P.R., Subburamu, K., and Gruber, D.A. 1990. Sediment oxygen demand model: methane and ammonia oxidation. *J. Environ. Engr. ASCE,* 116:945-986.

Di Toro, D.M. and J.F. Fitzpatrick. 1993. Chesapeake Bay sediment flux model. Tech. Report EL-93-2, U.S. Army Corps of Engineers, Waterways Experiment Station, Vicksburg, MS, 316 pp.

Di Toro, D.M., J.F. Fitzpatrick, and T.R. Isleib. 1994. "A model of manganese and iron fluxes from sediments," Contract Report W-94-1, U.S. Army Corps of Engineers, Waterways Experiment Station, Vicksburg, MS, 76 pp.

USACE. 2001. "Development of a Suspension Feeding and Deposit Feeding Benthos Model for Chesapeake Bay," Developed by the USACE Waterways Experiment Station for the Chesapeake Bay Program (contract report DACW39-96-D-0001), 177 pp.

Appendix B. Comparison of Ecology's SedFlux.xlsm with Professor James Martin's SED_JLM.FOR

The sediment flux model (SFM) developed for the EPA's WASP model has previously undergone rigorous review and testing (Martin, 2002). Professor James Martin at Mississippi State University has developed a stand-alone testing tool called SED_JLM.FOR that provides identical results compared with the WASP SFM. Ecology, in collaboration with Dr. Martin, also developed an Excel VBA version of the SFM called 'SedFlux.xlsm' that predicts nearly identical results (same within +/- 0.001%) compared with the SED_JLM.FOR for both time-variable and steady-state solutions (Ecology, 2013).

This appendix documents the results of comparison of Martin's SED_JLM.FOR with Ecology's SedFlux.xlsm tool for the time-variable model using the following test inputs using a model time step of 0.01 days:

Deposition fluxes from overlying water into the sediment:
Jcin = 0.3 gO2/m^2/d (deposition of POC)
Jnin = 0.005 gN/m^2/d (deposition of PON)
Jpin = 0.003 gP/m^2/d (deposition of POP)

Overlying water quality:
O20 = 5 mg/L (dissolved oxygen)
Depth = 2 m (depth of water)
Tw = 15 deg C (temperature)
NH30 = 0.015 mgN/L (ammonium N)
NO30 = 0.1 mgN/L (nitrate+nitrite)
PO40 = 0.004 mgP/L (soluble reactive P)
CH40 = 0 mg/L (dissolved organic C)
SALw = 30 psu (salinity)

Table B-1 presents the assumed initial conditions. Table B-2 presents the assumed kinetic rate parameter values.

Figures B-1 through B-10 show the comparison of results for SED_JLM and SedFlux.xlsm.

Table B-1. SedFlux.xls - Input of initial conditions (only used for Time Variable 2 option)

Name	Symbol	Units	Input value
Particulate organic C, N, and P in layer 2			
G class 1 POC in layer 2	POC2(1)	gO2/m^3	100.000
G class 2 POC in layer 2	POC2(2)	gO2/m^3	800.000
G class 3 POC in layer 2	POC2(3)	gO2/m^3	9100.000
G class 1 PON in layer 2	PON2(1)	gN/m^3	10.000
G class 2 PON in layer 2	PON2(2)	gN/m^3	80.000
G class 3 PON in layer 2	PON2(3)	gN/m^3	910.000
G class 1 POP in layer 2	POP2(1)	gP/m^3	2.500
G class 2 POP in layer 2	POP2(2)	gP/m^3	20.000
G class 3 POP in layer 2	POP2(3)	gP/m^3	227.500
Dissolved constituents in layer 1 and 2 porewater			
Dissolved ammonia N in layer 1 porewater	NH3(1)	mgN/L	0.000
Dissolved ammonia N in layer 2 porewater	NH3(2)	mgN/L	0.000
Dissolved nitrate+nitrite N in layer 1 porewater	NO3(1)	mgN/L	0.000
Dissolved nitrate+nitrite N in layer 2 porewater	NO3(2)	mgN/L	0.000
Dissolved phosphate P in layer 1 porewater	PO4(1)	mgP/L	0.000
Dissolved phosphate P in layer 2 porewater	PO4(2)	mgP/L	0.000

Table B-2. SedFlux.xls - Input of rate parameter values

Name	Symbol	Units	Input value
solids concentration in aerobic layer 1	m1	kgD/L	0.5
solids concentration in anaerobic layer 2	m2	kgD/L	0.5
bioturbation particle mixing coefficient	Dp	m^2/d	0.00006
pore water diffusion coefficient	Dd	m^2/d	0.0025
deep burial velocity	w2	m/d	6.85E-06
thickness of sediment anaerobic layer 2	H2	m	0.1
Reaction velocities			
freshwater nitrification velocity	KappaNH3f	m/d	0.1313
saltwater nitrification velocity	KappaNH3s	m/d	0.1313
freshwater denitrification velocity in layer 1	KappaNO3_1f	m/d	0.1
saltwater denitrification velocity in layer 1	KappaNO3_1s	m/d	0.1
denitrfication in the anaerobic layer 2	KappaNO3_2	m/d	0.025
methane oxidation in the aerobic layer 1	KappaCH4	m/d	0.7
Half saturation constants			
nitrification half saturation for NH4N	KM_NH3	mgN/L	0.728
nitrification half saturation for O2	KM_O2_NH3	mgO2/L	0.37
Partitioning coefficients			
partition coefficient for NH4 in layer 1 and 2	KdNH3	L/kgD	1
partition coefficient for PO4 in layer 2	KdPO42	L/kgD	20
freshwater factor that increases the aerobic layer partition coefficient of inorganic P	dKDPO41f	unitless	20
saltwater factor that increases the aerobic layer partition coefficient of inorganic P	dKDPO41s	unitless	20
critical O2 concentration in layer 2 for adjustment of partition coefficient for inorganic P	O2critPO4	mgO2/L	2
Temperature coefficients			
temperature theta for bioturbation mixing between layers 1 and 2	ThtaDp	unitless	1.117
temperature theta for pore water diffusion between layers 1 and 2	ThtaDd	unitless	1.08
temperature theta for nitrification	ThtaNH3	unitless	1.123
temperature theta for denitrification	ThtaNO3	unitless	1.08
temperature theta for methane oxidation	ThtaCH4	unitless	1.079
Salinity thresholds			
salinity above which sulfide rather than methane is produced from C diagenesis	SALTSW	psu	1
salinity above which saltwater nitrification/denitrification rates are used for aerobic layer	SALTND	psu	1
Sulfide constants			
aerobic layer reaction velocity for dissolved sulfide oxidation	KappaH2Sd1	m/d	0.2
aerobic layer reaction velocity for particulate sulfide oxidation	KappaH2Sp1	m/d	0.4
temperature coefficient for sulfide oxidation	ThtaH2S	unitless	1.079
sulfide oxidation normalization constant for O2	KMHSO2	mgO2/L	4
partition coefficient for sulfide in aerobic layer 1	KdH2S1	L/kgD	100
partition coefficient for sulfide in anaerobic layer 2	KdH2S2	L/kgD	100
Fractions of G classes 1 and 2 for settling PON, POC, and POP			
fraction of class 1 pon	frpon1	unitless	0.65
fraction of class 2 pon	frpon2	unitless	0.25
fraction of class 1 poc	frpoc1	unitless	0.65
fraction of class 2 poc	frpoc2	unitless	0.2
fraction of class 1 pop	frpop1	unitless	0.65
fraction of class 2 pop	frpop2	unitless	0.2
Diagenesis rate constants for G clase 1, 2, and 3 N/C/P			
G class 1 pon mineralization	kpon1	day^-1	0.035
G class 2 pon mineralization	kpon2	day^-1	0.0018
G class 3 pon mineralization	kpon3	day^-1	0
G class 1 poc mineralization	kpoc1	day^-1	0.035
G class 2 poc mineralization	kpoc2	day^-1	0.0018
G class 3 poc mineralization	kpoc3	day^-1	0
G class 1 pop mineralization	kpop1	day^-1	0.035
G class 2 pop mineralization	kpop2	day^-1	0.0018
G class 3 pop mineralization	kpop3	day^-1	0
Temperature coefficients for G class 1, 2, and 3 mineralization			
temperature theta for G class 1 pon	ThtaPON1	unitless	1.1
temperature theta for G class 2 pon	ThtaPON2	unitless	1.15
temperature theta for G class 3 pon	ThtaPON3	unitless	1.17
temperature theta for G class 1 poc	ThtaPOC1	unitless	1.1
temperature theta for G class 2 poc	ThtaPOC2	unitless	1.15
temperature theta for G class 3 poc	ThtaPOC3	unitless	1.17
temperature theta for G class 1 pop	ThtaPOP1	unitless	1.1
temperature theta for G class 2 pop	ThtaPOP2	unitless	1.15
temperature theta for G class 3 pop	ThtaPOP3	unitless	1.17
Parameters for partical mixing and benthic stress			
reference G1 at which w12base = Dp / H2 at 20 degC for DiToro eqn 13.1	POC1R	gO2/m^3	0.2667
first-order decay rate constant for benthic stress (d^-1) for DiToro eqn 13.3	kBEN_STR	day^-1	0.03
particle mixing half-saturation constant for O2 (mgO2/L)	KM_O2_Dp	mgO2/L	4

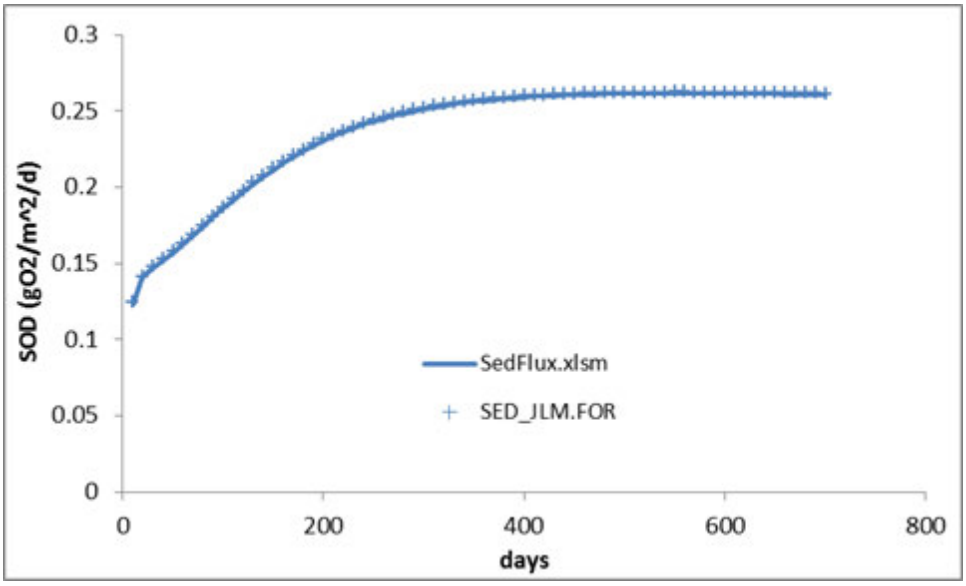

Figure B-1. Sediment oxygen demand (SOD).
(positive is flux from water into sediment)

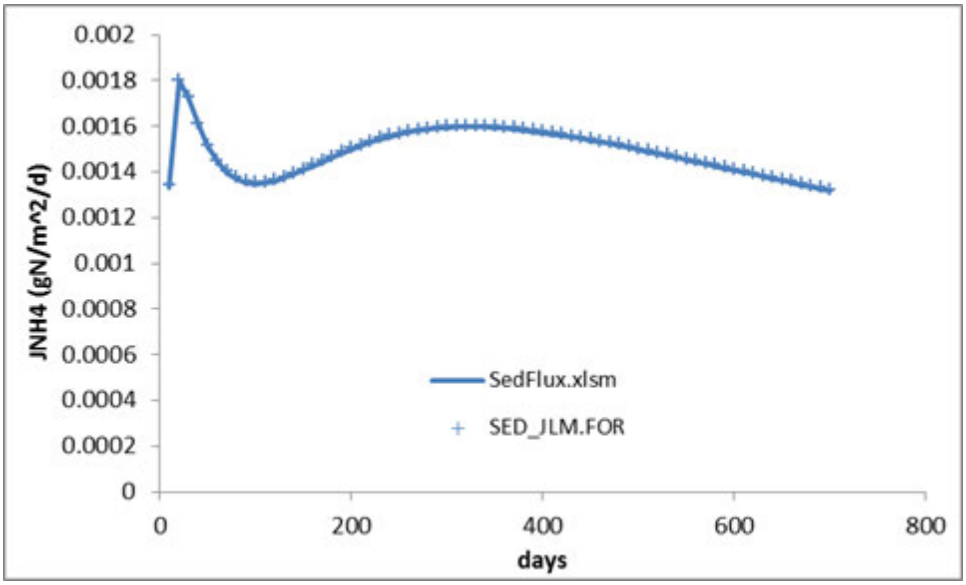

Figure B-2. Sediment-water flux of ammonium (JNH4).
(positive is flux from sediment into water)

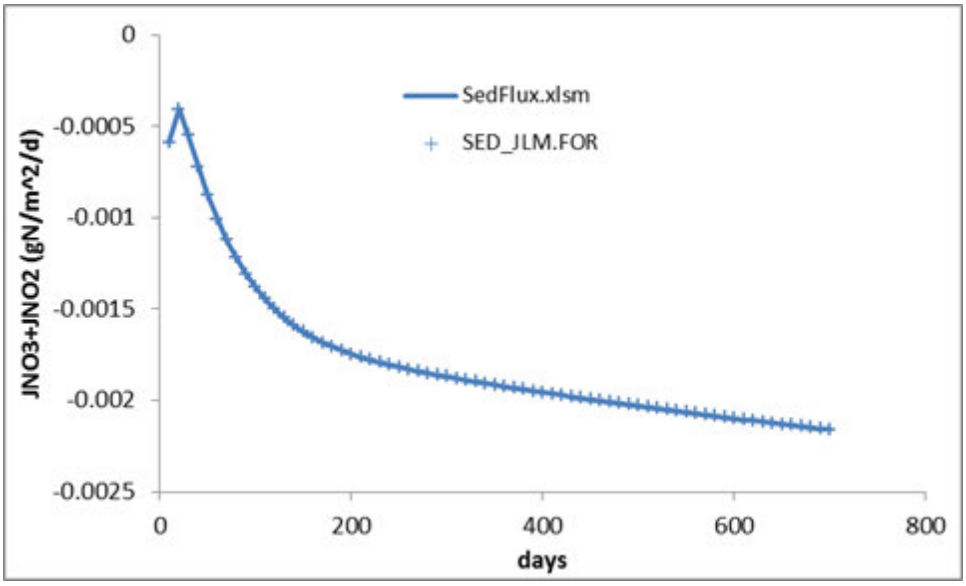

Figure B-3. Sediment-water flux of nitrate+nitrite (JNO3+JNO2).
(negative is flux from water into sediment)

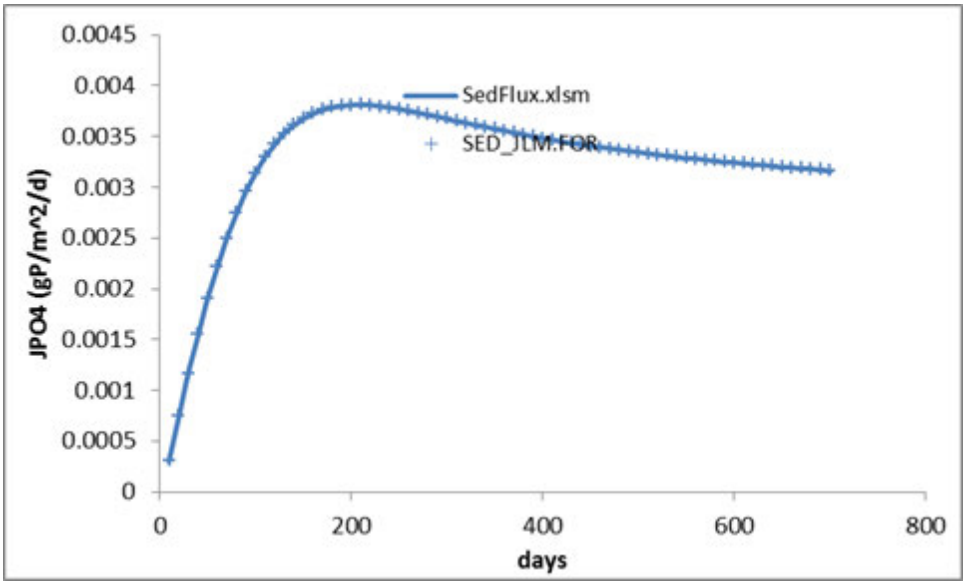

Figure B-4. Sediment-water flux of phosphate (JPO4).
(positive is flux from sediment into water)

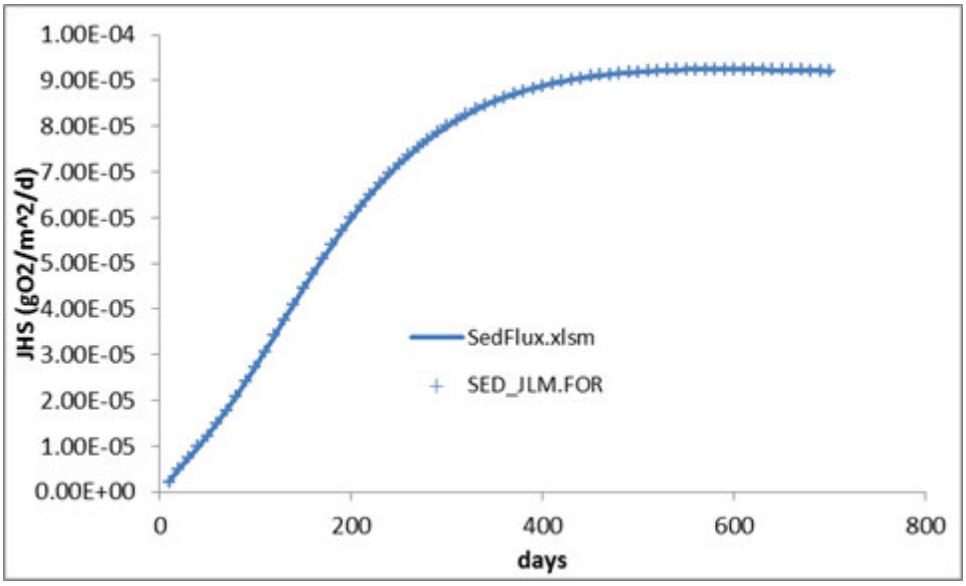

Figure B-5. Sediment-water flux of sulfide (JHS).
(positive is flux from sediment into water)

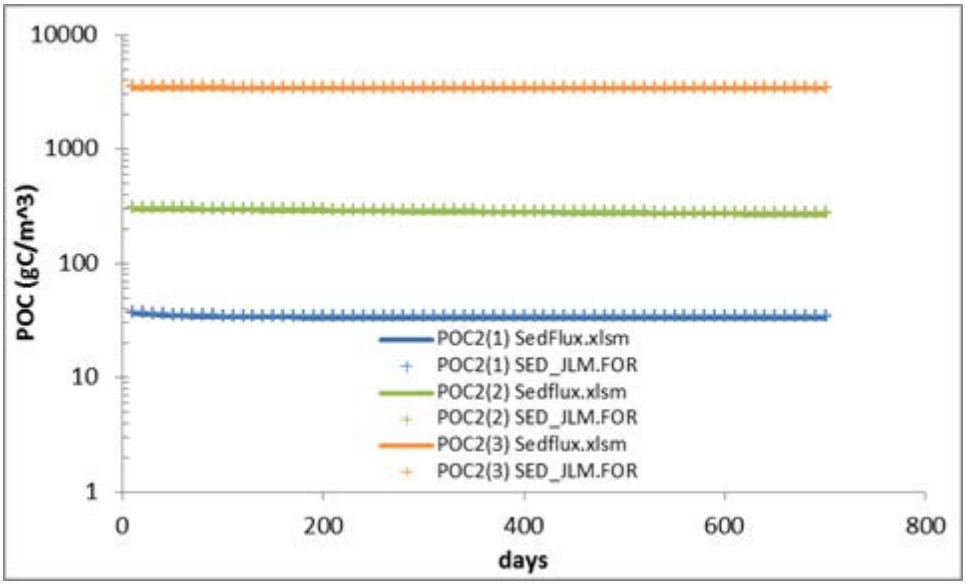

Figure B-6. Sediment layer 2 G classes of particulate organic C (POC).
POC in layer 2 in G class 1 is POC2(1), G class 2 is POC2(2), and G class 3 is POC2(3)

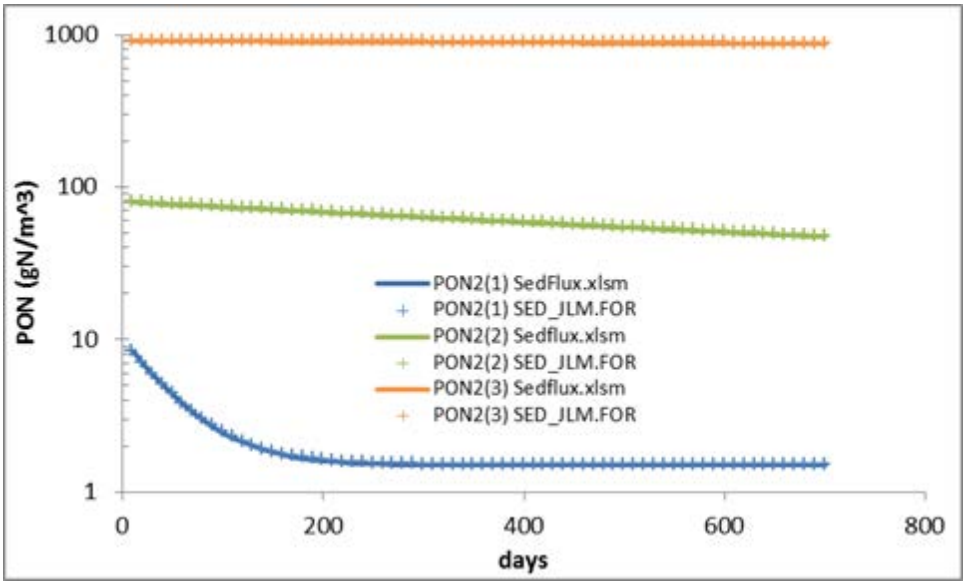

Figure B-7. Sediment layer 2 G classes of particulate organic N (PON).
PON in layer 2 in G class 1 is PON2(1), G class 2 is PON2(2), and G class 3 is PON2(3)

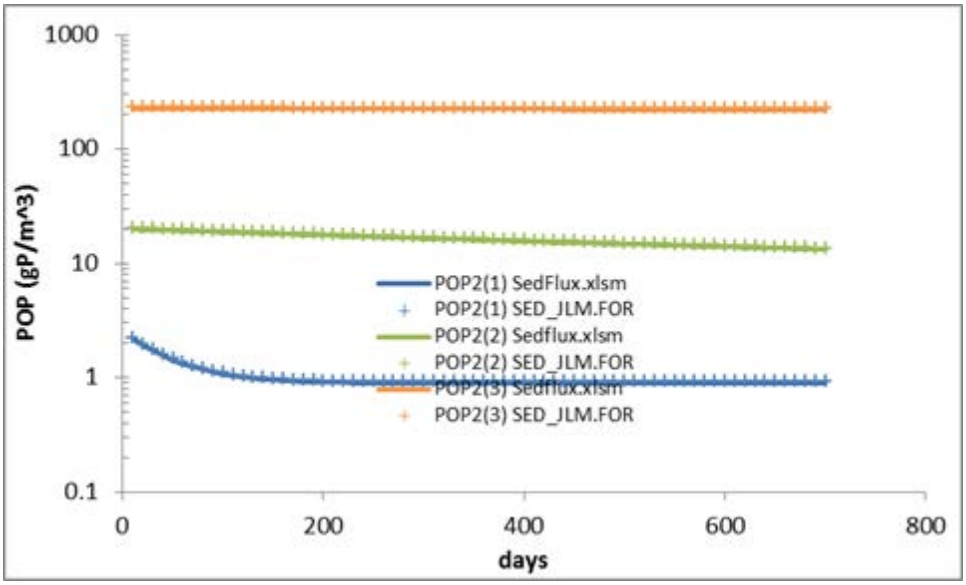

Figure B-8. Sediment layer 2 G classes of particulate organic P (POP).
POP in layer 2 in G class 1 is POP2(1), G class 2 is POP2(2), and G class 3 is POP2(3)

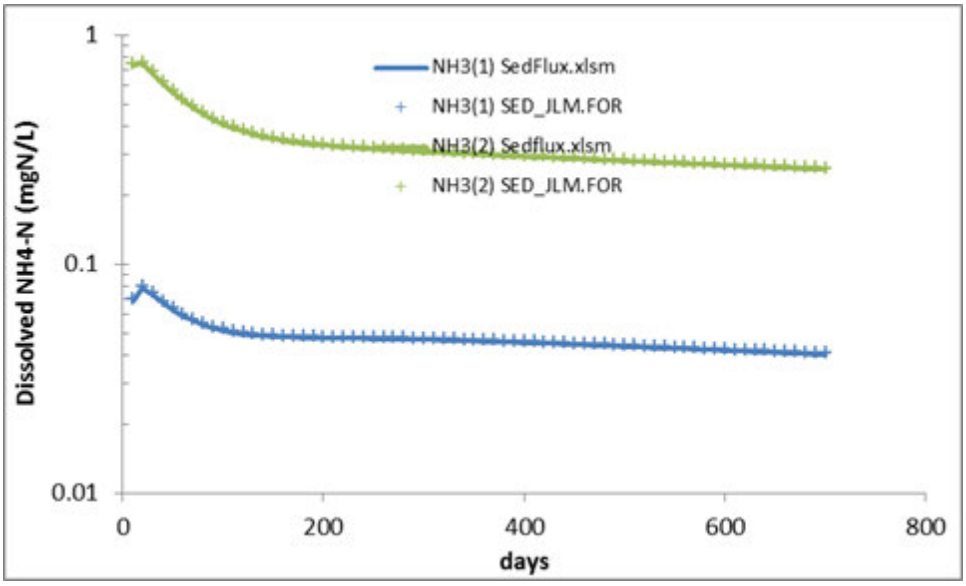

Figure B-9. Dissolved ammonium in sediment pore water in layer 1 (NH3(1)) and layer 2 (NH3(2)).

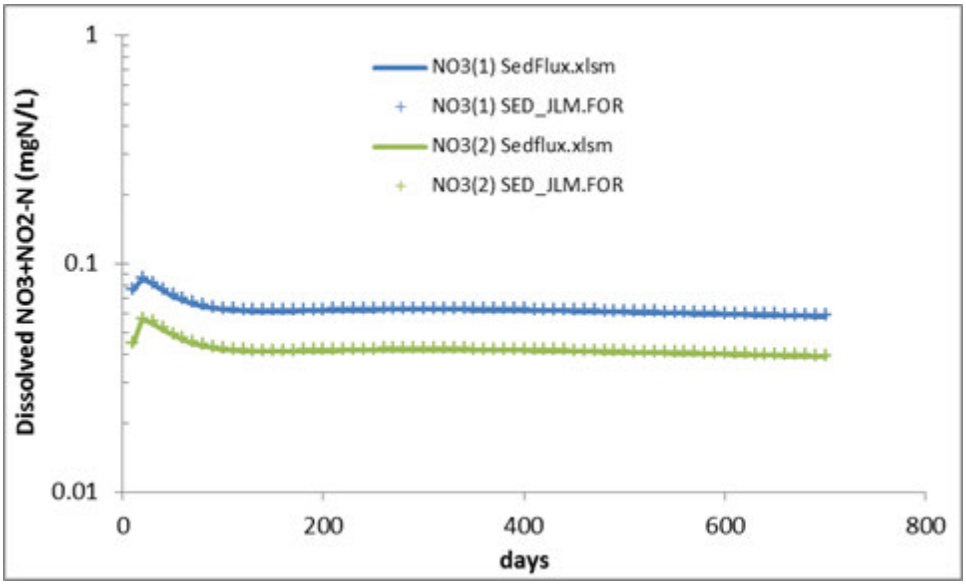

Figure B-10. Dissolved nitrate+nitrite in sediment pore water in layer 1 (NO3(1)) and layer 2 (NO3(2)).

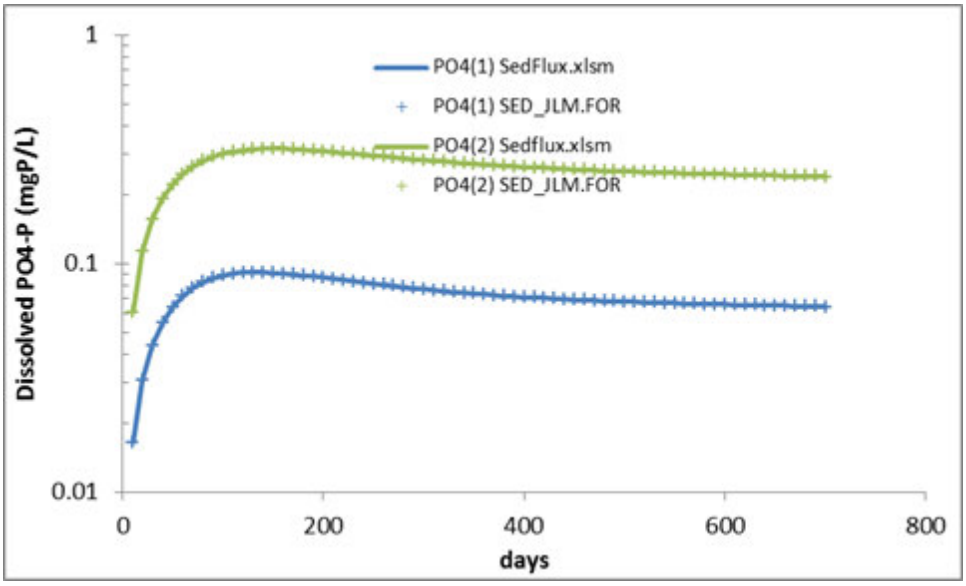

Figure B-11. Dissolved phosphate in sediment pore water in layer 1 (PO4(1)) and layer 2 (PO4(2)).

Appendix C. Results of Model Quality Assurance Testing with SedFlux.xlsm

Results of Testing Steps 2a-2e

From: Pelletier, Greg (ECY)
Sent: Wednesday, March 04, 2015 1:35 PM
To: Long, Wen <Wen.Long@pnnl.gov>
Cc: Roberts, Mindy (ECY) <MROB461@ECY.WA.GOV>; Mohamedali, Teizeen (ECY) <tmoh461@ECY.WA.GOV>; Bianucci, Laura <laura.bianucci@pnnl.gov>; Khangaonkar, Tarang P <Tarang.Khangaonkar@pnnl.gov>; Ahmed, Anise (ECY) <AAHM461@ECY.WA.GOV>
Subject: RE: Test A to Test E Results

The table below are the median relative percent differences (RPD) comparing Wen's Fortran code with Ecology's Excel benchmark for the outputs of the sediment flux model for tests 2a, 2b, 2c, and, and 2e specified in the Quality Assurance Project Plan (QAPP). The median across all output variables for all tests was within the QAPP goal of +/- 0.001%. All of the graphical comparisons look excellent.

Most of the individual outputs for tests 2a and 2b were within the QAPP goal of +/- 0.001%. All of the outputs for 2a and 2b were within +/- 0.01% which is also excellent. Therefore I am confident that both the steady state and time variable solutions are correct.

Some of the individual output variables for tests 2c, 2d, and 2e exceeded the QAPP goal (shown in gray in the table below), but all of those higher RPDs were within +/- 1% which is acceptable in my opinion. Some of these higher RPDs appear to be caused by fluxes correctly changing from positive to negative values during the integration, and when the values passed through zero there were some tiny differences that became relatively large but are insignificant.

Overall I recommend that the test results for 2a-2e should be approved.

	Test 2a	Test 2b	Test 2c	Test 2d	Test 2e
SOD	-0.0008%	-0.0006%	-0.1021%	-0.0007%	-0.0973%
Jnh4	-0.0049%	-0.0030%	-0.2020%	-0.0035%	-0.1000%
Jno3	0.0002%	0.0001%	-0.1877%	0.0000%	-0.1876%
JDenitT	0.0001%	0.0000%	0.1103%	0.0000%	0.0865%
Jhs	-0.0085%	-0.0018%	-0.5174%	-0.0024%	-0.4937%
NH3(1)	-0.0012%	-0.0008%	0.0888%	-0.0009%	0.1197%
NH3(2)	-0.0002%	-0.0001%	0.0313%	-0.0001%	0.0370%
NO3(1)	-0.0013%	-0.0010%	-0.0634%	-0.0010%	-0.0712%
NO3(2)	-0.0013%	-0.0010%	-0.0623%	-0.0011%	-0.0709%
HS(1)	-0.0017%	-0.0011%	-0.6231%	-0.0014%	-0.2507%
HS(2)	0.0000%	0.0000%	0.9179%	-0.0001%	0.9226%
POC2(1)	0.0000%	0.0000%	-0.0920%	0.0000%	-0.0920%
POC2(2)	0.0000%	0.0000%	0.0003%	0.0000%	0.0003%
POC2(3)	0.0000%	0.0000%	0.0000%	0.0000%	0.0000%
PON2(1)	0.0000%	0.0000%	-0.0175%	0.0000%	-0.0175%
PON2(2)	0.0000%	0.0000%	0.0058%	0.0000%	0.0059%
PON2(3)	0.0000%	0.0000%	-0.0001%	0.0000%	0.0000%
H1	0.0008%	0.0006%	0.0912%	0.0007%	0.0830%
BEN_STR		0.0000%	0.0000%	0.0000%	0.0000%
Median	0.0000%	0.0000%	-0.0001%	0.0000%	0.0000%
Average	-0.0010%	-0.0005%	-0.0327%	-0.0006%	-0.0066%
Min	-0.0085%	-0.0030%	-0.6231%	-0.0035%	-0.4937%
Max	0.0008%	0.0006%	0.9179%	0.0007%	0.9226%

Results of Testing Step 3 – comparison of SedFlux.xlsm with linked Puget Sound model at node 3801

The following are the median relative percent differences (RPD) between output from the linked FVCOM-ICM-SFM model with Ecology's SedFlux.xlsm model at model node 3801. Median RPDs for all variables are within +/- 0.1% and are considered to be acceptable.

	Median RPD
Jcin	0.00%
Jnin	0.00%
Jpin	0.00%
Jsin	0.00%
O20	0.00%
Depth	0.00%
Tw	0.00%
NH30	0.00%

NO30	0.00%
PO40	0.00%
SALw	0.00%
SOD	-0.02%
Jnh4	-0.02%
Jno3	-0.02%
JDenitT	-0.01%
Jhs	-0.06%
Jpo4	0.04%
Jsi	0.02%
NH3(1)	-0.01%
NH3(2)	0.00%
NO3(1)	-0.03%
NO3(2)	-0.01%
PO4(1)	0.03%
PO4(2)	0.01%
Si(1)	0.00%
Si(2)	0.01%
HS(1)	-0.04%
HS(2)	0.02%
POC2(1)	0.00%
POC2(2)	0.00%
POC2(3)	0.00%
PON2(1)	0.01%
PON2(2)	0.00%
PON2(3)	0.00%
POP2(1)	0.00%
POP2(2)	-0.01%
POP2(3)	0.00%
POS2	0.00%
H1	0.02%
BEN_STR	0.00%
Median	0.00%
Min	-0.06%
Max	0.04%

Appendix D. Binders of Comparison of Predicted and Observed Water Quality Variables in Time Series and Profile Plots

The following tables are available only online as zip files. They are linked to this report at: https://fortress.wa.gov/ecy/publications/SummaryPages/1703010.html

Appendix D.1 Binders for all variables

Appendix D.2 Binders for dissolved oxygen, chlorophyll, and DIN

Appendix E. Listing of Key Model Parameters – Salish Sea Model (SSM) Water Quality Model (FVCOM-ICM) with pH and Sediment Diagenesis

Table E-1. Parameters for phytoplankton, mineralization, and settling.

Symbol	Value	Unit	Literature Range	Definition
Algae parameters (inputs/algae.dat)				
G1	calculated	d^{-1}	–	growth rate of diatom
G2	calculated	d^{-1}	–	growth rate of dinoflagellates
PM1	300-525[a]	g C g^{-1} Chl d^{-1}	200 – 350	maximum photosynthetic rate of diatom
PM2	357-525[a]	g C g^{-1} Chl d^{-1}	200 – 350	maximum photosynthetic rate of dinoflagellates
BM1	0.1	d^{-1}	0.01 – 0.1	basal metabolic rate of diatom
BM2	0.1	d^{-1}	0.01 – 0.1	basal metabolic rate of dinoflagellates
BPR1	1.0	d^{-1}	0.05 – 1.0	base predation rate of diatom
BPR2	0.5	d^{-1}	0.05 – 1.0	base predation rate of dinoflagellates
FNIP	0.4	$0 \leq$ FNIP ≤ 1	0 – 1	fraction of algal predation released as NH_4
FNLP	0.3	$0 \leq$ FNLP ≤ 1	0 – 1	fraction of algal predation released as LPON
FNRP	0.1	$0 \leq$ FNRP ≤ 1	0 – 1	fraction of algal predation released as RPON
FNLDP	0.18	$0 \leq$ FNLDP ≤ 1	0 – 1	fraction of algal predation released as LDON
FNRDP	0.02	$0 \leq$ FNRDP ≤ 1	0 – 1	fraction of algal predation released as RDON
FPIP	0.5	$0 \leq$ FPIP ≤ 1	0 – 1	fraction of algal predation released as PO_4
FPLP	0.07	$0 \leq$ FPD ≤ 1	0 – 1	fraction of algal predation released as LDOP
FPRP	0.03	$0 \leq$ FPD ≤ 1	0 – 1	fraction of algal predation released as RDOP
FPLDP	0.36	$0 \leq$ FPLP ≤ 1	0 – 1	fraction of algal predation released as LPOP
FPRDP	0.04	$0 \leq$ FPRP ≤ 1	0 – 1	fraction of algal predation released as RPOP
FDOP	0.0	$0 \leq$ FDOP ≤ 1	0 – 1	Fraction of algal predation released as DIC
FCLP	0.5	$0 \leq$ FCLP ≤ 1	0 – 1	fraction of algal predation released as LPOC
FCRP	0.2	$0 \leq$ FCRP ≤ 1	0 – 1	fraction of algal predation released as RPOC
FCLDP	0.1	$0 \leq$ FCLDP ≤ 1	0 – 1	fraction of algal predation released as LDOC
FCRDP	0.2	$0 \leq$ FCRDP ≤ 1	0 – 1	fraction of algal predation released as RDOC
FSAP	0.3	$0 \leq$ FSAP ≤ 1	0 – 1	fraction of algal silica recycled to the dissolved pool via predation
ANC1	0.175	g N g-1 C		algal group 1 diatom nitrogen-to-carbon ratio
CCHL1	37	g C g^{-1} Chl	30 – 143	carbon-to-chlorophyll ratio for diatoms
KHN1	0.06	g N m^{-3}	0.003 – 0.923	half-saturation concentration for nitrogen uptake by diatoms
KHP1	0.02	g P m^{-3}	0.001 – 0.163	half-saturation concentration for phosphorus uptake by diatoms
ALPHMN1	6.0	g C g^{-1} Chl $(E\ m^{-2})^{-1}$		initial slope of PvsI curve for algal group diatom
PRSP1	0.25	$0 \leq$ PRSP1 ≤ 1	0 – 1	fraction of production consumed in photorespiration for diatoms
TMP1	12	°C	up to 35	optimal temperature for growth of diatom
KTG11	0.008	$°C^{-2}$	-	effect of sub-optimal temperature on growth algae group1
KTG12	0.2	$°C^{-2}$	-	effect of sub-optimal temperature on growth algae group1

Table E-1. Parameters for phytoplankton, mineralization, and settling.

Symbol	Value	Unit	Literature Range	Definition
FNI1	0.55	$0 \leq$ FNI1 ≤ 1	0 – 1	fraction of algal 1 metabolism released as NH_4
FNLP1	0.02	$0 \leq$ FNLP1 ≤ 1	0 – 1	fraction of algal 1 metabolism released as LPON
FNRP1	0.05	$0 \leq$ FNRP1 ≤ 1	0 – 1	fraction of algal 1 metabolism released as RPON
FNLD1	0.18	$0 \leq$ FNLD1 ≤ 1	0 – 1	fraction of algal 1 metabolism released as LDON
FNRD1	0.1	$0 \leq$ FNRD1 ≤ 1	0 – 1	fraction of algal 1 metabolism released as RDON
FPI1	0.75	$0 \leq$ FPI1 ≤ 1	0 – 1	fraction of algal 1 metabolism released as PO_4
FPLP1	0.0	$0 \leq$ FPLP1 ≤ 1	0 – 1	fraction of algal 1 metabolism released as LPOP
FPRP1	0.0	$0 \leq$ FPRP1 ≤ 1	0 – 1	fraction of algal 1 metabolism released as RPOP
FPLD1	0.2	$0 \leq$ FPLD1 ≤ 1	0 – 1	fraction of algal 1 metabolism released as LDOP
FPRD1	0.05	$0 \leq$ FPRD1 ≤ 1	0 – 1	fraction of algal 1 metabolism released as RDOP
FCI1	1.0	$0 \leq$ FCI1 ≤ 1	0 – 1	fraction of algal 1 metabolism released as CO2
FCLP1	0.0	$0 \leq$ FCLP1 ≤ 1	0 – 1	fraction of algal 1 metabolism released as LPOC
FCRP1	0.0	$0 \leq$ FCRP1 ≤ 1	0 – 1	fraction of algal 1 metabolism released as RPOC
FCLD1	0.0	$0 \leq$ FCLD1 ≤ 1	0 – 1	fraction of algal 1 metabolism released as LDOC
FCRD1	0.0	$0 \leq$ FCRD1 ≤ 1	0 – 1	fraction of algal 1 metabolism released as RDOC
ANC2	0.175	g N g-1 C		algal group 2 dinoflagellates nitrogen-to-carbon ratio
CCHL2	50	g C g^{-1} Chl	30 – 143	carbon-to-chlorophyll ratio for dinoflagellates
KHN2	0.06	g N m^{-3}	0.005 – 0.589	half-saturation concentration for nitrogen uptake by dinoflagellates
KHP2	0.02	g P m^{-3}	0.0003 – 0.195	half-saturation concentration for phosphorus uptake by dinoflagellates
ALPHMN2	6	g C g^{-1} Chl $(E\ m^{-2})^{-1}$		initial slope of PvsI curve for algal group 2 dinoflagellate
PRSP2	0.25	$0 \leq PRSP_{dia} \leq 1$	0 – 1	fraction of production consumed in photorespiration for diatoms
TMP2	18	°C	up to 35	optimal temperature for growth of dinoflagellates
KTG21	0.05	$°C^{-2}$	-	effect of sub-optimal temperature on growth algae group 1
KTG22	0.008	$°C^{-2}$	-	effect of sub-optimal temperature on growth algae group 2

Table E-1. Parameters for phytoplankton, mineralization, and settling.

Symbol	Value	Unit	Literature Range	Definition
FNI2	0.55	$0 \leq$ FNI2 ≤ 1	0 – 1	fraction of algal 2 metabolism released as NH_4
FNLP2	0.2	$0 \leq$ FNLP2 ≤ 1	0 – 1	fraction of algal 2 metabolism released as LPON
FNRP2	0.05	$0 \leq$ FNRP2 ≤ 1	0 – 1	fraction of algal 2 metabolism released as RPON
FNLD2	0.18	$0 \leq$ FNLD2 ≤ 1	0 – 1	fraction of algal 2 metabolism released as LDON
FNRD2	0.02	$0 \leq$ FNRD2 ≤ 1	0 – 1	fraction of algal 2 metabolism released as RDON
FPI2	0.75	$0 \leq$ FPI2 ≤ 1	0 – 1	fraction of algal 2 metabolism released as PO_4
FPLP2	0.0	$0 \leq$ FPLP2 ≤ 1	0 – 1	fraction of algal 2 metabolism released as LPOP
FPRP2	0.0	$0 \leq$ FPRP2 ≤ 1	0 – 1	fraction of algal 2 metabolism released as RPOP
FPLD2	0.2	$0 \leq$ FPLD2 ≤ 1	0 – 1	fraction of algal 2 metabolism released as LDOP
FPRD2	0.05	$0 \leq$ FPRD2 ≤ 1	0 – 1	fraction of algal 2 metabolism released as RDOP
FCI2	1.0	$0 \leq$ FCI2 ≤ 1	0 – 1	fraction of algal 2 metabolism released as CO2
FCLP2	0.0	$0 \leq$ FCLP2 ≤ 1	0 – 1	fraction of algal 2 metabolism released as LPOC
FCRP2	0.0	$0 \leq$ FCRP2 ≤ 1	0 – 1	fraction of algal 2 metabolism released as RPOC
FCLD2	0.0	$0 \leq$ FCLD2 ≤ 1	0 – 1	fraction of algal 2 metabolism released as LDOC
FCRD2	0.0	$0 \leq$ FCRD2 ≤ 1	0 – 1	fraction of algal 2 metabolism released as RDOC
Mineralization constants				
KHONT	3.0	g O_2 m^{-3}	-	half-saturation constant of dissolved oxygen required for nitrification
KHNNT	0.5	g N m^{-3}	-	half-saturation constant of NH4 required for nitrification
KHODOC	0.5	g O_2 m^{-3}	-	half-saturation concentration of dissolved oxygen required for oxic respiration
KHNDN	0.1	g N m^{-3}	-	half-saturation concentration of nitrate required for denitrification

Table E-1. Parameters for phytoplankton, mineralization, and settling.

Symbol	Value	Unit	Literature Range	Definition
PN1	calculated	$0 \leq$ PN ≤ 1	0 – 1	preference for ammonium uptake of diatom
PN2	calculated	$0 \leq$ PN ≤ 1	0 – 1	preference for ammonium uptake of dinoflagellates
AOCR	2.37	g O_2 g^{-1}C	-	oxygen-to-carbon mass ratio in production and respiration
AONT	4.33	g O_2 g^{-1} N	-	oxygen consumed per mass ammonium nitrified
KTCOD	0.041	$°C^{-1}$	-	effect of temperature on COD exertion
KTMNL	0.092	$°C^{-1}$	-	effect of temperature on dissolved organic matter mineralization rates
KTHDR	0.092	$°C^{-1}$	-	effect of temperature on particulate organic matter hydrolysis rates
KTSUA	0.092	$°C^{-1}$	-	effect of temperature on particulate biogenic silica dissolution rates
KTNT1	0.0045	$°C^{-2}$	-	effect of sub-optimal temperature on nitrification
KTNT2	0.0045	$°C^{-2}$	-	effect of super-optimal temperature on nitrification
TMNT	30	°C	25 – 35	optimal temperature for nitrification
KADPO4	0.66	m^3 g^{-1}	-	partition coefficient of sorbed vs. dissolved phosphate
KADSA	0	m^3 g^{-1}	-	partition coefficient of sorbed vs. dissolved silicate
AANOX	0.5		0 – 1	ratio of denitrification to oxic carbon respiration rate
ANDC	0.933	g N g^{-1} C	0.933	mass nitrate-nitrogen reduced per mass dissolved organic carbon
Kr	calculated as a function of wind speed		–	reaeration coefficient, depends on AREAR, BREAR, and CREAR
AREAR	0.1	-	0.1-0.157	empirical constant in reaeration equation (≈0.1)
BREAR	1	-	-	exponent of wind in reaeration equation
CREAR	1.5	-	-	exponent of wind in reaeration equation
DENIT	calculated	d^{-1}	0.0	denitrification rate
KLDC	0.025	d^{-1}	0.005 – 0.25	minimum respiration rate of LDOC
KRDC	0.0015	d^{-1}	–	minimum respiration rate of RDOC
KLPC	0.05	d^{-1}	0.005 – 1.5	dissolution rate of LPOC
KRPC	0.0015	d^{-1}	0.001 – 0.005	dissolution rate of RPOC
KLDN	0.050	d^{-1}	0.02 – 2.0	minimum mineralization rate of LDON
KRDN	0.0025	d^{-1}	–	minimum mineralization rate of RDON
KLPN	0.075	d^{-1}	0.03 – 0.08	minimum hydrolysis rate of LPON
KRPN	0.0025	d^{-1}	0.001 – 0.005	minimum hydrolysis rate of RPON
KLDP	0.1	d^{-1}	0.05 – 0.2	minimum mineralization rate of LDOP

Table E-1. Parameters for phytoplankton, mineralization, and settling.

Symbol	Value	Unit	Literature Range	Definition
KRDP	0.01	d^{-1}	–	minimum mineralization rate of RDOP
KLPP	0.075	d^{-1}	0.075 – 0.12	minimum hydrolysis rate of LPOP
KRPP	0.005	d^{-1}	0.001 – 0.005	minimum hydrolysis rate of RPOP
KSUA, KCOD – not used				
KDCALG	0.0075	$m^3\ g^{-1}\ C\ d^{-1}$	-	Constant that relates DOC respiration to algal biomass
KLCALG	0.05	$m^3\ g^{-1}\ C\ d^{-1}$	-	Constant that relates LPOC hydrolysis to algal biomass
KRCALG	0.001	$m^3\ g^{-1}\ C\ d^{-1}$	-	Constant that relates RPOC hydrolysis to algal biomass
KDNALG	0.05	$m^3\ g^{-1}\ N\ d^{-1}$	-	Constant that relates DON mineralization to algal biomass
KLNALG	0.01	$m^3\ g^{-1}\ N\ d^{-1}$	-	Constant that relates LPON hydrolysis to algal biomass
KDPALG	0.2	$m^3\ g^{-1}\ N\ d^{-1}$	-	Constant that relates DOP mineralization to algal biomass
KLPALG	0.4	$m^3\ g^{-1}\ N\ d^{-1}$	-	Constant that relates LPOP hydrolysis to algal biomass
NT_m	0.4	$g\ N\ m^{-3}\ d^{-1}$	0.01 – 0.7	Maximum nitrification rate
Settling (* inputs/settling.dat*)				
SS	0.25	$m\ d^{-1}$		fixed solids settling rate
WSLAB	10	$m\ d^{-1}$		labile particulate organic solids settling rate
WSREF	10			refractory particulate organic matter (POM) settling rate
WS1	0.6	$m\ d^{-1}$	0 – 30.	settling velocity of diatom
WS2	0.3	$m\ d^{-1}$	0 – 30.	settling velocity of dinoflagellates

Table E-2. Parameters for sediment diagenesis and carbonate chemistry.

Sediment Diagenesis (**inputs/sediments.dat*)**				
pH and Carbonate Chemistry				
Parameter	**Value**	**Unit**	**Meaning**	**Comments**
HSEDALL	10	cm	Depth of sediment	
SSTATEG3	0	0 or 1	1 means do steady state calculation for G3 of POM in sediments	
SSTATEIC	1	0 or 1	=1 for using steady state solution based as initial condition for sediments	
SSTATAV	0	0 or 1	=1 for using time averaged water column conditions to calculate steady state solution	Obsolete (was in old ICM, and not implemented)
ITVWCLF	0	0 or 1	=1 for reading time varying input file for water column conditions for sediment	=0 to use model calculated overlying condition
NTVWCLF	1	Integer	Number of files to read if ITVWCLF==1	
WCFLDAY	360.0	day	Length of each file for reading water column data	
DIFFT	1.0	cm^2/sec	Diffusion rate between water and sediment for calculating sediment temperature	Used only if SEDTC=ON in wqm_con.npt file. Otherwise, sediment temperature is set to same as water column bottom temperature
SALTSW	1.0	ppt	Critical salinity for fresh/salt water CSOD	When Salt< SALTSW, CSOD is calculated using HS Otherwise, using CH4
SALTND	1.0	ppt	Critical salinity for fresh/salt water rates for nitrification/denitrification	When salt < SALTND, using KAPPNH4F KAPPNO3F otherwise using KAPPNH4S and KAPPNO3S
FRPALG1(1:3)	0.65 0.2 0.15	None	Algae 1 split of P for G1, G2, G3 in sediments	
FRPALG2(1:3)	0.65 0.2 0.15		Algae 2 split of P for G1, G2, G3 in sediments	
FRPALG3(1:3)	0.65 0.2 0.15		Algae 3 split of P for G1, G2, G3 in sediments	Obsolete, no ALG3 in current model, was in ICM
FRNALG1	0.65 0.25 0.10		Algae 1 split of N for G1, G2, G3 in sediments	
FRNALG2	0.65 0.25 0.10		Algae 2 split of N for G1, G2, G3 in sediments	
FRNALG1	0.65 0.25 0.10		Algae 3 split of N for G1, G2, G3 in sediments	Obsolete, no ALG3 in current model, was in ICM
FRCALG1	0.65 0.2 0.15		Algae 1 split of C for G1, G2, G3 in sediments	
FRCALG2	0.65 0.2 0.15		Algae 2 split of C for G1, G2, G3 in sediments	
FRCALG3	0.65 0.2 0.15		Algae 3 split of C for G1, G2, G3 in sediments	Obsolete, no ALG3 in current model, was in ICM
KPOP1	0.035	1/day	Decay rate of POP1 in sediments	Used for POP diagenesis
THTPOP1	1.1	None	Temperature theta of KPOP1	
KPOP2	0.0018	1/day	Decay rate of POP2 in sediments	Used for POP diagenesis
THTPOP2	1.15	None	Temperature theta of KPOP2	

Parameter	Value	Unit	Meaning	Comments
KPOP3	0.0	1/day	Decay rate of POP3 in sediments	Used for POP diagenesis
THTPOP3	1.17	none	Temperature theta of KPOP3	
KPON1	0.035	1/day	Decay rate of PON1 in sediments	Used for PON diagenesis
THTPON1	1.1	None	Temperature theta of KPON1	
KPON2	0.0018	1/day	Decay rate of PON2 in sediments	Used for PON diagenesis
THTPON2	1.15	None	Temperature theta of KPON2	
KPON3	0.0	1/day	Decay rate of PON3 in sediments	Used for PON diagenesis
THTPON3	1.17	None	Temperature theta of KPON3	
KPOC1	0.035	1/day	Decay rate of POC1 in sediments	Used for POC diagenesis
THTPOC1	1.1	None	Temperature theta of KPOC1	
KPOC2	0.0018	1/day	Decay rate of POC2 in sediments	Used for POC diagenesis
THTPOC2	1.15	None	Temperature theta of KPOC2	
KPOC3	0.0	1/day	Decay rate of POC3 in sediments	Used for POC diagenesis
THTPOC3	1.17	None	Temperature theta of KPOC3	
KSI	0.5	1/day	Decay rate of particulate biogenic silicate POS in sediments	Used for POS diagenesis
THTASI	1.1	None	Temp theta of KSI	
THTASISAT	1.023	None	Temp theta of Si saturation concentration in sediment	
M1	0.5	Kg/L	Sediment concentration in aerobic layer	
M2	0.5	Kg/L	Sediment concentration in anaerobic layer	
THTADP	1.117	None	Temp theta for sediment-water particle mixing	
THTADD	1.08	None	Temp theta for sediment-water diffusion	
KAPPNH4F	0.131	m/d	Freshwater depth integrated nitrification rate	In aerobic layer (layer 1 of sediment)
KAPPNH4S	0.131	m/d	Salt water depth integrated nitrification rate	In aerobic layer (layer 1 of sediment)
PIENH4	1.0	L/kg	Layer 1 Sediment NH4 partitioning coefficient	
THTANH4	1.123	None	Temp theta for KAPPNH4S and KAPPNH4F	
KMNH4	728.0	mgN/L	Nitrification half constant for NH4	Di Toro book (3.30)
KMNH4O2	0.37	mgO2/L	Nitrification half constant for oxygen	
THTAKMNH4	1.0	None	Temp theta for KMNH4	
KAPPNO3F	0.1	m/d	Freshwater depth integrated denitrification rate in layer 1	
KAPPNO3S	0.1	m/d	Salt water depth integrated denitrification rate in layer 1	
K2NO3	0.25	m/d	Depth integrated denitrification rate in layer 2	
THTANO3	1.08	None	Temp theta for K2NO3, KAPPNO3F, KAPPNO3S	
KAPP1HSD	0.2	m/d	Dissolved hydrogen sulfide oxidation rate in layer 1	
KAPP1HSP	0.4	m/d	Particulate hydrogen sulfide oxidation rate in layer 1	
PIE1HS	100	L/kg	Partitioning coefficient for hydrogen sulfide in layer 1	
PIE2HS	100	L/kg	Partitioning coefficient for hydrogen sulfide in layer 2	

Parameter	Value	Unit	Meaning	Comments
THTAH2S	1.079	None	Temp theta for KAPP1HSD and KAPP1HSP	
KMHSO2	4.0	mgO2/L	Half constant for HS oxidation in layer 1	
CSISATT20	40000.0	mgSi/m^3	Saturation concentration of Silicate at T=20degC	
DPIE1SI	10.0	None	Oxygen control coefficient on Silicate partitioning in layer 1 based on PIE2Si	Di Toro book (7.18)
PIE2SI	100.0	L/kg	Silicate partitioning coefficient	
KMPSI	50000.0	gSi/m^3	Half constant for Silicate dissolution	
O2CRITSI	2.0	mgO2/L	Critical oxygen concentration for varying silicate partitioning in sediment	An indication of partitioning coefficient based on different oxygen level in layer 1
JSIDETR	0.0	Mg Si/m^2/day	Source to biogenic silica in sediments	This is obsolete and only used for tuning purposes, give zero here. Otherwise, it will be extra source/sink to particulate organic silicate in sediments
DPIE1PO4F	20.0	None	Oxygen control parameter on fresh water layer 1 sediment PO4 partitioning	Di Toro book (16A.18)
DPIE1PO4S	20.0	None	Oxygen control parameter on salt water layer 1 sediment PO4 partitioning	Di Toro book (16A.18)
PIE2PO4	20.0	L/kg	Layer 2 PO4 partitioning coefficient	Di Toro book (16A.18)
O2CRITPO4	2.0	mgO2/L	Critical oxygen for	
KMO2DP	4.0	mgO2/L	Half constant for oxygen regulated particle mixing across sediment-water interface due to bioturbation	
TEMPBEN	-999	degC	Temperature at which benthic stress is reset to zero	Obsolete, this is disabled in current model. It is a formulation to calculate benthic stress
KBENSTR	0.03	1/day	Rate benthic stress is released	Mainly used in calculating layer 1-layer 2 sediment particle mixing rate due to bioturbation which is regulated by benthic stress
KLBNTH	0.0	None	Rate of bio-irrigation to bioturbation	Parameter used for regulating diffusion rate across layer 1 and layer 2 due to bioturbation.
DPMIN	0.0	m^2/day	Minimum particle diffusion rate across layer 1 and layer 2	Used for calculating how particles go across layer 1 and layer 2
KAPPCH4	0.7	m/day	Methane oxidation rate in layer 1 (depth integrated)	
THTACH4	1.079	None		
KMCH4O2	30.0640	mgO2/L	Half constant of oxygen concentration for calculating methane oxidation rate in layer 1	
KMSO4	-999.0	gO2-eq/m^3	SO4 saturation concentration (in oxygen equivalents)	Obsolete, currently disabled in model
SPVARS	CONSTANT	String	Whether to have spatial varying net settling rates of organic matter from water column to sediment	If non constant, then WSSNET etc below need to be specified for all model nodes

Parameter	Value	Unit	Meaning	Comments
PRINTS	NO	String	Whether or not to print settling rates	Obsolete, unused
WSSNET	0.2	m/d	Net settling rate of inorganic suspended sediments in bottom layer of water column	
WSLNET	2.0	m/d	Net settling rate of Labile POM in bottom layer of water column	
WSRNET	2.0	m/d	Net settling rate of refractory POM in bottom layer of water column	
WS1NET	0.4	m/d	Net settling rate of algae1 in bottom layer of water column	
WS2NET	0.15	m/d	Net settling rate of algae2 in bottom layer of water column	
WS3NET	0.05	m/d	Net settling rate of algae 3 in bottom layer of water column	Useless, as ALG3 is turned off in current model
WSUNET	0.2	m/d	Net settling rate of un-available biogenic silica in bottom layer of water column	
POC1R	0.1	mgC/gSediemnt	Reference POC concentration for calculating particle mixing across layer 1 and layer 2.	POC represents amount of bioturbation activity. When there is plenty of POC, then animals have more food and be more active.
SPVARB	CONSTANT	String	Whether to have constant or spatial varying sedimentation, sediment - water mixing and diffusion rates	If non CONSTANT, then must provide VSED, VPMIX, VDMIX below for all nodes.
PRINTB	NO	String	Whether or not to print sedimentation, diffusion and mixing rates	Obsolete, not used
VSED	0.2502	cm/yr	Sedimentation rate	
VPMIX	0. 00018	m^2/day	Particle mixing rate between layer 1 and 2	
VDMIX	0. 0075	m^2/day	Diffusion rate across sediment-water interface	
SPVARLR	CONSTANT	String	Whether or not to provide constant POP, POC, PON fractions of different G classes for Refractory POP in water column upon settling into sediments	If non CONSTANT, then must provide FRPOP2, etc. below for all nodes.
PRINTLR	NO			Obsolete
FRPOP2	0.65		Fraction of RPOP assigned to G2 upon settling	Note FRPOP2+ FRPOP3=1.0 i.e. there is no spill over to G1 upon settling. For G1 is supposed to be labile.
FRPOP3	0.35		Fraction of RPOP assigned to G3 upon settling	
FRPON2	0.65		Fraction of RPON assigned to G2 upon settling	Note FRPON2+ FRPON3=1.0, i.e. there is no spill over to G1 upon settling. For G1 is supposed to be labile.
FRPON3	0.35		Fraction of RPON assigned to G3 upon settling	
FRPOC2	0.65		Fraction of RPOC assigned to G2 upon settling	Note FRPOC2+ FRPOC3=1.0, i.e. there is no spill over to G1 upon settling. For G1 is supposed to be labile

Parameter	Value	Unit	Meaning	Comments
FRPOC3	0.35		Fraction of RPOC assigned to G3 upon settling	
SWITCH_LAB	1	1 or 0	1 to use FRACL1, FRACL2, FRACL3 below to split 3 G classes up on POM settling from water column, rather than splitting RPOM in water column into G2 and G3	If turned on to 1, then all POM fluxes into sediments are aggregated first and then split by FRACL1, FRACL2, FRACL3 into 3 G classes.
FRACL1	0.65	Unitless		Note FRACL1+ FRACL2+ FRACL3=1.0
FRACL2	0.25	Unitless		
FRACL3	0.1	unitless		

Parameter	Value	Unit	Meaning	Comments
WHICH_K1K2	10		Choice of parameter set	1-Roy 2-Goyet 3-Hansson 4-Mehrbach 5-Hansson and Mehrbach 6-GEOSECS 7-Peng 8-Millero 1979 9-Cai 10-Lueker 11-Prieto 2002 12-Millero 2002 13-Millero 2006 14-Millero 2010
WHOSEKSO4	1		Choice of KSO4	1-Dickson & TB 1979 2-Khoo 1979 3-Dickson 2010 4- Khoo & TB 2010

Table E-3. Parameters for air/water CO_2 exchange, settling, and light attenuation.

Air/Water CO2 (inputs/input_pCO2atm.dat)

Parameter	Value	Unit	Meaning	Comments
AIRSEA_OPTION	5	None	Choice of air sea CO2 flux formula	1-reaeration 2-Wanninkhof (1992) 3-Nightingale (2000) 4-Ho (2016) 5-Wanninkhof (2014)
MAPCO2ATM	UNIFORM	String	Way of specifying pCO2	If UNIFORM, then only need one number for entire domain
UNITCO2ATM	fCO2	String	Input data in CO2 or fCO2 format	If pCO2, then will calculate CO2 saturation in water using fugacity, otherwise, no fugacity is needed
pCO2atm	400	Microatm or ppmv	pCO2 pressure	Value for pCO2 concentration in pCO2 or fCO2 units

pCO2 = atmospheric CO2

Settling Rates (*inputs/settling.dat*)

WSS	0 25	m/d	Water column settling rate of suspended solids	This is not used for now as we have turned off suspended sediment
WSLAB	10 0	m/d	Water column LPOC/LPON/LPOP settling rate	
WSREF	10 0	m/d	Water column RPOC/RPON/RPOP settling rate	
WS1	0 6	m/d	Algae 1 settling rate	
WS2	0 3	m/d	Algae 2 settling rate	
WS3	0 1	m/d	Algae 3 settling rate	
WSU	0 25	m/d	Settling rate of particulate biogenic silicate	Not used for now as we turned off silicate calculation in water column and suspended sediments

W_l	10.0	m d^{-1}	settling velocity of labile particles (i.e., WSLAB)
W_r	10.0	m d^{-1}	settling velocity of refractory particles (i.e., WSREF)

Light Attenuation Rates (inputs/wqm_kei.dat)

INITKE	1	1/m	initial light attenuation coefficient Actual attenuation is calculated based on light absorbance spectra , turbidity and chlorophyll and detritus content
TURB	5	NTU	initial light attenuation coefficient
COLOR	70 0	dimensionless	indication of CDOM content in water , then calculated as 12 2*exp(0 14*(LDOC+RDOC)) with max value set to 10
BNCHL	0 111	1/(gCHL/m^3)	coefficient of CHLA for calculating light absorbance spectra
BNNTU	1 146	1/(NTU)	coefficient of Turbidity for calculating light absorbance spectra
PCOLOR	0 31931	dimensionless	coefficient of COLOR for calculating light absorbance spectra

[a] Value specified in subbasins – Hood Canal, Whidbey Basin, Bellingham Bay, and South Puget Sound.
[b] Value specified in selected shallow regions of Puget Sound known for low values of near-bed DO.

Table E-4. Parameters for main control file and meteorology.

Main Control file (wqm_con.npt)

File Handle CON – wqm_con.npt

Parameter	Value	Unit	Meaning	Comments
MGL	16012	None	# of nodes	
NGL	25019	None	# of elements	
TMSTRT	0.0	Day	Starting time	
TMEND	366.0	Day	Ending time	
YRSTRT	2014	Year	Year	
DTI	20.0	Sec	Time step of WQ model	Obsolete, Now replaced by DLTVAL
DLTVAL	20.0	Sec	Time step of WQ model	DTI is set to DLTVAL
AHMDLT	100.0	Sec	Time step of Hydro	Obsolete (ignored)
FILGTH	730.0	Days	Time length of hydro results	Used for reading meteorology file MET. The model reads MET for WQ and assumes it will repeat. The MET is supposed to have this length of data in it. Also used for BFI benthic flux condition, if no Sediment Diagenesis Module (SDM), and force with benthic flux condition (when BFC is turned on)
BFC	OFF	Logical	Whether or not to use externally forced benthic flux	If use the SDM, this should be turned off
SNPC	ON			Obsolete Old ICM snapshots output control
SNPD			Snapshot frequency change dates	Obsolete
SNPF		Day	Snapshot frequency	Obsolete
PLTC	ON			Obsolete, old ICM plot output control
PLTD			Plot frequency change dates	Obsolete
PLTF		Day	Plot frequency	Obsolete
APLTC	ON			Obsolete ICM average results output control
APLTD		Day		Obsolete
APLF		Day		Obsolete
TFLC	ON			Obsolete, old ICM transport flux calculation control
TFLD		Day		Obsolete
TFLF		Day		Obsolete
OPLC	OFF			Obsolete, old ICM oxygen output control
OINT		Integer	Box ID for output oxygen	Obsolete
OPLD		Day		Obsolete
OPLF		Day		Obsolete
NOPL	1	Integer	# of frequency changes for output oxygen	Obsolete
NOINT	8	Integer	# of boxes to output oxygen	Obsolete
MBLC	OFF		Whether to calculate mass balance of C, N, P, etc.	Obsolete
NMBL	1	Integer	# of frequency changes for outputting mass balance	Obsolete
MBLD		Day		Obsolete
MBLF		Day		Obsolete
DIAC	ON		Diagenesis output control	Obsolete, old ICM diagnostics of model run
DIAD		Day		Obsolete

Parameter	Value	Unit	Meaning	Comments
DIAF		Day		Obsolete
RSOC	ON		Turn on/off writing restart files	
NRSO	9	Integer	# of restart output s	
RSOD		Day	Array for restart output times	
RSIC	OFF		Turn on reading restart file as initial condition. If turned on, model will use restart file as initial condition. So far not coded.	Obsolete, this is not use for now. Needs thorough checking to make sure restart file can be written and read correctly for all kinds of combinations of model run controls
SLC	QUICKEST	String	Method for solving equations	Obsolete, Old ICM transport scheme
CONSC	MASS	String		Obsolete, Old ICM mass conservation control
TH	1.0			Obsolete
MINSTEP	10.0	Sec		Obsolete, Old ICM parameter for automatic change of time step
SEDC	ON		Turn on Sediment Diagenesis Module (SDM)	
AUTOC	ON		Turn on automatic time step change	Obsolete, Old ICM automatic time step calculation
VBC	ON		Volume Balance Control	Obsolete, Old ICM flag
BFOC	ON		Turn on output of benthic flux of SDM	
STLC	ON		Turn on settling calculation	If on, will read settling rates from STL
ICIC	UNIFORM	String	Data type of initial condition of WQ	So far only using uniform initial condition for WQ. Associated with ICI file
ICOC	ON		Turn on writing output file for use as initial condition for future runs	Obsolete
SAVMC	OFF		Turn on SAV calculation	Not working yet
BAOC	OFF		Output control for benthic algae	Not working yet
SEDTC	OFF	Logical	ON to calculate sediment temperature when SDM is on	
SFLC	OFF		Turn off suspension feeder module	Not working yet
DFLC	OFF		Turn off deposition feeder module	Not working yet
SFLOXC	ON		Low oxygen impact on suspension feeder	Not working yet
DFLOXC			Low oxygen impact on deposition feeder	Not working yet
BALC	OFF		Turn off benthic algae module	Not working yet
DFOC	OFF		Turn off outputs of deposition feeder	Not working yet
FLC	ON		Turn on U,V,W	If off, will model a dead sea case with no u,v,w
XYDFC	ON		Turn on horizontal diffusion calculation	If off, will simulate case without horizontal turbulent mixing
ZDFC	ON			If off, will model without vertical turbulent mixing
XYDF	0.2	m^2/sec	Basic horizontal diffusion coeff	
ZDFMUL	1.0			Obsolete
ZDFBCK	0.000001		Molecular viscosity m^2/sec	
ZDFMAX	0.1			Obsolete

Parameter	Value	Unit	Meaning	Comments
XYDFU	ON		Turn on horizontal turbulent eddy viscosity calculation	If off, will use XYDF directly
BCC	OFF		Boundary condition	Obsolete, OLD ICM boundary treatment
S1C	OFF		Point Source 1	Obsolete
S2C	OFF		Point Source 2	Obsolete
S3C	OFF		Point Source 3	Obsolete
MDC	OFF		Modify Initial Condition after reading it	Obsolete
BFC	OFF		Simple Diagenesis model (alternative)	This is pre-diagenesis model, where a simple reflective model is used for sediment fluxes. Should be turned off if we use SEDC=ON
ATMC	OFF		Atmospheric deposition	If turned on, will read ATM file. Not working yet
SAVLC	OFF		SAV loading on WQ models	This is to simulate effect of SAV on WQ model without using SAV model. Basically a simplified SAV representation for WQ. Not working yet
REDS1C	1.0		Factor to reduce Point Source 1 Carbon	Obsolete
REDS1N	1.0		Factor to reduce Point Source 1 Nitrogen	Obsolete
REDS1P	1.0		Factor to reduce Point Source 1 Phosphorus	Obsolete
REDS2C	1.0		Ditto	Obsolete
REDS2N	1.0		Ditto	Obsolete
REDS2P	1.0		Ditto	Obsolete
REDS3C	1.0		Ditto	Obsolete
REDS3N	1.0		Ditto	Obsolete
REDS3P	1.0		Ditto	Obsolete
REDCBC	1.0		Reduce boundary condition	Obsolete
REDCBN	1.0			Obsolete
REDCBP	1.0			Obsolete
BNDTC	INTERP	String	Control on Boundary condition (stepwise or using interpolation over time)	Obsolete
ACC	ON/OFF		Activate various WQ state variables	Fixed now. Needs more explanation on all of them.
NHYDF	4		# of hydrodynamics input file	Obsolete
NTVDF	4		# of time varying data files	Used for reading MET, ATM, BFI, CBC,SVI,S1,S2,S3 etc loading data. Currently on affecting MET, as the rest of them are either obsolete or turned off.
MAPFN				Obsolete
GEOFN				Obsolete
ICIFN	inputs/ssm_initial_wq_hotstart_364.dat			
RSIFN	inputs/restart.140			Not used
AGRFN	inputs/wqm_algae_Grx1half.3_yr_7_t1_ssm.dat		Algae growth parameters file	
ZOOFN	inputs/zooplankton npt		Zooplankton parameters file	Not used
SFIFN	inputs/susp_feeder npt		Suspension feeder file	Not used
STLFN	inputs/settling.dat		Settling rates	
MRLFN	inputs/mineralization.dat		Detritus Remineralization rates	
EXTFN	inputs/wqm_kei.dat		Light attenuation (extinction)parameters	

Parameter	Value	Unit	Meaning	Comments
S1FN	inputs/s1_load npt		Source 1 loading	Obsolete
S2FN	inputs/s2_load npt		Source 2 loading	Obsolete
S3FN	inputs/s3_load npt		Source 3 loading	Obsolete
ATMFN	inputs/atmospheric npt		Atm deposition	Not used
SAVFN	inputs/sav npt		SAV input parameters control file	Not used
BFIFN	inputs/sediments.dat		Sediment diagenesis control file or sediment flux (prescribed)	
CBCFN	inputs/wqm_cbc.w_iss			Obsolete
BAIFN	inputs/bai_chn.npt		Benthic Algae Input control	Not used
DFIFN	inputs/dfi_chn npt		Deposition feeder input file	Not used
ICOFN	outputs/initial_conditions .3_yr_11		Output for use as initial condition	
SNPFN	outputs/snapshot.3_yr_11		Snapshots output	Obsolete
RSOFN	outputs/restart.3_yr_11		Restart output file	Used for creating initial condition
PLTFN				Obsolete
APLFN				Obsolete
DIAFN				Obsolete
TFLFN				Obsolete
KFLFN				Obsolete
OPLFN				Obsolete
MBLFN				Obsolete
ALOFN				Obsolete
ZFOFN				Not used
BFOFN	outputs/benthic_flux.3_yr_11		Sediment flux output file	Obsolete. Currently hardwired in history outputs and station outputs directed by the linkage file
SVOFN				Not used
SFOFN				Not used
BAOFN				Not used
DFOFN				Not used

File MET inputs/meteorologic_fullgrid.dat

```
==== inputs/meteorologic_fullgrid.dat ===
MET file converted from FVCOM file psm_mc_wrf_2008.dat
KT = coef of heat exchange (watts/m2/C) (not used), TE = equil temp (C) (not used)
IO = PAR (E/m2/day), FD=Fraction of day, and WS = wind speed (m/s)
   JDAY    KT     TE     IO     FD     WS
  0.000 14.940 23.030  6.262 0.4580  7.680
  0.500 14.940 23.030  6.262 0.4580  7.680
  1.500 14.940 23.030  3.086 0.4580  7.658
  2.500 14.940 23.030  2.521 0.4580 10.393
  3.500 14.940 23.030  3.958 0.4580 10.135
  4.500 14.940 23.030  9.307 0.4580  8.483
...
 364.500 14.940 23.030  5.597 0.4580  7.140
 365.500 14.940 23.030  6.038 0.4580  7.412
 366.083 14.940 23.030  6.038 0.4580  7.412
================
```

The above file gives time-series of KT, TE, IO, FD, WS, all created based on the meteorological file based on Hydrodynamics run. First four lines are comments. Rest of them are data.

JDAY - Julian day of the year

KT - coef of heat exchange (watts/m2/C) (obsolete, it was in old ICM model for simulating T in ICM, now we are using T from HYD directly)
TE - TE = equil temp (C) (obsolete, it was in old ICM model for simulating T in ICM, now we are using T from HYD directly)
IO - PAR (E/m2/day) Photosynthetically active radiation, converted from short wave radiation
FD - fraction of day
WS - wind speed (m/s)

Appendix F. Glossary, Acronyms, and Abbreviations

Glossary

Clean Water Act: A federal act passed in 1972 that contains provisions to restore and maintain the quality of the nation's waters. Section 303(d) of the Clean Water Act establishes the TMDL program.

Diagenesis: The transformation of organic nitrogen and carbon into inorganic forms in the sediment.

Dissolved oxygen (DO): A measure of the amount of oxygen dissolved in water.

Effluent: An outflowing of water from a natural body of water or from a human-made structure. For example, the treated outflow from a wastewater treatment plant.

Eutrophic: Nutrient-rich and high in productivity resulting from human activities such as fertilizer runoff and leaky septic systems.

Model skill: Measures of the ability of a model to reproduce characteristics in the processes and parameters being simulated.

Nonpoint source: Pollution that enters any waters of the state from any dispersed land-based or water-based activities. This includes, but is not limited to, atmospheric deposition, surface-water runoff from agricultural lands, urban areas, or forest lands, subsurface or underground sources, or discharges from boats or marine vessels not otherwise regulated under the NPDES program. Generally, any unconfined and diffuse source of contamination. Legally, any source of water pollution that does not meet the legal definition of "point source" in section 502(14) of the Clean Water Act.

Nutrient: Substance such as carbon, nitrogen, and phosphorus used by organisms to live and grow. Too many nutrients in the water can promote algal blooms and rob the water of oxygen vital to aquatic organisms.

Parameter: A physical chemical or biological property whose values determine environmental characteristics or behavior.

Point source: Sources of pollution that discharge at a specific location from pipes, outfalls, and conveyance channels to a surface water. Examples of point source discharges include municipal wastewater treatment plants, municipal stormwater systems, industrial waste treatment facilities, and construction sites where more than 5 acres of land have been cleared.

Pollution: Contamination or other alteration of the physical, chemical, or biological properties of any waters of the state. This includes change in temperature, taste, color, turbidity, or odor of the waters. It also includes discharge of any liquid, gaseous, solid, radioactive, or other substance into any waters of the state. This definition assumes that these changes will, or are likely to, create a nuisance or render such waters harmful, detrimental, or injurious to

(1) public health, safety, or welfare, or (2) domestic, commercial, industrial, agricultural, recreational, or other legitimate beneficial uses, or (3) livestock, wild animals, birds, fish, or other aquatic life.

Salish Sea: Puget Sound, the Strait of Georgia, and the Strait of Juan de Fuca.

Sediment oxygen demand (SOD): Consumption of oxygen in the sediments due to oxidation of organic matter. Dissolved oxygen moves from the water into the sediment to supply the oxidation reactions that occur in the sediment. Therefore SOD reduces the dissolved oxygen concentration in the water overlying the sediment.

Total Maximum Daily Load (TMDL): A distribution of a substance in a waterbody designed to protect it from not meeting (exceeding) water quality standards. A TMDL is equal to the sum of all of the following: (1) individual wasteload allocations for point sources, (2) the load allocations for nonpoint sources, (3) the contribution of natural sources, and (4) a margin of safety to allow for uncertainty in the wasteload determination. A reserve for future growth is also generally provided.

Watershed: A drainage area or basin in which all land and water areas drain or flow toward a central collector such as a stream, river, or lake at a lower elevation.

303(d) list: Section 303(d) of the federal Clean Water Act requires Washington State to periodically prepare a list of all surface waters in the state for which beneficial uses of the water – such as for drinking, recreation, aquatic habitat, and industrial use – are impaired by pollutants. These are water quality-limited estuaries, lakes, and streams that fall short of state surface water quality standard and are not expected to improve within the next two years.

Acronyms and Abbreviations

C	Carbon
CBOD	Carbonaceous biochemical oxygen demand
Chl	Chlorophyll-a
DIN	Dissolved inorganic nitrogen (sum of nitrate, nitrite, and ammonium)
DO	(See Glossary above)
DOC	Dissolved organic carbon
Ecology	Washington State Department of Ecology
e.g.	For example
EPA	U.S. Environmental Protection Agency
et al.	And others
FVCOM	Finite-volume Coastal Ocean Model
ICM	Integrated Compartment Model
i.e.	In other words
MQO	Measurement quality objective
N	Nitrogen
NH4	Ammonia
NO3	Nitrate
P	Phosphorus
PNNL	Pacific Northwest National Laboratory

PO4	Phosphate phosphorus
POM	Particulate organic matter
QA	Quality assurance
RMSE	Root mean squared error
SAV	Submerged aquatic vegetation
SDM	Sediment Diagenesis Module
SFM	Sediment flux model
SOD	(See Glossary above)
SSM	Salish Sea Model
TMDL	(See Glossary above)
TOC	Total organic carbon
WAC	Washington Administrative Code
WASP	Water Analysis Simulation Program
WWTP	Wastewater treatment plant

Units of Measurement

m^3/s	cubic meters per second, a unit of flow
g	gram, a unit of mass
kg	kilograms, a unit of mass equal to 1,000 grams
kg/d	kilograms per day
kgD	kilograms of detritus
m	meter
mgd	million gallons per day
mg/L	milligrams per liter (parts per million)
mL	milliliters
mmol	millimole or one-thousandth of a mole
mole	an International System of Units (IS) unit of matter
psu	practical salinity units
ug/L	micrograms per liter (parts per billion)